Titre: Title:	Preliminary studies of some acetals polymer electrolyte membrane fuel cells (PEMFC)
Auteur: Author:	Xiangyang Yang
Date:	2002
Type:	Mémoire ou thèse / Dissertation or Thesis
Référence: Citation:	Yang, X. (2002). Preliminary studies of some acetals polymer electrolyte membrane fuel cells (PEMFC) [Master's thesis, École Polytechnique de Montréal]. PolyPublie. https://publications.polymtl.ca/26181/

UNIVERSITÉ DE MONTRÉAL

PRELIMINARY STUDIES OF SOME ACETALS POLYMER ELECTROLYTE MEMBRANE FUEL CELLS (PEMFC)

XIANGYANG YANG

GÉNIE METALLURGIQUE

ÉCOLE POLYTECHNIQUE DE MONTRÉAL

MEMOIRE PRÉSENTÉE EN VUE DE L'OBTENTION

DU DIPLÔME DE MAÎTRISE ÈS SCIENCES APPLIQUÉES

(GÉNIE METALLURGIQUE)

AOÛT 2002

UNIVERSITÉ DE MONTRÉAL

ÉCOLE POLYTECHNIQUE DE MONTRÉAL

Ce mémoire intitulé:

PRELIMINARY STUDIES OF SOME ACETALS POLYMER ELECTROLYTE MEMBRANE FUEL CELLS (PEMFC)

Présenté par: YANG Xiangyang

en vue de l'obtention du diplôme de: Maîtrise ès sciences appliquées

a été dûment accepté par le jury d'examen constitué de:

M. RIGAUD Michel, D.Sc.A., président
M. ROBERGE Raymond, Ph.D., membre
M. SAVADOGO Oumarou, D.d'ETAT, membre et directeur de recherche

To my wife and my son, Huifang and Rui

Acknowledgment

I would like to express my sincere appreciation to Professor O. Savadogo, my supervisor, for his guidance and constant encouragement throughout this research. Without his support and direction, I would not have completed my study in École Polytechnique.

I am also thanks to Mr. Xing Baozhong, Hugo Chagnon, Marc Lacroix, Teko, Ms. Tian Huimin, and Mr. Javier Rodriguez for their suggestions and helps during my experiments. I benefit and learned a lot from their advices and helps.

Thanks should give to André Désilets, Carole Massicotte, Jacques Desrochers for their assistance in experiments and their help in the preparation of this thesis. During my study and research in École Polytechnique, personnel and friends in the Département de Métallurgie et de Génie des Matériaux gave me enthusiastic support. I would like to repeat my acknowledgment for the help I received from many of them.

Résumé

Ce travail a pour objectif de développer les piles à combustible à consommation directe d'acétals à l'état liquide. Nous avons conçu et réalisé le montage du dispositif qui permet l'alimentation des piles à des températures de fonctionnement variant entre 25 et 80 °C avec un système de contrôle de la température et de débit du combustible dans chaque pile. Nous avons développé une méthode de fabrication de catalyseurs multicouches minces à base de matériaux binaires comme le platine – ruténium (Pt-Ru), le platine – étain (Pt – Sn), le platine – palladium, le platine – Iridium (Pt – Ir), le platine – rhodium (Pt – Rh), etc. Le principe de cette méthode repose sur l'utilisation le catalyseur binaire Pt – Ru supporté sur du carbone comme support, sur lequel sera étalé un deuxième catalyseur binaire. Le comportement de ses catalyseurs multicouches est comparé à celui des catalyseurs binaires simples. Nous montrons pour la première fois que l'électroxydation de l'éthylal et du dioxolane sur plusieurs électrodes différentes compositions. Les surtensions de leurs réactions sont plus faibles que celle du méthylal. Les surtensions d'électroxydation de tous les acétals sont inférieurs à ceux du méthanol. Ceci montre que ces combustibles sont plus efficaces dans une pile à combustible que le méthanol. La variation de la densité de courant, pour un potentiel donné, en fonction de la différence des rayons atomiques des deux éléments de l'alliage passe par un maximum pour l'alliage ayant la différence de rayon la plus élévée. Ainsi, les alliages métalliques ayant une différence de rayons atomiques élevée donnent les meilleures performances

d'électroxydation. Ceci explique pourquoi le platine- ruthénium et le platine – étain donnent les meilleures électrochimiques.

Les caractéristiques courant-potentiel des piles PEM à consommation directe d'acétals utilisant des anodes composites basées sur les alliages de platine et de platine – oxyde de platine ont été déterminées pour la première fois. Les conditions de préparation de ces électrodes d'utilisation de ses combustibles dans des piles PEM ont été déterminées. Les effets du type de combustible et des anodes sur les performances ont été étudiés. Les assemblages membranes – électrodes basées sur différentes anodes sur le nafion 117 ont été élaborés. La pile à base de platine – ruthénium sur lequel le platine – étain a été déposé présente les meilleures performances. La pile à base d'éthylal est meilleure que celle à base de diméthylal et du 1, 3 –dioxolane. La performance de la pile augmente avec la différence de rayon atomique entre les deux éléments qui forment le composé. Ainsi les alliages comme le platine – ruthénium et le platine – étain donne les meilleures performances pour les piles à combustible à consommation directe de méthanol.

L'étude des caractéristiques des piles à combustible à base d'anodes utilisant des catalyseurs composés d'alliages binaires simples (comme par exemple Pt – Ru) et des anodes à base de catalyseurs composés d'alliages déposés en multicouches (comme par exemple Pt – Sn déposé sur Pt – Ru) montre que les piles à base d'anodes de catalyseurs d'anodes multicouches sont plus performantes que celles avec anodes avec catalyseurs simples. Ceci indique que l'anode multicouche dispose de plus de catalyseurs disponibles

à la réaction que l'anode simple. L'empoisonnement diminue également avec les anodes multicouches. Ceci montre que les anodes multicouches sont bien indiquées pour améliorer les performances des piles à consommation directe de d'acétals.

Abstract

This thesis focuses on studying new fuels and electrocatalysts used in PEMFCs. As a very important type of fuel cell, PEMFC has attracted more and more attentions during the past few years. Along with its successful use in transportation and portable applications, the demands for PEMFCs, especially for direct fuel electro-oxidation will have a huge increase in the near future. At the same time the limitations still hinder the progress of PEMFC in several aspects, among them the high cost due to very expensive electrocatalysts and low efficiency due to slow direct electro-oxidation rate of liquid-storage fuel (methanol or other hydrocarbon fuel cell) are real challenges to the marketing of PEMFC. Keeping our eyes on these challenges is our initial motivation to look for new fuels and electrocatalysts. The primary half cell results of methylal on different electrocatalysts encourage us to continue our studies on other acetals.

First, for transportation application, methanol, which is inexpensive and relatively abundant, is an attractive alternative fuel to hydrogen in PEMFC and also only choice in today's practice direct-PEMFC. However, there are common problems related to direct methanol fuel cells, the main ones are as follows: a) low electrocatalytic activity and stability of the anodes; b) self-poisoning effects due to strong CO adsorption on Pt-based anodes and; c) a high degree of methanol cross-over through the Nafion membranes. All of these problems are due to the lack of good electrocatalysts and suitable fuels. So far,

the only catalysts that have been shown to exhibit good activity to promote the methanol/O_2 reactions in acid media are Pt and Pt-based alloys.

Second, demand for more-efficient portable power sources is steadily rising as equipment manufacturers add more features to their products, and at the same time hope them to run longer time. What are needed to replace the conventional rechargeable batteries are power sources with very high energy densities. Since fuel cell's energy density is ten times that of conventional rechargeable batteries, they are candidates to replace these batteries in portable equipments.

When hydrogen is used as a fuel, however, pumps, pipes and fans are needed to move the fuel to the cells that are stacked and connected in series. These additional mechanical devices would make the cells too big for portable equipments such as cell phones and notebook computers. PEMFCs for portable applications must also exhibit high energy density at room temperature. Consequently, fuel cells based on direct liquid fuel consumption at room temperature without any storage will be more competitive than hydrogen fuel cells equipped with mechanical devices. Thus, the development of low-temperature (room-temperature) PEMFC fed with high-energy organic substances, such as hydrocarbons, methanol and its derivatives, is of particular importance for the integration of fuel cell technology in transportation and portable applications.

The acetals are new fuels that are fabricated from natural gas, the world's reserves of which are in terms of a promising long-lasting supply. There are advantages to using them as direct fuels in fuel cells: a) they are completely electro-oxidized to carbon dioxide and water; b) their high energy content per molecule is attractive compared to that of methanol; c) their boiling point, flash point and toxicity are more adequate for this application than those of methanol; d) their cross-over rate in membranes may be lower than of methanol because of their greater size; and e) their electro-oxidation reaction involves a larger number of electrons per molecule than does the methanol electro-oxidation reaction. The technology of acetals formation on a large scale is well known.

In our half cell experiments, acetals (e.g. methylal, ethylal and 1,3-dioxolane) were oxidized in different supporting electrolytes and on various electrodes, including oxide-based electrodes dispersed onto carbon powder. The electro-oxidation of ethylal and 1,3-dioxolane was demonstrated for the first time. The fuel that exhibited the lowest over voltage was deduced from the electro-oxidation curve. Then, from an analysis of the reaction products from long-term anodic experiments, the electrode reactions were deduced. It was shown that the anodic polarization of the electro-oxidation of acetals in an acid medium is lower than that of methanol. Thus, acetals seem to be better fuels for fuel cell applications than methanol.

For methylal direct electro-oxidation the most of electrodes have an open-circuit potentials values at 220mv to 350mv. The open-circuit potential is a mixed potential resulting from the electrochemical reactions related to hydrogen atoms formed by the dissociate adsorption of the organic molecules or water and then ionisation of adsorbed hydrogen atoms. Ethylal has a lower open-circuit potential than methylal and 1,3-dioxolane, it maybe means that ethylal has more activated C-H bonds compared to latter, and then has a higher coverage of the surface adsorbed by hydrogen atoms.

From direct electro-oxidation of methylal we can see among the single noble metal electrodes that Pt/C is the best catalyst for oxidation of methylal. For Pt-metal oxides electrodes, at a given current the overpotential of the reaction increases in the order Pt-RuO_2 < Pt-Ru <Pt-Fe_3O_4 < Pt-SnO_2 < Pt-WO_3, only when current density is high than 10mA.cm^{-2}, the Pt-Ru/C is better than Pt-RuO_2/C. On the other hand for a fixed concentration of Pt in the Pt-RuO_2 alloy, the overpotential changes with the RuO_2 concentration in the electrode. For RuO_2 concentration from 5% to 40% w/w, the lowest overpotential is obtained on 5%Pt-10%RuO_2. These different results may be explained by the synergetic effect that between Pt and the ruthenium oxides for this reaction, the optimum value obtained for the overpotential when %RuO_2 changes supports this synergetic effect.

For Pt-noble metal alloy series electrode, the best electrode among them is still Pt-Ru alloy, Pt-Ir alloy also show a good properties, and Pt-Co-Cr has a big improvement as

temperature rising from 25°C to 60°C. The overpotential increase in the order Pt-Ru < Pt-Ir< Pt-Co-Cr< Pt-Rh< Pt-Pd.

The polarization curves of ethylal and 1,3-dioxolane in 1 M H_2SO_4 on various electrodes including Pt mixed with oxides electrodes were drawn and similar trends to those obtained on methylal electrooxidation were observed. The best characteristics are obtained in the ethylal solution among these acetals. The high number of electrons produced from acetals electrooxidation may explain why the polarization curves of acetals are better than that of methanol.

Volcano behavior was obtained for the plot of direct oxidation current density vs. metal radius for various single noble-metal electrodes. The highest current density was obtained with the Pt electrode. Similar behavior was obtained with electrodes based on noble binary platinum alloys, where the electrooxidation current density increases with the difference in metal radius in each alloy (ΔR). Thus, the alloys that give the highest $|\Delta R|$, e.g. Pt-Ru and Pt-Sn, exhibited the best electro-oxidation current density.

The results based on fuel cell station experiments also give us some promotion information. The electrode (Pt-Ru + Pt-Sn)/C, which was prepared by our lab, has the best performance in H_2/O_2. The other electrodes prepared by ourselves (Pt-Ru + Pt-Pd/C, Pt-Ru + Pt-Ir/C, Pt-Ru + RuO_2/C) also have better performance compared to Pt-Ru/C electrode. The performances of all electrodes have the order (Pt-Ru + Pt-Sn) > (Pt-Ru +

Pt-Pd) > (Pt-Ru + Pt-RuO_2) > (Pt-Ru + Pt-Ir), it is shown that Pt-Sn has the strongest synergetic effect on Pt-Ru.

Poisoning effect is inevitable to all these electrodes just like methanol electro-oxidation because either acetals or their intermedia will produce CO_2 during reaction processing. But the performance of (Pt-Ru + Pt-Sn) in our studies has shown this electrode has good resistance to CO/CO_2 poison. From our curves we also can guess that the product composition of electrooxidation processes is dependent on the electrocatalyst materials. Such differences have been observed in the oxidation of methanol on Pt and Pt-Ru catalysts where the kinetic of oxidation and the stability of intermediates is altered by the chemisorptions characteristics of the Ru sites.

Differences in product composition can also arise from the extreme water activity at the site of reaction. In water-deficient environment other oxygen-deficient intermediate products such as dimethyl ether or methyl formate could be formed electrochemically. This affirms that in order to attain complete oxidation of the organic molecules, the nature of the electrocatalyst and electrolyte are of fundamental important.

From our figures we can see ethylal and 1,3-dioxolane have similar reaction trend as methylal, the mechanism of electrodes on acetals should has some kind of common characters. The (Pt-Ru + Pt-Sn) has a good performance. For acetals performance on

same electrode the ethylal always exhibits the best performance except on Pt-Ru-RuO_2, on which 1,3-dioxolane was better than other acetals.

Condensé en français

La pile à combustible à électrolyte polymère solide est un dispositif électrochimique de conversion de l' énergie chimique en énergie électrique. C'est un dispositif de production de l'énergie qui fournit des rendements de conversion au moins deux fois supérieure au rendement de conversion des moteurs thermiques qui fonctionnent selon le cycle de Carnot. Ceci fait qu'il est nettement moins polluant que les moteurs thermiques présentement utilisés. Les combustibles utilisés peuvent être sous forme liquide où sous forme gazeux. Des combustibles comme l'hydrogène et les hydrocarbures légers à densité énergétique élevée comme le méthanol, l' éthanol, le propane, et les acétals peuvent être utilisés. Malgré ces aspects avantageux, la fabrication industrielle des piles à combustible est limitée par plusieurs facteurs :i) la performance limitée des systèmes; i) le coût élevé des matériaux (plaques bipolaires, électrocatalyseurs, membranes, etc.); iii) le manque de réseau de distribution des combustibles; iv) le coût élevé de fabrication; v) l'absence de secteur d'application commerciale très porteuse, etc. Pour résoudre ses difficultés, il est important de continuer à développer de nouvelles connaissances liées aux différents aspects de ses systèmes. Un des aspects qui contribuerait à ce développement consiste à étendre l'utilisation des combustibles autres que l'hydrogène et d'électrocatalyseurs autres que le platine.

Ce travail porte sur le développement de nouveaux électrocatalyseurs à base d'alliage de platine et d'alliages d'oxydes et de platine qui pour les piles à combustible à consommation directe d'acétals à basse températures. Le développement de piles à combustible à basse température alimentés par des hydrocarbures légers à hautes valeurs énergétiques est important pour assurer l'intégration de la technologie des piles à combustible pour des applications stationnaires, mobiles et de transport. Néanmoins, plusieurs difficultés liées au développement de ces systèmes existent : a) faible activité catalytique et stabilité des électrocatalyseurs pour l'oxydation de ces hydrocarbures; b) l'empoisonnement des catalyseurs due à la forte adsorption en CO sur les anodes à base de platine, et c) le passage important du combustible à travers la membrane comme le méthanol. En 1997, l'oxydation directe du dymethoxymethane(DMM), trimethoxymethane(TMM) et du trioxane ont montré l'alliage platine-ruthenium donnait des performances meilleures que l'alliage platine-étain et le platine seul. DMMconduit à la formation du méthanol, puis du dioxyde de carbone. Celle du TMM est précédée par une hydrolyse qui catalyse la réaction sur le Nafion en milieu acide. Lorsque le polybenzimidazole est utilisé comme membrane, la performance des piles est meilleure. Ces combustibles doivent passer aissi à travers la membrane de la pile mais en quantités moins importantes que le methanol. Les avantages des comme combustibles dans les piles à combustibles sont : a) ils peuvent facilement être comlèt5ement électrolysés en dioxyde de carbone, b) leur desité énergétique est plus élevée que le méthanol., c) ils sont moins toxiques que le methanol; d) comme ils sont plus gros que le méthanol, ils passent

moins vite à travers la membrane, e) le nombre d' électrons impliqués dans leur elecro-oxydation est plus élevé que celle du méthanol.

Ce travail a pour objectif de développer les piles à combustible à consommation directe d'acétals à l'état liquide. Nous avons conçu et réalisé le montage du dispositif qui permet l'alimentation des piles à des températures de fonctionnement variant entre 25 et 80 °C avec un système de contrôle de la température et de débit du combustible dans chaque pile. Nous avons développé une méthode de fabrication de catalyseurs multicouches minces à base de matériaux binaires comme le platine – ruténium (Pt-Ru), le platine – étain (Pt – Sn), le platine – palladium, le platine – Iridium (Pt – Ir), le platine – rhodium (Pt – Rh), etc. Le principe de cette méthode repose sur l'utilisation le catalyseur binaire Pt – Ru supporté sur du carbone comme support, sur lequel sera étalé un deuxième catalyseur binaire. Cette approche présente l'avantage d'augmenter la performance du catalyseur pour l'éléctroxydation des acétals. Le comportement de ses catalyseurs multicouches est comparé à celui des catalyseurs binaires simples.

Dans ce travail nous montrons pour la première fois que l'électroxydation, de l'éthylal et du dioxolane sur plusieurs électrodes différentes compositions. Les surtensions de leurs réactions sont plus faibles que celle du méthylal. Les surtensions d'électroxydation de tous les acétals sont inférieurs à ceux du méthanol. Ceci montre que ces combustibles sont plus efficaces dans une pile à combustible que le méthanol. La variation de la densité de courant, pour un potentiel donné, en fonction de la différence des rayons atomiques

des deux éléments de l'alliage passe par un maximum pour l'alliage ayant la différence de rayon la plus élévée. Ainsi, les alliages métalliques ayant une différence de rayons atomiques élevée donnent les meilleures performances d'électroxydation. Ceci explique pourquoi le platine- ruthénium et le platine – étain donnent les meilleures électrochimiques.

Les caratéristiques courant-potentiel des piles PEM à consommation directe d'acétals utilisant des anodes composites basées sur les alliages de platine et de platine – oxyde de platine ont été déterminées pour la première fois. Les conditions de préparation de ses électrodes d'utilisation de ses combustibles dedans des piles PEM ont .t. déterminées. Les effets du type de combustible et des anodes sur les performances ont été étudiées. Les assemblages membranes – électrodes basées sur différentes anodes sur le nfion 117 ont été élaborées. La pile à base de platine – ruthénium sur le quel le platine – étain a été déposé présentae les meilleures performances. Lapile à ase d »éthylal est meilleure que celle diméthylal et du 1, 3 –dioxolane. La perforamance de la pile augmente avec la différence de rayon atome entre les deux éléments qui forment le composé. Ainsi les alliages comme le platine – ruthénium et le platine – étain donne les meilleures performances pour les piles à combustible à consommation directe de méthanol.

L'étude des caractéristiques des piles à combustible à base d'anodes utilisant des catalyseurs composés d'alliages binaires simples (comme par exemple Pt – Ru) et des anodes à base de catalyseurs composés d'alliages déposés en multicouches (comme par

exemple Pt – Sn déposé sur Pt – Ru) montre que les piles à base d'anodes de catalyseurs d'anodes multicouches sont plus performantes que celles avec anodes avec catalyseurs simples. Ceci indique que l'anode multicouche dispose de plus de catalyseurs disponibles à la réaction que l'anode simple. L'empoisonnement diminue également avec les anodes multicouches. Ceci montre que les anodes multicouches sont bien indiquées pour améliorer les performances des piles à consommation directe de d'acétals.

Table of Contents

List of Figures

LIST OF TABLES

CHAPTER 1

INTRODUCTION

1.1 Fuel Cells and PEMFC

A Fuel cell is an electrochemical cell that can continuously convert the chemical energy of a fuel and an oxidant to electrical energy by a process involving an essentially invariant electrode-electrolyte system [1]. Fuel cells work at high efficiency with very low emission levels.

The basic principles of a fuel cell are similar to well-known electrochemical batteries. The big difference is that, in the case of batteries, the chemical energy is stored in substances located inside them. When this energy has been converted to electrical energy, the battery must be thrown away or recharged appropriately. In a fuel cell, the chemical energy is provided by a fuel and an oxidant stored outside the cell in which the chemical reactions take place. As long as the cell is supplied with fuel and oxidant, electrical power can be obtained.

Presently, different types of fuel cells are being studied and developed for various applications. Of these applications, PEMFC (polymer electrolyte membrane fuel cell) has been one of the important types because they may provide and actually already provide power source for transportation [2-21]. When PEMFC applied to transportation, it has a

lot of advantages, such as (a) High-energy efficiency that is not limited by Carnot efficiency like thermal cycles. (b) Clean exhaust gas because it does not exhaust any nitrogen oxide, which is one of the major pollutants of combustion engines, high efficiency also means that less carbon dioxide exhaust for a given work. (c) Quiet operation. There is no major mechanic part in the system except pumps to carry air and fuel to the cell. Whether such vehicles should carry methanol fuel or hydrogen fuel, the PEMFC cathode will operate on air in all of these terrestrial transportation systems.

On the other hand, PEMFC applied to portable systems also has a bright future [22-25]. These portable fuel cell systems may one day replace the traditional batteries include miniature fuel cell power telecommunication equipments from cellular phones and notebook PCs to cameras and electronic games, small and lightweight fuel cell supplied power sources for medical applications such as total artificial hearts (TAH), left ventricular assist devices (LVAD).

1.2 Limitations and Problems

However, PEMFC to replace internal combustion engine or batteries still have a long way ahead. Many factors have to be considered for designing a fuel cell, such as fuel type, electrolyte and catalyst for electrode, etc. As a fuel, hydrogen is probably the best candidate because it can be generated from reformed hydrocarbons and its oxidation product is non-toxic to the environment. However, hydrogen is not a liquid fuel that

makes it inconvenient to store and transport. Also, the use of a fuel reformer increases the weight, volume and cost of the fuel cell.

Methanol (MeOH), being inexpensive and relatively abundant, is an attractive alternative fuel to hydrogen in PEMFC. In contrast to hydrogen, MeOH is a liquid fuel that makes it convenient to store and transport. Presently, direct MeOH/O_2 PEMFC operate between 60 and 80°C and use Nafion as a proton conducting membrane. However, the anode and cathode reactions are kinetically slow and the only catalysts that have been shown to exhibit activity to efficiently promote these reactions in acid media are Pt and Pt-based alloys. The direct oxidation of MeOH in a fuel cell may have to work in acid electrolyte because an alkaline electrolyte would be intolerant to the CO_2 produced. In alkaline media, carbon dioxide, the final product of methanol oxidation, is adsorbed and accumulated in the electrolyte:

$$CO_2 + OH^- \rightarrow HCO^{3-} \qquad (1\text{-}1)$$

This phenomenon leads to decrease of conductivity of the electrolyte and reactivity of methanol and results in the necessity of periodical maintenance of the electrolyte. In acid media, in contrast, carbon dioxide is ejected and causes no maintenance problems.

In acid media, methanol is oxidized by the following reaction:

$$CH_3OH + \rightarrow CO_2 + 6H^+ + 6e^- \qquad (1\text{-}2)$$

The thermodynamic potential for this reaction is –0.03V against the standard hydrogen electrode (SHE). At present, however, the oxidation occurs at an appreciable rate at no less than +450 mV versus SHE even on freshly made best electrocatalysts. Accumulation of poisoning species reduces the current density and/or raises the oxidation potential. As the result, only small voltage would remain when it is combined with a air electrode, in which the reduction potential is practically no more than 0.9V, in spite of the thermodynamic potential of 1.23V.

The difficulty of electrochemical oxidation of methanol is due to the lack of a good electrocatalyst. It is not over-stated, therefore, that ultimate goal of all studies on methanol oxidation is to find a better electrocatalyst.

At present, the only material that shows reasonable electrocatalytic activity on methanol direct electro-oxidation is platinum and platinum based alloys. A major problem of these catalysts, aside from the high price of platinum, is rapid decrease of the catalytic activity after starting oxidation.

As shown by (1-2), methanol oxidation to carbon dioxide is a six-electron reaction. This reaction, however, does not proceed by a simple single step. On the contrary, it is considered as a complex multi-step reaction involving several intermediates and by-

product that may be different depending on the catalysts, media, temperature and other conditions. Although the details are yet to be found, it is widely agreed that some intermediates or by-product accumulate on the surface and poison the catalyst to decrease its activity. Overcoming this poisoning effect is a major challenge in a study in electrocatalyst for methanol oxidation.

For commercial use the cost of the stack of fuel cell must be decreased significantly. This has enormous technological implication and material as well as manufacturing issues has to be addressed:

Electrolyte Membrane: The PEMFC uses a polymer membrane as its electrolyte. This membrane is an electronic insulator, but an excellent conductor of hydrogen ions. The materials used to date such as Nafion consists of a fluorocarbon polymer backbone, similar to Teflon, to which sulfuric acid groups are attached. The acid molecules are fixed to the polymer and cannot "leak" out, but the protons on these acid groups are free to migrate through the membrane. The disadvantages of membranes in PEMFC are:

- The fluorinated polymer electrolyte is traditionally expensive and cell costs are high.
- Water-management in the membrane is critical for efficient operation.
- CO tolerance is poor.
- Difficulty in thermally integrating with a reformer.

Catalysts: The archetype of the PEMFC catalyst is Pt-black, traditionally used at a high loading of a 4 mg/cm^2. Two efforts had been made in order to reduce the catalyst costs: First the amount was lowered and second supported catalysts are currently being used. This type of catalyst is characterized by a catalyst support of a conductive material, i.e. carbon. The support is impregnated with very small clusters of precious metal, consisting of not more than a few hundred atoms per catalyst particle. With such catalysts, loading of precious metal of only 0.1mg/cm^2 has been successfully demonstrated, without loss of performance. The ultimate goal of catalyst research may be to avoid precious metals completely.

Electrode preparation techniques: The catalyst can be applied to either on the electrode support material or on the membrane. Both are possible and at present neither one has clear advantages. For the application of the catalyst a variety of techniques are possible.

Bipolar plates: The prototype of a PEMFC-bipolar plate is machined graphite plate; neither graphite nor machining will succeed if commercial aspects are considered. Alternatives have to be found.

1.3 Solutions

Although hydrogen and methanol are currently the practical fuels for use in the present generation of fuel cells, all of these problems and limitations in existing fuel cell systems require us to look for new fuels and more efficient electrocatalysts. Especially direct-oxidation of hydrocarbon used in acid media PEMFC has attracted a lot of attention. Unfortunately, simple hydrocarbon gases were shown to be anodic oxidized at unacceptably low rates, while higher molecular weight compounds generally proved to be less reactive. To find new fuels and new electrocatalyst therefore become a double difficult challenge.

1.4 Aims of the Works

Various metal oxides have been shown to exhibit great promise for enhancing the catalysis of methanol oxidation. So along with these studies we try to find some electrocatalysts that can be practically used as anodes for direct-oxidation of new fuels (e.g. acetals) in PEMFC. At same time just as we addressed above to look for and test new fuels that maybe will replace methanol for direct electro-oxidation used in PEMFC is another major objective of this works. Thus the aims of this works are:

- Development of Direct Acetals PEM Fuel Cells (DAPEMFC).
- Development of new composite anodes for DAPEMFC.

CHAPTER 2

LITERATURE REVIEW

2.1 TYPES OF FUEL CELLS

Fuel cell systems can be classified according to the working temperature: high, medium and low (ambient) temperature systems, or referring to the pressure of operation: high, medium and low (atmospheric) pressure systems. They may be further distinguished by the fuels and/or the oxidants they use: (1) gaseous reactants (such as hydrogen, ammonia, air and oxygen), (2) liquid fuels (alcohols, hydrazine and hydrocarbons) or (3) solid fuels (coal, hydrides).

For practical reasons fuel cell systems are simply distinguished by the type of electrolyte used and the following names and abbreviations are now frequently used in publications: Alkaline fuel cells (AFC), phosphoric acid fuel cells (PAFC), molten carbonate fuel cells (MCFC), solid oxide fuel cells (SOFC) and polymer electrolyte membrane fuel cells (PEMFC).

Subsequent classifications are also available with the systems. The principle division into direct and indirect fuel cells has its basis at the electrode level. For instance, hydrogen gas is ionized at the hydrogen electrode and participates directly in the electric power generating reaction. In direct cells, chemicals e.g., ammonia, alcohol, cyclohexane,

methane or aviation turbine fuels are cracked or steam reformed to hydrogen containing mixture gases. This is usually done outside of the fuel cell with the aid of catalysts at high temperatures. Only the hydrogen in the gas mixture reacts electrochemically at the electrode.

The summary review of different fuel cell systems are simply shown as tables 2-1. The individual electrode reactions listed in table 2-2. The overall corresponding electrochemical reactions are given in table 2-3, along with the appropriate form of the Nernst equation. The Nernst equation provides a relationship between the standard potential (E^0) for the cell reaction and the equilibrium potential (E) at various temperature and partial pressures (activities) of reactants and products. According to the Nernst equation, the equilibrium cell potential at a given temperature can be increased by operating at higher reactant pressures and improvements in fuel cell performance have been observed at higher pressures (often continuing life-time).

Table 2-1. Applications for technical H_2/O_2-fuel cell systems

Fuel Cell System	Temperature Range	Efficiency (Cell)	Electrolyte	Application Area
Alkaline fuel cell (AFC)	60-90 °C	50-60%	35-50% KOH	Space applications/ Traction applications
Polymer Electrolyte Fuel Cell (PEFC)	50-80°C	50-60%	Polymer Membrane (Nafion/Dow)	Traction applications/ Portable application/ Space applications
Phosphoric Acid Fuel cell (PAFC)	160-220°C	55%	Concentrated Phosphoric acid	Predominantly dispersed Power applications (50-500kw, 1MW, 5MW, 11MW)
Molten Carbonate Fuel Cell (MCFC)	620-660°C	60-65%	Molten Carbonate Melts (Li_2C0_3/Na_2CO_3)	Power generation
Solid Oxide Fuel Cell (SOFC)	800- 1000°C	55-65%	Yttrium-stabilized Zincdioxide (ZrO_2/Y_2O_3)	Power generation

Table 2-2. Typical Electrochemical Reactions in Fuel Cells

Fuel Cell	Anode Reaction	Cathode Reaction
Alkaline Fuel Cells	$H_2 + 2(OH)^- \rightarrow 2\,H_2O + 2e^-$	$\frac{1}{2}O_2 + H_2O + 2e^- \rightarrow 2OH^-$
Polymer electrolyte Fuel Cells	$H_2 \rightarrow 2H^+ + 2e^-$	$\frac{1}{2}O_2 + 2H^+ + 2e^- \rightarrow H_2O$
Phosphoric Acid Fuel Cells	$H_2 \rightarrow 2H^+ + 2e^-$	$\frac{1}{2}O_2 + 2H^+ + 2e^- \rightarrow H_2O$
Molten Carbonate Fuel Cells	$H_2 + CO_3^{2-} \rightarrow H_2O + CO_2 + 2e^-$	$\frac{1}{2}O_2 + 2e^- \rightarrow CO_3^{2-}$
Solid Oxide Fuel Cells	$H_2 + O^{2-} \rightarrow H_2O + 2e^-$	$\frac{1}{2}O_2 + 2e^- \rightarrow O^{2-}$

Table 2-3. Corresponding Nernst Equations

Cell Reactions (total)	Nernst Equation
$H_2 + \frac{1}{2}O_2 \rightarrow H_2O$	$E = E^0 + (RT/2F)\ln [(P_{H2} * P_{O2}^{1/2}) / P_{H2O}]$
$H_2 + \frac{1}{2}O_2 + CO_2(c) \rightarrow H_2O + CO_2\,(a)$	$E = E^0 + (RT/2F) * \alpha$ $\alpha = \ln [(P_{H2} * P_{O2}^{1/2} * (P_{CO2})_c\,] / [P_{H2O} * (P_{CO2})_a\,]$

(a) - Anode
(c) - Cathode
E – Equilibrium potential
E^0 - Standard potential
P - Gas pressure
R - Universal gas constant
T – Temperature

2.2 PEMFC

2.2.1 Introduction

Application of the polymer electrolyte fuel cell (PEMFC) as a primary power source in electric vehicles has received increasing attention in the last few years. This attention has been fueled by a combination of significant technical advances and by the initiation of projects for the demonstration of a complete, PEMFC-based power system in a bus or in a passenger car. Whether such vehicles should carry methanol fuel (to be reformed on board) or hydrogen fuel (in pressurized, liquefied, or hydride form), the PEMFC cathode will operate on air in all of these terrestrial transportation systems.

The PEMFC uses a polymer membrane as its electrolyte. This membrane is an electronic insulator, but an excellent conductor of hydrogen ions. The materials used to date consist of a fluorocarbon polymer backbone, similar to Teflon, to which sulfuric acid groups are attached. The acid molecules are fixed to the polymer and cannot "leak" out, but the protons on these acid groups are free to migrate through the membrane. The advantages of PEMFCs against AFCs are:

- there is no free corrosive liquid in the cell,
- it is simple to fabricate the cell,
- they are able to withstand large pressure differentials

- material corrosion problems are minimal, and
- they have demonstrated long life.

The disadvantages of PEMFCs are:

- the fluorinated polymer electrolyte is traditionally expensive and cell costs are high,
- water-management in the membrane is critical for efficient operation,
- CO tolerance is poor,
- long-term, high performance with low catalyst loadings in the electrodes needs to be demonstrated , and
- difficulty in thermally integrating with a reformer.

The electrode reactions in the PEMFC are analogous to those in the PAFC. Hydrogen from the fuel gas stream is consumed at the anode, yielding electrons to the anode producing hydrogen ions that enter the electrolyte. At the cathode, oxygen combines with electrons from the cathode and hydrogen ions from the electrolyte to produce water.

anode: $2H_2 \rightarrow 4\,H^+ + 4e^-$ (2-1)

cathode: $O_2 + 4H^+ + 4e^- \rightarrow 2\,H_2O$ (2-2)

The water does not dissolve in the electrolyte and is, instead, expelled from the back of the cathode into the oxidant gas stream. As the PEMFC operates at about 80°C, the water is produced as liquid and is carried out of the fuel cell by excess oxidant flow.

2.2.2 OPERATING PRINCIPLE

The cross-section of a single polymer-electrolyte fuel cell is shown schematically in Figure 2-1 [26]. The cell typically consists of graphite bipolar plates, which are pressed against membrane-electrode assembly. These plates have a manifold of grooves to distribute the reactant gases to the electrodes. They are also sufficiently electrically conductive to pass the generated current to the adjacent cell.

The membrane-electrode assembly is the electrochemical heart of the system. On the anode, or hydrogen side, hydrogen gas is catalytically disassociated according to the reaction (2-1). The hydrogen ions pass through the polymer electrolyte to the cathode, or oxygen side, of the cell. There they are combined catalytically with oxygen and electrons from the adjacent cell to form water according to the reaction (2-2).

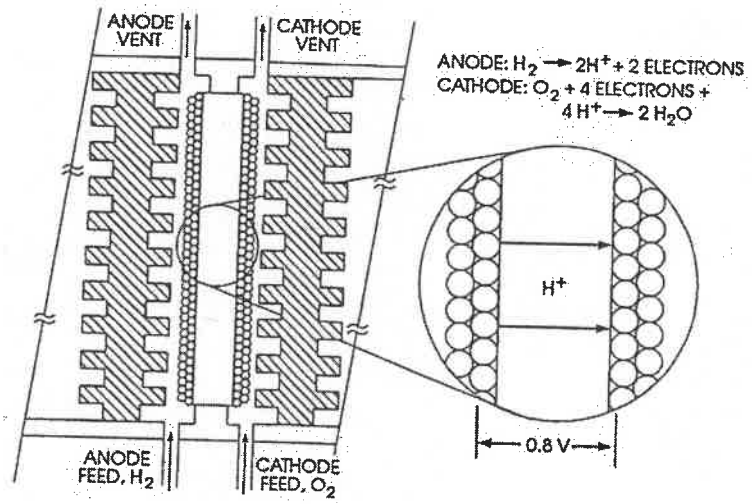

Figure 2-1 Schematic cross section of a PEMFC [26]

The membrane functions twofold, it acts as the electrolyte, which provides ionic communication between the anode and the cathode, and it serves as a separator for the two reactant gases. Optimized proton and water transport properties of the membrane and proper water management are crucial for efficient fuel cell operation. Dehydration of the membrane reduces proton conductivity and excess of water can lead to flooding of the electrodes. Both conditions result in poor cell performance.

2.2.3 ELECTRODES

The electrodes are typical gas-diffusion electrodes. The backing is a porous carbon cloth with a hydrophobic coating. In order for the electrochemical reactions to take place at a useful efficiency, they must be catalyzed [27-29]. To date, platinum has proven to be the best catalyst for both the hydrogen oxidation and the oxygen-reduction reactions. The problem of high platinum loading (typically 4 mg of platinum per square centimeter) was solved by the use of supported platinum catalysts similar to those used in liquid-electrolyte fuel cells. These consist of 2 to 5 nm diameter Pt particles on the surface of fine carbon particles. This greatly increases the effective surface area of the platinum. Ticianelli and co-workers used several methods to incorporate changes in the electrode structure and to have electrodes with platinum layers at the front surface. They also determined the electrochemically active surface areas in fuel cell electrodes by the cyclic voltammeter technique, and found that only about 10-20% of the platinum was electrochemically active in the fuel cell reaction [30-31].

To function, the catalyst must have access to the gas and must be in contact with both the electrical and protonic conductors. A certain procedure of making effective contact with the protonic conductor is by impregnating the supported-catalyst electrode with protonic conducting material. This is achieved by covering the surface with a solution of solubilized membrane material (Nafion) (see Figure 2-2 to 2-3 [32]). Also, sulfuric acid solutions containing 0.001M perfluorooctane sulfonic acid were found to similarly enhance the wettability of the electrode-electrolyte interface.

New electrochemical canalization techniques for producing gas-diffusion electrodes for PEMFC applications, in which platinum catalyst particles are in regions of the electrode that are in ionic contact with the proton-exchange membrane and in electronic contact with the carbon support, propose 0.05 mg/cm^2 [33].

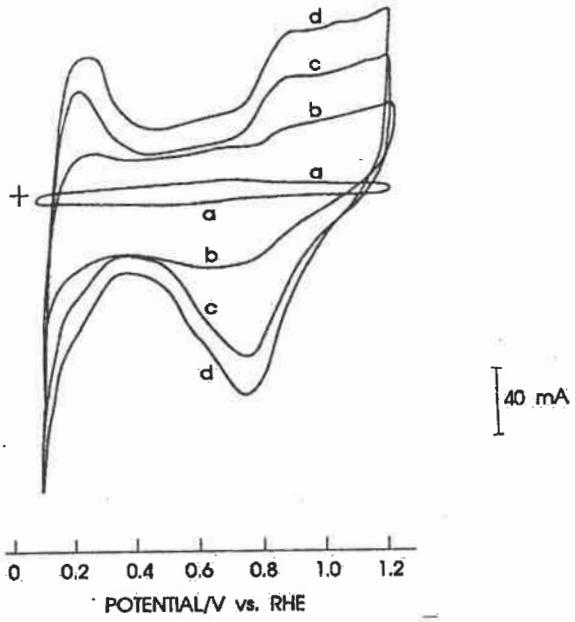

Figure 2-2 Cyclic Voltammograms at 50°C on Prototech Electrodes: (a) uncatalyzed, (b) 10 wt % Pt/C, (c) 20 wt % Pt/C plus 50 nm sputtered film of Pt (v = 100 mV/s). [32]

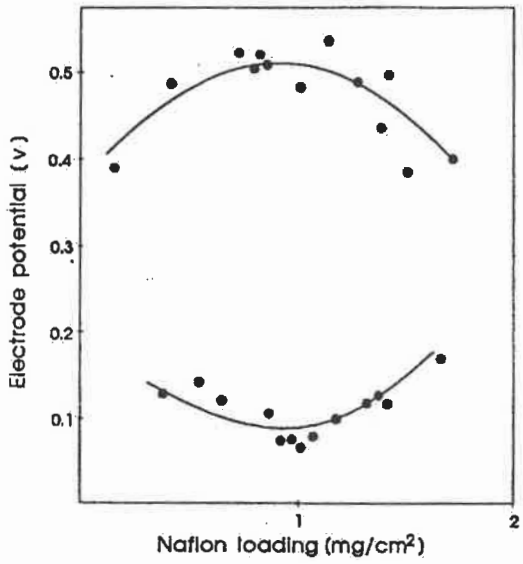

Figure 2-3 Effect of Nafion Loading on Anodic and Cathodic Volt. of 200mA/cm^2 [32]

2.2.4 ELECTROLYTES MEMBRANES

The PEMFC uses one of several ion-exchange polymers as its electrolyte. These polymers are electronic insulators, but excellent conductors of hydrogen ions. The early membranes tested in PEMFCs include the hydrocarbon-type polymers such as cross-linked, polystyrene-divinylbenzene sulfuric acids and sulfonated phenolformaldehyde. Hydrocarbon-type polymers are unstable because of C-H bond cleavage, particularly at the α-H sites where the functional groups are attached. When these polystyrenes were replaced with fluorine-substituted polystyrenes, the life of the PEMFCs was extended by a factor of four to five. The research started in the early 1960s with the development of Nafion. This material, which is still used to date, consists of a fluorocarbon polymer backbone, similar to Teflon, to which sulphuric acid groups have been chemically bonded. The acid molecules are fixed to the polymer and cannot be leached out, but the protons on these acid groups are free to migrate through the electrolyte (see Figure 2-4 and 2-5 [34-35]).

The electrolyte is used in the form of a very thin membrane, typically 50 to 175 μm thick, and can be handled easily and safely. The material is a relatively dilute acid with about the same conductivity as 1 M sulphuric acid. It behaves as a typical aqueous acid from the viewpoint of conductivity, so that their use is limited to temperatures below the boiling point of water.

The latest version from DuPont is Nafion-105, which has similar ionic properties to materials from the Dow Chemical Company (for which n = 0 and m = 2) and the materials known as Aciplex-S from the Asahi Chemical Industry Company, in which n = 0-2, and m = 2-5. The materials are made using a slightly different chemistry and have slightly different properties, with equivalent weights of 1100, 800 and 1000 respectively. Figure 2-6 [36-37] shows performance data achieved with different Nafion membranes.

However, the open-circuit potential of the thinner membranes (Nafion-105) show a lower open circuit Voltage (50-100 mV) than the thicker ones (Nafion-117) because of cross-over of the hydrogen gas. The cross-over effect is also reflected by a lower potential in the cell with the 50 μm thick membrane compared to the cell with a 175 or 125 μm thick membranes at low current densities.

The PEMFCs with Aciplex-S and the Dow membranes show considerably better performances than the PEMFC with the Nafion membrane, mainly because of the considerably lower R values for these two cells. Figure 2-7 [38] also shows that the PEMFC with the Dow membrane exhibits the pseudo-linear behavior even at current densities higher than 2 A/cm2, but above this current density the PEMFC with the Aciplex-S membrane shows some mass-transport limitations. Comparisons between Nafion117 and Aciplex-S in which the transport parameters of hydrogen and oxygen were investigated reported in references [39,40]. Arrhenius plots for diffusion coefficients are show Figure 2-8 [41].

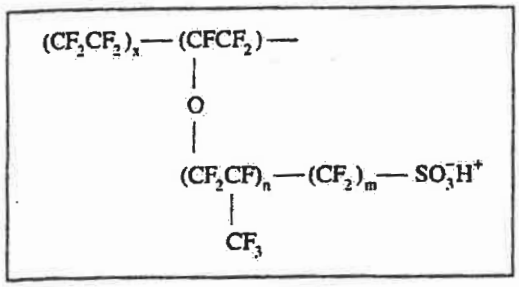

Membrane	Equiv. weight g/mol SO_3^-	Thickness in dry state, µm	Water Content %	Conductivity Ω^{-1} cm^{-1}
Dow	800	125	54	0.114
Aciplex®-S	1000	120	43	0.108
Nafion®-115	1100	100	34	0.059

Figure 2-4 Structure of perfluorocarbon ion exchange polymers [34]

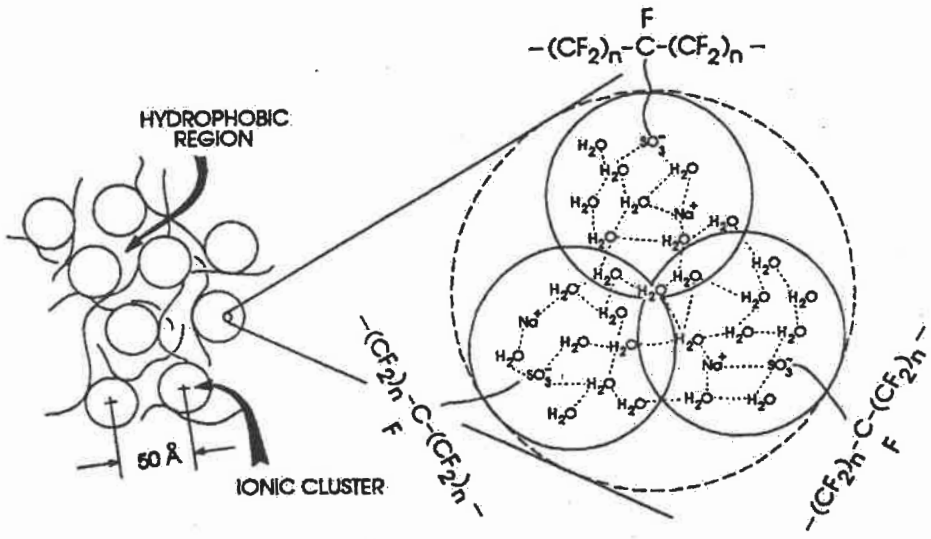

Figure 2-5 Schematic representation of ion clustering in Nafion [35]

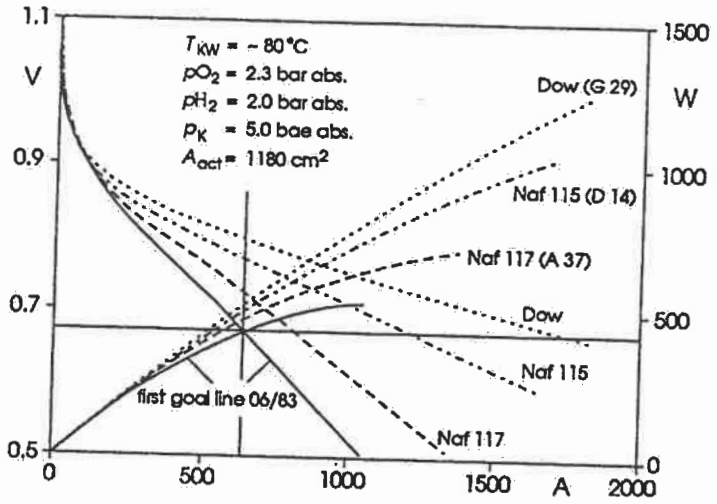

Figure 2-6 Potential performance increase with the use of different Nafion and Dow membranes [36-37]

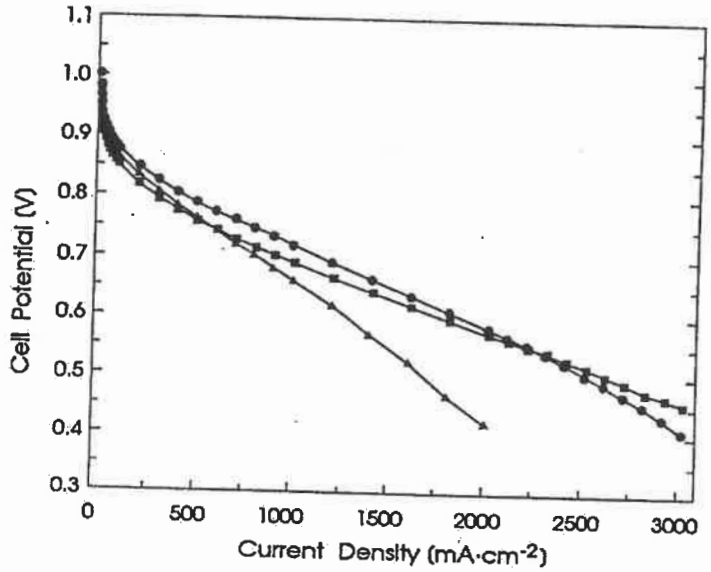

Figure 2-7 Effect of poton conducting membrane on PEMFC performance – H2/O2 reactants (E-TEC electrodes – 20% Pt/C, o.4 mg/cm^2), 95°C, 5atm; Aciplex-S 1004(•); Dow(■); Nafion-115 (▲) [38]

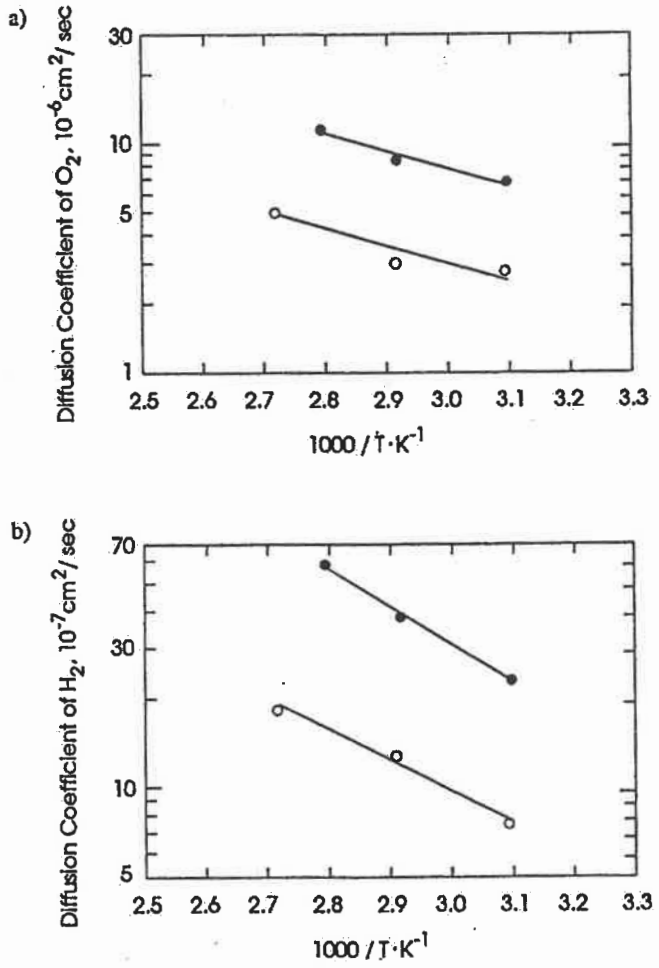

Figure 2-8 Diffusion coefficients of H_2 and O_2 in PEMFCs with a) Aciplex-S (μ) and b) Nafion-117 membrane (λ) [41].

2.2.5 INFLUENCE FACTORS OF PERFORMANCE

2.2.5.1 Influence of Temperature

Both the temperature and pressure of operation of the cell have a significant influence on its performance. The effect of temperature on performance is illustrated in Figure 2-9 [42] for the temperatures 50 to 95°C at a pressure of 5 atm. The slope of the linear region of the cell potential versus current density plot decreases, which is indicative of a lowering of the internal resistance of the cell. This decrease is predominantly due to the decrease in ohmic resistance of the electrolyte. The mass transport limitations caused by diffusion of reactants through the PEM assembly to the active Pt sites, the movement of protons from the anode to the cathode and the removal of product water is also reduced with the increase in temperature.

2.2.5.2 Influence of Cathodic Reactant Composition and Pressure

For terrestrial applications, the source of oxygen is air, whereas for extraterrestrial (space, underwater) applications pure oxygen is used. Experiments using both these gases in single cells operating at pressures from 1 to 5 atm show the significant influences of mass transport phenomena in the cell. Figure 2-10 [43] demonstrates the effect of pressure at 50°C on the cell potential versus current density plot using H_2/O_2 and H_2 /air as reactants.

Two effects are apparent on changing over from oxygen to air as the cathodic reactant:

- the slope of the linear region of the V-I plot is 50% higher, and
- deviation from the linear region is visible at lower current densities.

In the higher-temperature fuel cells (PAFC, MCFC, SOFC), the oxygen gain in potential is constant at all current densities in the linear region, and thus the slopes of the V-I plot are the same with H_2/O_2, and H_2 /air as reactants. The dependence of the slope of the V-I plot on the oxygen partial pressure is indicative of mass-transport limitations, which also cause a linear variation of V with I at lower current densities. It is generally accepted that there is a 'nitrogen barrier layer effect', which causes this mass transport limitation. The second effect, i.e. deviation from the linear region of the V versus I plot at lower current densities with air, is clearly due to the effect of oxygen partial pressure. Figure 2-11 [44] shows the effect of parasitic losses for air compression on performance efficiency.

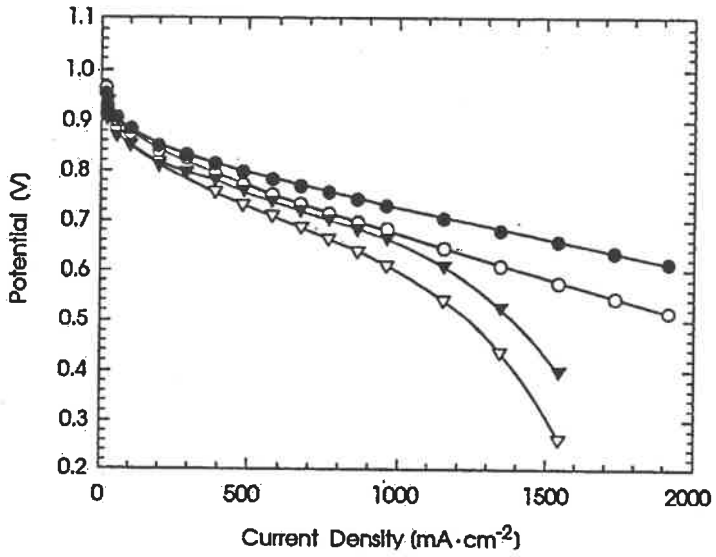

Figure 2-9 Effect of Temperature and Reactant Gas on the Performance of a PEMFC, Pt loading of electrodes 0.45 mg/cm2, Dow membrane, 5 atm. (●) 95°C oxygen (o) 50°C oxygen, (▼) 95°C air, (∇) 50°C air [42].

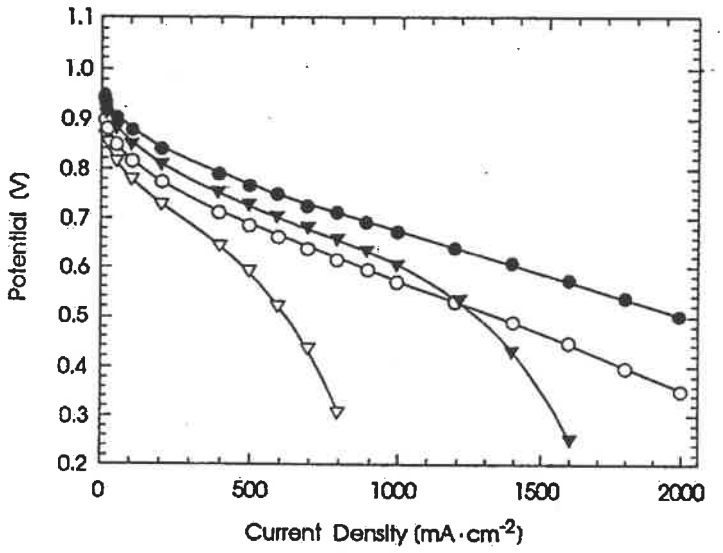

Figure 2-10 Effect of pressure and reactant gas on the performance of a PEMFC. Pt loading of electrodes 0.45 mg/cm_2, Dow membrane, 50°C. (●) 5 atm, O_2 (o) 1 atm, O_2 (▼)5 atm, air (∇) 1 atm, air [43].

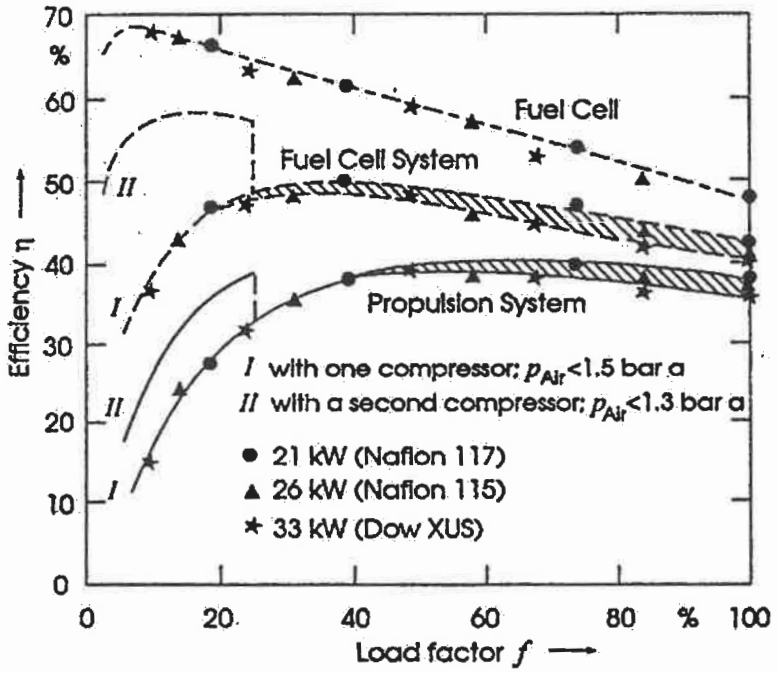

Figure 2-11 Performance losses in a PEMFC with varying load factor [44]

2.2.5.3. Influence of CO in the Fuel Gas

One of the problems with methanol-water reformers is that the reaction is often not complete, leaving small concentrations (approximately 1%) of carbon monoxide in the fuel stream. This carbon monoxide is an extremely effective poison for the fuel cell catalyst. Even a few parts per million CO produce a substantial degradation in fuel cell performance, particularly at high current densities [45, 46] (see Figure 2-12 [47]).

One approach to solve this problem is to reduce the carbon monoxide content of the reformate. This has been achieved by selectively oxidizing the CO to CO_2. To achieve this, the reformate passes through a small reactor containing a platinum catalyst. The injection of a small amount of oxygen or air into this reactor causes a significant reduction of the CO content with relatively little hydrogen consumption [48] (see Figure 2-13 [49]).

The removal of CO in the reformate by partial oxidation to below shift-equilibrium levels may be thwarted by a reverse water-gas shift of reformate, i.e. the formation of a few ppm of CO from CO_2 and H_2 on the anode catalyst, which causes poisoning.

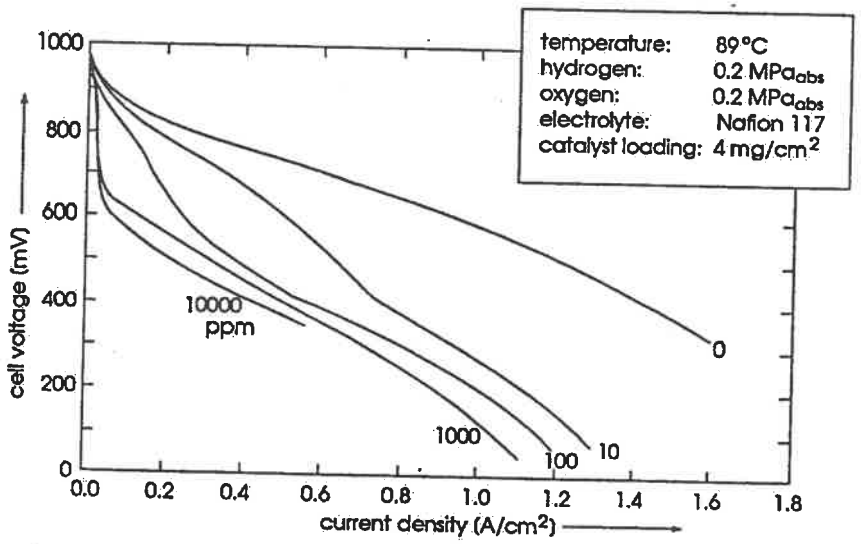

Figure 2-12 Influence of CO on the V-I characteristics of a PEMFC Single Cell [47].

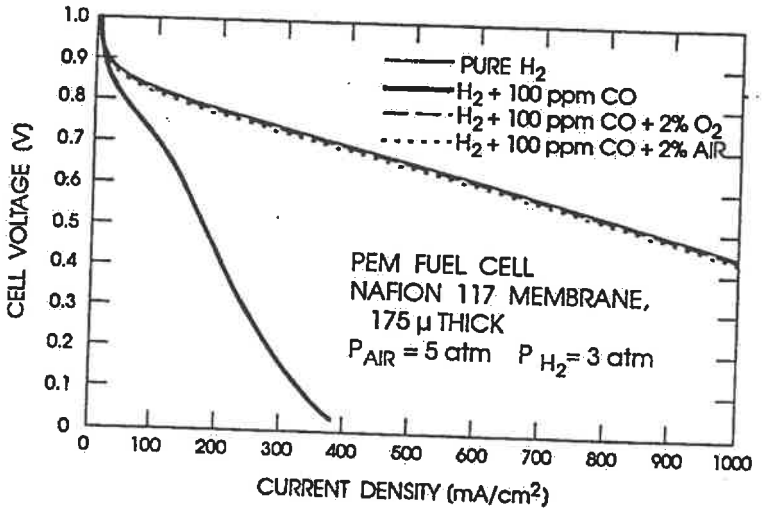

Figure 2-13 Residual catalyst poisoning by trace amounts of CO with/without injecting ~ 2% air into the fuel feed stream [49].

2.3 APPLICATIONS OF PEMFC

2.3.1 Transportation application

PEMFC has been believed to have significant advantages over the PAFC system when both used in transportation application:

- Reduced weight and size, due to high current density output.
- Fast start up from room temperatures and operation at 80-100°C.
- Lower cost over a longer operational life span.
- Operation on air (tolerating the CO_2) and simple reformates.
- The immobilized electrolyte should make the stack design (sealing) easy.

The principal difference to the alkaline system is that the proton (H^+) is the migrating species and the water is produced at the cathode (oxygen electrode). With the PAFC fuel cell it shares the possibility to use CO_2-containing hydrogen as fuel gas. However, there are also serious disadvantages that may not be easily eliminated:

- A high sensitivity to a few ppm CO in the fuel, requiring extreme cleaning efforts.
- The high cost of the platinum, which is used at the 4mg/cm^2 level a few years ago. But now at the 1-0.1mg/cm^2 level.
- The high cost of the membrane in spite of great efforts to lower the price.

- The system must be pressurized, which leads to inefficiencies on the air side.
- The water content of the fuel gas must be kept high to prevent dehydration of the membrane and an increase in resistance.

The high loading problem has been solved at the Los Alamos Natl. Laboratory: in experimental cells the Pt-level has been lowered to 0.1 mg/cm^2 with a tolerable loss in cell performance [50]. The other points have been the subjects of development efforts: an oxidizer must be added to the fuel to eliminates the CO. Presently just air is added to the fuel to reduce he CO from about 0.5% to a few ppm. A turbocompressor pressurizes the air to at least 3 bars. An additional water removal system must be designed, because extra water is added to the gas entering the stacks for keeping the humidity above 400 mmH_2O [51].

The very high current densities, which are possibly drawn from the PEM electrodes led to suggestions to operate without a booster battery (Ballard). However, there is a trade-off between power output, need for expensive accessories, size and above all, cost. Heat management is also an important point.

It should be recognized that the idea to use an organic ion exchange membrane as solid electrolyte and separator in an electrochemical cell was first described in the early 1960's by W. T. Grubb of General Electric Co. and that it took nearly 40 years until the first practical applications were found. The use in vehicles was always contemplated, research

into membrane cells for space applications was a continuous project for General Electric Co and NASA Space efforts, but the key question was the reliability and the absence of 11 pinholes" in the membranes. The situation changed when DuPont Co. introduced t6e NAFION membranes. Further progress after the introduction of new membranes by DOW led to the general decision that electric vehicles should use PEM-Fuel cells [52]. The Company that was most active in the field and practically assured a covering of the field was BALLARD in Vancouver, BC, Canada.

2.3.2. The Ballard PEMFC Transportation Activities

The main Canadian expertise in the PEMFC technology rests with Ballard Power Systems. Its PEMFC technology is considered by many to be the world-leading technology. Ballard in conjunction with the Province of British Columbia and the Government Of Canada has begun a program to develop a commercial transit bus powered by Ballard's PEMFC. The bus was designed to operate solely on the Fuel Cell System. The goal is to demonstrate the same performance capability as the corresponding commercial Diesel bus. The hydrogen is supplied from 6 steel cylinders stored under the bus floor.

The Ballard PEMFC Bus Program consists four phases:

Phase 1: Proof of Concept with a 20 passengers transit bus, with traction power only from fuel cells, and with a 160 km/100 mile range.

Phase 2: A Prototype 40 passenger transit bus with a 280 km/175 mile range.

Phase 3: A Demonstration Fleet, based on a 75 passenger bus with fuel cell traction power and regenerative braking and with a 400km/250mile range.

Phase 4: Commercial Production of a 75 passenger bus with a 560 km/350mile range.

The phase 1 Transit Bus, the world's first fuel-cell powered ZEV (Zero Emission Vehicle) bus, was completed on schedule and within budget. This proof-of-concept vehicle is meeting its performance targets and is providing valuable data for the subsequent development phases. The fuel cell bus was designed and built, starting with a National Coach Corporation Model RE-32 bus, by Ballard Power Systems (fuel cell array and associated equipment) and SAIC Canada (systems integration etc.) with valuable assistance from BC Transit. Note that this bus relies solely on the Ballard PEFC stacks for its motive power; lead/acid batteries provide auxiliary power for start-up, lights etc. The bus power plant consists of 24 of the 5 kW stacks arranged in a series-parallel string providing 120 kW of gross power. Air is supplied by a combination of a motor-driven automotive supercharger and a turbocharger driven by the air exhaust stream. The fuel is compressed pure hydrogen gas, stored in 3000 psig in transportation- approved fibreglass-wrapped aluminum cylinders, is the on-board fuel. This storage option does, however, result in a limited but still useful range of about 160 km/100 miles. Ballard also has finished the phase 2 to 4 in the last few years. In 1999 the final commercial PEMFC Bus has already been used in Vancouver, in Los Angeles, and in Sacramento, California.

Ballard has also collaboration agreements with different auto manufacturers with specific manufacturing expertise and an intimate knowledge of end-users. Ballard's cooperation with Daimler-Benz started in 1993 to develop a high Power density PEMFC fuel cell stack using methanol and related manufacturing processes. General Motors is using Ballard Fuel Cells to develop a methanol fueled hybrid electric vehicle.

Figure 2-14 Picture of the Ballard PEMFC Bus operated in Chicago (www.ballard.com).

2.3.3 Daimler Benz NECAR II [53]

2.3.3.1 Hydrogen/Air Systems

Daimler Benz presented in 2000/2001 its new fuel cell car NECAR IV & V, which attracted much international attention. The electricity needed to drive the motor is produced on board by two fuel cell stacks with a total electrical power of 50KW. These stacks are fed by hydrogen gas from pressurized gas tanks that are positioned on top of the car. The overall efficiency of the car is high enough to drive six occupants for more than 250 km with a single tank.

The power density of the complete fuel cell system is rather high: The weight/power ratio is 6 kg/kW. The entire system fits behind the last two seats in the bottom of the car. It comprises two fuel cell stacks, 25 kW each. The development of these stacks, which were constructed and developed by scientists and engineers both from the Canadian company Ballard Power System and from Daimler-Benz is a real technological breakthrough: For the first time a power density for a full scale PEMFC stack of more than I kW/l has been demonstrated. In comparison to the previous Ballard Mk5 stacks, the power density has been increased more than six fold. Also the tie-rods are integrated into the stack and the end plate design has been improved.

There are two reasons that made this possible:

1. Careful design of tile bipolar plates, i.e. reduction of their thickness and proper flow-field design, and
2. Excellent current/voltage characteristics of the single cell.

Under operating conditions at a cell temperature of 80°C and a pressure of 2.6 bar, at a current density of 0.7 A/cm^2 a voltage of 0.7 V is still achieved with hydrogen and air as oxidant (Figure 2-16). This performance is achieved with a low catalyst loading of the electrodes and with a preparation method for the electrodes that is suitable for mass production,

This described the status oil hydrogen/air-systems at Daimler-Benz. Of course, buses are another excellent opportunity to realize vehicles for environmentally sensitive areas. Although hydrogen vehicles have many advantages, i.e. they are real zero-emission-vehicles, their usefulness might still be hampered by the low volumetric energy density of the hydrogen. Even with the very high efficiency of fuel cell systems their range is still limited. Also the infrastructure for hydrogen is still missing and might not be as easy to implement as for a fuel that is liquid at room temperature.

2.3.3.2 Methanol/Air-Systems

For that reason Daimler-Benz is evaluating alternative fuels for fuel cell systems, such as methanol. The first approach here is to keep the hydrogen consuming fuel cell and to generate the hydrogen on board i.e. in a steam reforming process. Thus the research at Daimler-Benz is focusing on fuel cell systems with methanol reforming. Here promising results in component development and system research have been already achieved.

In such a system the methanol first has to be vaporized. Then it enters the reformer. The reformate gas contains besides the hydrogen approximately 25% of carbon dioxide and 1 to 3% of carbon monoxide. The latter is a very potent poison of the platinum catalysts in the fuel cell. For that reason this gas has to be cleaned in some way, i.e. in a selective oxidation process. In that way the carbon monoxide content can in principal be reduced to an extremely low level.

Nevertheless new catalysts for the fuel cell have to be developed which can tolerate carbon oxide and to a certain amount also of carbon monoxide. Carbon dioxide can also be harmful cause of the reversed water gas equilibrium. The research effort has made available excellent catalysts, which can tolerate carbon monoxide up to 100 ppm without significant performance losses (Figure 2-17).

Figure 2-15 Daimler Benz fuel cell car NECAR IV & V (www.ballard.com)

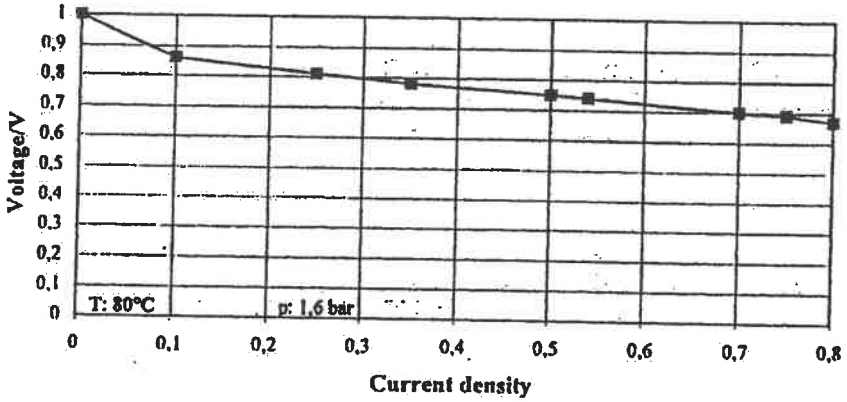

Figure 2-16 Polarization characteristic of a single cell in H_2/air.

T_{cell}: 80°C; Pressure 2.6 bar [53].

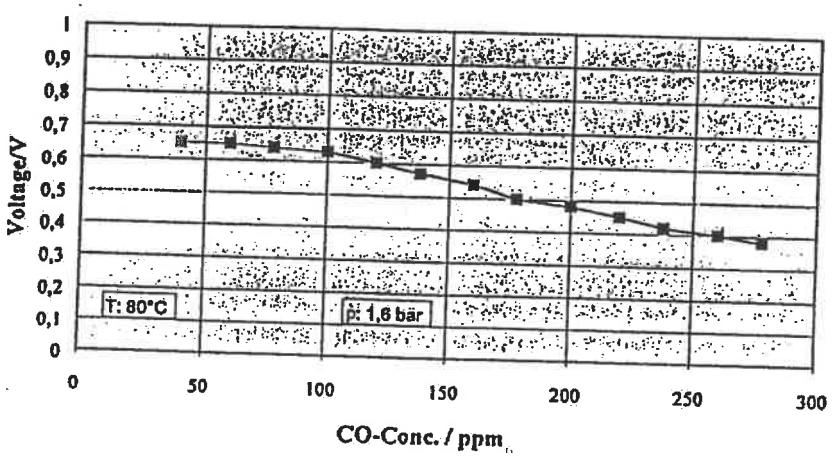

Figure 2-17 Carbon monoxide tolerance of Dalmer-Benz electrodes at a fixed current density of 0.9A/cm^2 [53].

2.3.4 General progress in PEMFC transportation application [54]

The development of a commercially viable PEMFC transportation application is a system design exercise, which is dependent on the application, available fuel, oxidant supply, available fuel cell hardware and related system components. The overall system must be revaluated and design compromises made to achieve an optimal design based on functionality, reliability, manufacturability and cost. There has been a general trend toward reducing the number of required system components by incorporating system requirements into the fuel cell stack. This has included all increased focus on fuel cell operation with zero humidification, direct fuels and oxidant operation at ambient (or near ambient) pressure. A significant portion of research and development effort of different group is directed towards these areas, especially Ballard's PEMFC. The following sectors will discuss progress in some of these key topics during past few years.

2.3.4.1 Reformed Fuels

For applications requiring reformed fuels there are generally performance issues with CO, CO_2 and residual methanol for methanol reformate which have to be dealt with. Improvements in the development of fuel supply systems (reformer, shift reactor and CO selective oxidizer) has been able to reduce CO levels to < 50 ppm and in some cases to a few ppm. In earlier work done at Ballard [55] it was found that a small air bleed was able to reduce the CO content of the fuel and subsequent work was directed at integration of

selective oxidation with the fuel cell stack and providing the air bleed directly within the stack [56-57]. With the improvements in fuel processing and a small air bleed to the fuel cell a remaining performance issue is due to CO_2 and residual methanol in the case of methanol reformate. Work with an air bleed was done as early as 1988 by Ballard. The use of an oxygen or air bleed directly into the anode gas stream just before it enters the anode chamber of the fuel cell has also been described elsewhere in the literature [58]. The reaction of CO2 at catalyst surfaces within anodic potentials can form CO-like adsorbed poisons. The short term goals for fuel cell anode development are to reduce the CO_2 induced losses on reformate operation with an air bleed. The long-term goal is to improve both intrinsic (no air bleed) CO and CO_2 catalyst tolerance in order to eliminate the use of an air bleed altogether.

Ballard has developed important diagnostic tools for understanding and determining performance sensitivity to reformate. Such diagnostics permit the assessment of the effects of changes in catalyst, electrode structure, operating conditions and cell design on reformate tolerance. In collaboration with Johnson Matthey significant progress has been made in the development of more reformate tolerant catalysts and electrodes. Addition of a deliberate gas-phase layer to the active catalyst layer improves the CO air bleed sensitivity (lower air bleed required) and significantly improves lifetime degradation in the presence of an air bleed [59].

2.3.4.2 Direct Methanol Fuel Cell

General interest in the direct methanol fuel cell is increasing largely because of general technical progress, the potential of system simplification and increased system power density, and its potential application in the automotive area. However, general problems still exist with the technology, particularly with respect to methanol cross-over and high anode overpotentials [60-61]. Performance levels achieved on air by Ballard and others are now in the range of 180 MW/cm^2 to 250 MW/ cm^2 [62-64] considered to be the threshold value for introduction into these types of applications. However, for practical applications low oxidant stoichiometries on air and high fuel utilization will also be required. The air stoichiometry required for stable operation is higher than that required for conventional hydrogen/air fuel cells because of methanol crossover. Figure 2-18 [65] shows a plot of cell voltage versus percent fuel utilization for the direct methanol fuel cell operating at constant current density. Fuel utilizations in the range of 75 % to 85% have been achieved with the primary reason for fuel utilization loss being methanol crossover. Special diagnostic techniques have been useful in understanding these effects and giving a new insight into the direct methanol cell.

2.3.4.3 Unit Cell / Flow Field Development

Prior art flow field design was exemplified by that used by the General Electric Company and Hamilton Standard and consisted of a number of parallel channels formed in an

electrically conductive plate [66]. This type of flow field resulted in water coalescence in the channels and poor reactant gas distribution over the active area. Current preferred now field technology for the PEMFC is based on grooved continuous serpentine flow fields through which gaseous reactant and liquid coolant now. Some of the fundamental principles of this type of flow field have been developed by Ballard [67-68] and have resulted in significant performance improvements for the PEMFC. Specifically, better reactant distribution over the active area and from cell to cell in the stack, improved water management, and less scale up effects (number of cells, cell area). Again, work done at Ballard in the design of liquid coolant flow fields for liquid distribution and commensurately cell temperature distribution [69-70] has resulted in significant performance improvements. These flow field designs have much better thermal management and control of temperature profiles over the active area.

Some newer approaches to now field design for the PEMFC have been based on the use of porous components in which the reactant gas is forced to flow laterally through the component. This has been successfully demonstrated at Ballard [71] and later by others [72] using an interdigitated flow field. Reactant gases are delivered down inlet manifold channels and forced through the porous gas diffusion electrode to exit manifold channels. A further modification [73] has been to incorporate flow field channels directly into the porous gas diffusion electrode. For the PEMFC there have been some issues with these approaches with respect to channeling of reactant gas flows and poor distribution due to water coalescing and blocking regions. Sealing concepts that use gasket materials to

directly seat against the solid polymer membrane have been successfully developed by different groups [74-75].

It is important to maximize active area in the cell design to reduce effective component cost and increase power density. More advanced Ballard cell/stack design(s) for the PEMFC [76-77] have achieved high utilization of the cell area (> 80%). Area utilization is defined as the ratio of electro-active area to the cell envelope area. In addition, these hardware have much better thermal management and control of temperature profiles over the cell active area. High power densities in excess of 700 W/kg and 1000 W/l have been achieved for the PEMFC on air and hydrogen at practical operating conditions [78], and scale up issues from single cells to larger 150 cell stacks have been minimal. In general, advanced Ballard stack designs now meet or exceed the power density targets identified by the automakers, by the US Department of Energy, and by the Partnership for a New Generation Vehicle (PNGV).

2.3.4.4 Advancement water management towards zero humidification

Effective water management in the solid polymer fuel cell has a major impact on cell performance and lifetime. Peak fuel cell power is achieved typically at higher current densities at which performance is limited by mass transport issues usually associated with water management. Cell performance may be adversely affected by the formation of liquid water, the dilution of reactant gases by water vapor or by dehydration of the

solid polymer membrane. Fuel cell water management can be achieved by a number of approaches, which include system design, stack operating conditions, cell/stack hardware and the membrane electrode assembly design and its components. These approaches need to be evaluated with respect to the overall system performance, complexity and cost [79]. Novel methods of water management have been developed at Ballard such as the "anode water removal approach". By appropriate cell, membrane electrode assembly (MEA) and stack design, liquid water accumulated in the cathode catalyst layer can be drawn by a forced concentration gradient across the membrane to the anode and removed in the fuel stream. This method of water management can significantly reduce parasitic loads and performance issues with the oxidant side of the fuel cell. It can also be used as a fuel cell diagnostic technique and it can lead to new approaches to fuel cell system design [80-81].

A number of water management strategies have been considered but perhaps the most easy and reliable methods to implement are those based on flow field design and operating conditions. The benefits of these types of water management strategies are largely dependent on the use of a continuous flow field design. They have included the use of pressure drop and temperature rise between the inlet and outlet of the flow field to increase the water vapor carrying capacity of the gas streams. The use of pressure drop or increased gas flow velocity to evaporate liquid water and/or assist liquid water to become entrained into the gas stream usually has an associated system parasitic load because the energy required for gas delivery is directly related to pressure, volume flow rate and

pressure drop. For this reason the use of temperature gradients has been preferred. More recently, these flow field water management approaches in conjunction with appropriate operating conditions have allowed fuel cell operation with zero humidification [82].

2.3.4.5 Development of higher/ambient pressure operation

Performance sensitivity to reactant pressure has been tested over a wide range of pressure. This has been modeled mathematically using Butler Volmer kinetics or similar equivalent forms. The measurement of voltage gain with oxidant pressure has been found the reaction order with respect to oxidant pressure is near unity, i.e., first order. Empirical fitting of the observed cell voltage gain with both the oxygen and hydrogen pressure gains has led to the predicted voltage gain for a PEMFC as a function of pressure shown in Figure 2-19 [83]. These predicted gains have shown a good fit with experimentally measured data up to 500 psig. The gains due to hydrogen partial pressure are assumed not to be kinetic (i.e., purely thermodynamic or "Nernstian"), mass transport issues have been minimized, and the catalyst temperature has been assumed to be 100°C. Performance gains with oxygen pressure in the range of 31 to 39 mV per doubling of pressure above 100 psi are achieved. At lower pressures the water vapor dilution effect causes a steeping of the gain with respect to total pressure.

The improvement in performance gained by increased pressure have to be evaluated from an overall system point of view since energy is required to pressurize the reactant gases.

Optimal pressure must take into consideration system performance, efficiency, cost, operating and maintenance costs, weight and size.

Initial work in 1992 at Ballard in the area of ambient pressure operation focused on cell designs that were self-regulating without any of the system requirements of conventional fuel cells [84]. Continuous fuel cell operation over 25,000 hours has been achieved without forced airflow, without humidification and without active cooling. Lightweight fuel cell systems in the 25 to 500 watt range have been developed which operate with a fuel source and at pressures approximating ambient air. This technology has the potential to replace batteries in some applications as a result of tile potentially superior energy density and tile possibility of mechanical refueling.

2.3.4.6 Low cost electrode and membrane development

Initial electrode development of PEMFC of transportation application focused on improving performance and lifetime of high loaded Pt black electrodes. This was to provide a stable baseline electrode for stack and system development. In March of 1994 Ballard and Johnson Matthey signed a joint collaboration agreement to undertake low cost electrode development. The goal of this collaboration was to develop and implement high performance catalyst/electrodes, low catalyst loading, and MEA manufacturing technology, i.e., into Ballard production fuel cells [85]. Major activities in this program have included the development of advanced catalysts with high surface area, carbon

supported catalyst development, the design of low catalyst loading electrode structure to maximize effective catalyst utilization and to minimize losses resulting from mass transport effects.

Total catalyst loadings in the range of 0.6 to 1.0 mg/cm^2 have been shown to give equivalent performance to higher unsupported platinum black loadings in the range of 8.0 mg/cm^2. In general, the performance, reproducibility and lifetime of these printed low catalyst loaded electrodes meet present to midterm requirements for commercial fuel cell stacks in applications ranging from transportation to stationary uses. Further development work at Ballard is focused on integration of this low cost electrode technology with other low cost fuel cell components while maintaining reproducibility, reliability and lifetime. Additional cost reduction is anticipated through further significant reductions in the catalyst loading and improved performance through improved MEA and cell design. Although very low catalyst loadings (< 0.1 mg/cm^2) have been demonstrated by Ballard and others, its use in practical applications and with reformate fuels has yet to be proven.

Although perfluorosulfonic acid membranes show good performance and are noted for their stability in electrochemical devices the current price of 50-70 \$US/ft^2 is unacceptably high for PEMFCs to be commercially viable in most markets. Recent work of membrane has concentrated on ion-exchange membranes based on trifluorostyrene and substituted trifluorostyrelle copolymeric compositions [86-87]. The development of this new family of polymers has been previously discussed in a review of advances and

activities in membrane development [88]. To date, these third generation membranes (BAM3G) have demonstrated tens of thousands of hours of cumulated performance in a variety of commercial Ballard fuel cell hardware. The performance of the BAM3G membrane is comparable and, over 700 ASF, better than the best performing perfluorinated membranes. Membrane work now is largely focused on optimization and integration of the BAM3G membrane into various stack hardware to suit specific applications. Polymer and membrane production has reached the pilot plant stage.

2.3.4.7 Low cost bipolar plate development

At Present, most proton exchange fuel cells use machined graphite plates for current collection/distribution, thermal management and gas distribution. Other candidate materials for bipolar plates in PEMFC stacks such as conductive plastics, plated metals such as aluminum and stainless steel are under consideration [89-90]. In general, these materials are inferior to graphite plates due to contact resistance and potential problems with longevity. Graphitized or at least high temperature heat-treated carbons and several types of resin used as binders for the carbon or graphite have been found to be stable in the phosphoric acid fuel cell (PAFC) and PEMFC environments. Ballard has developed low cost, lightweight graphite materials that yield comparable Performance to the expensive high purity graphite bipolar plates commonly employed [91]. Other approaches developed by Ballard include embossed, laminated and stamped materials [92-93].

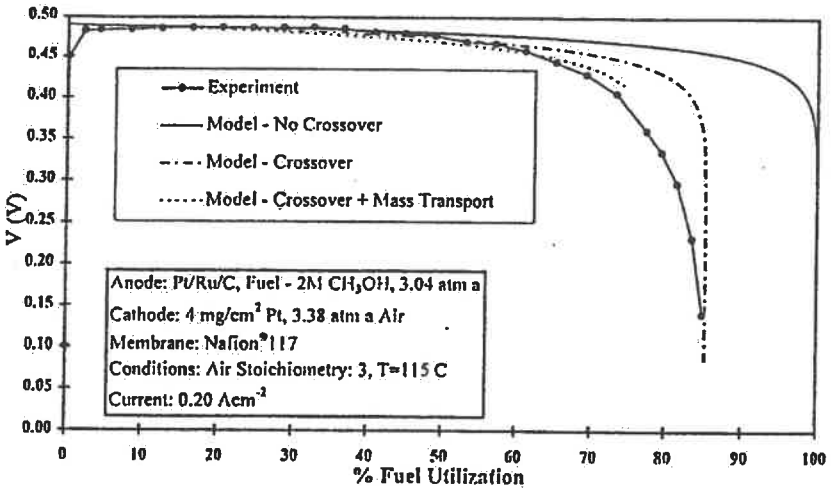

Figure 2-18 Effect of methanol crossover on DMFC fuel utilization [65].

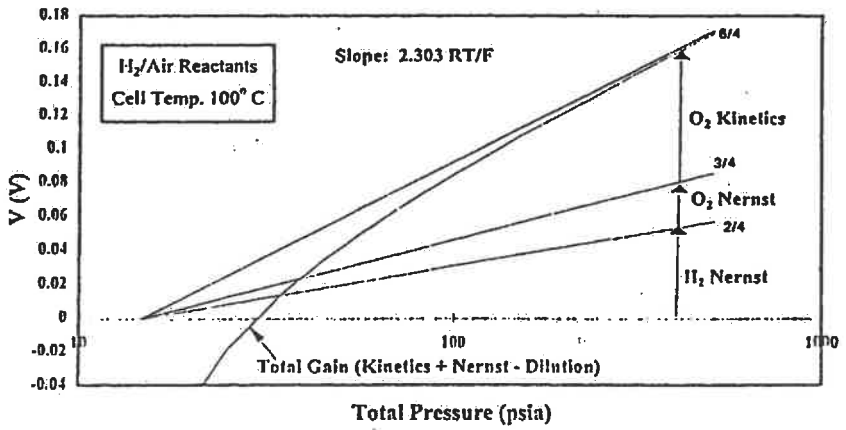

Figure 2-19 Effect of pressure on PEMFC performance [83].

2.3.5 Portable Application

Although PEMFC technology has advanced substantially since the Gemini space program of the mid 1960s, small devices have not received as much attention. Much of the interest has focused on developing multi-kilowatt PEMFC power plants for high power applications in automotive and stationary energy conversion systems. Miniaturization of the PEMFCs for portable and mobile applications, that require low power has only recently received attention [94-96]. The main application of these portable PEMFC include telecommunication and medical mini-equipments applied on human body. The simple summary is given as following.

2.3.5.1 Portable application in telecommunications

The importance of portable emergency power to handle power stoppages has been increasing, because telecommunications equipment is installed in many users' buildings. To date, portable engine generators have been used as the emergency power source for small and medium-sized telecommunications equipment, but they are noisy and produce toxic exhaust gas. Thus, a portable indoor-use emergency power source that generates power quietly and cleanly is desirable.

In U.S.A Motorola Labs (Tempe, AZ) and Los Alamos National Laboratory (Los Alamos, NM) have recently developed a miniature fuel cell that may one day replace the

traditional batteries now powering everything from cellular phones and laptop computers to portable cameras and electronic games. The cell - measuring about 1 in^2 and less than 0.10 in thick - is powered by liquid methanol and can easily be installed in electronic devices. Each cell has an energy density 10 times that of conventional rechargeable batteries. At the same time, when the cells are in production in a projected three to five years, they will be significantly lighter and less expensive than rechargeable batteries. While hydrogen has been the most common fuel cell element, methanol has more recently been considered an alternative fuel because it has a higher energy density than hydrogen.

The new PEMFC uses a reservoir of inexpensive methanol that produces electricity when combined with oxygen. Since fuel cells have low-voltage outputs, typical designs normally would require stacking several cells together to increase voltage. However, Motorola labs has designed circuitry that efficiently converts the low voltage to the higher voltage required to replace conventional batteries and directly drive portable electronics. The cell converts the energy in methanol directly to electricity and operates at normal room temperatures. The cell's simplified design eliminates the need for air pumps, heat exchangers, and other complex devices that previous fuel cells required and that excluded them from use in small, portable electronic products.

On the same time some Japanese group also focused on portable PEMFC applied on telecommunications. Two types of recently developed portable fuel cell systems are

described in Japan in some literature [97-99]: one with dc output and one with ac output. The systems consist of a small fuel cell stack, two hydrogen cylinders, and a power converter. They are completely contained in one cabinet that can be separated into two sections, making it easy to move. Each system can generate power within 5 min of the start-up time and can supply between 200 and 250 W of power for more than 6 h using two 6.7-liter hydrogen cylinders. The dc-output system supplies dc 55 V for telecommunications use and dc 12 V for general use, and the ac-output system supplies ac 100 V. The output power of these systems can be increased by operating multiple units in parallel. These systems generate power quietly and cleanly, and are thus suitable for use as an indoor emergency-power source for telecommunications use and for various types Pf equipment.

The design of the fuel cell system for a portable emergency power source should be simpler than that of a large-scale fuel cell, which includes a reformer for converting natural gas into hydrogen and a heat exchanger for exhausting heat to the atmosphere. The start-up time should be shortened to a few minutes for easy use. These power sources are generally used for numerous short periods, unlike large-scale fuel cells that must generate power continuously for a long time. They should run stably for many cycles, but may be required to generate power suddenly in an emergency after not being used for a long time. Therefore, their long-term reliability should be evaluated.

2.3.5.2 Portable application in medical equipments

In assessing the applicability of a mobile power source, cost and energy density are not only two of the characteristics that need to be considered. Safety, hand portability, and operational features are equally important. Most conventional batteries suffer from environmental problems. Higher energy density primary batteries, such as lithium batteries, present a considerable safety risk as a result of cell reversal caused by uneven discharge in series connected cells, whereas secondary batteries require long recharge times with a rapidly declining capacity on deep discharge.

An attractive alternative power source is under development, which relies on small air-breathing PEMFCs fueled by gaseous hydrogen. The reaction products are environmentally benign oxides and water. The power source will be designed to operate at near ambient temperature. Fuel cell product water is stored in porous carbon elements and removed with the oxygen-depleted air by evaporative cooling or released from the carbon structure as liquid water. Recovery of the water as a liquid for use in the hydrogen generator is possible, but adds to the complexity of the device. Such clean device is especially important to some medical equipment.

Thus small, lightweight PEMFC power sources for total artificial hearts (TAH), left ventricular assist devices (LVAD), and other medical products are under development in Japan and U.S.A. The new power source will provide 2 to 3 times the capacity of

conventional batteries. The implications of this new power source are profound. For example, for the Heart-mate LVAD, 5 to 8 hours of operation are obtained with 3 lb of lead acid batteries. With the same weight, as much as 14 hours of operation appear achievable with the PEMFC power source. Energy densities near 135 watt-hour/kg and 137 watt-hour/L are achievable. These values significantly exceed those of most conventional and advanced primary and secondary batteries. The improvement is mission dependent and even applies for the short deployment cited above. The comparison to batteries becomes even more favorable if the mission length is increased. The higher capacity requires only replacement of lightweight hydride cartridges and logistically available water. Therefore, when one spare 50 L hydride cartridge weighing 115 g is added to the reactant supply the energy density of the total system increases to 230 watt-hour/kg.

The PEMFC power source is comprised of two main subsystems: 1) the PEM fuel cell assembly and 2) the miniature hydrogen generator. In addition to the fuel cell and hydrogen generator, ancillary components will include a microprocessor based controller and power conditioner, as well as a residual capacity indicator. A small rechargeable battery provides redundant power during cartridge replacement and initial start-up.

2.4 Electrocatalysts

2.4.1 Electrocatalysis and Electrocatalysts

Chemical catalysis is a well-known phenomenon. A given reaction occurs at a different rate upon different substrates, and the action of the substrate in changing the rate is called catalysis. The substrate itself suffers no change.

The situation is similar with reaction on electrode. What the term electrocatalysis usually means is the variation of the rate of an electrochemical reaction with change of substrate at the same over-potential. These substrates are electrocatalysts. In practical they are used only of those catalysts that can promote a desired reaction on a technically interesting scale. For low-temperature fuel cell, adequate electrocatalytic activity of electrodes is an essential consideration.

The electrocatalytic activity of an electrode depends on a number of properties of electrocatalyst. The three most important functions are:

- Chemisorption of the reactant at the electrode surface
- Facilitation of the interface reaction by the dissociation of the adsorbed molecules into atoms or by the cleavage of the reactive groups
- Lowering of the activation energy of charge transfer

In addition, the affinity of the electrode for the components of the electrolyte has a consider influence and the electrode must possess good electronic conductivity.

In theory the best way of comparing the velocity of various reactions is to extrapolate each to equilibrium potential ($\eta = 0$). Thus electrocatalysis is measured by i_0 (exchange current density), the equal (and opposite) rates of the electron emission and the electron acceptance when the electrode is at the equilibrium potential for the reaction concerned. In practice, the term electrocatalysis has a relative rather then an absolute meaning. One electrode is regarded as being more electrocatalytically active then another when at a constant over-potential a given reaction proceeds faster on one than on the other. Alternatively, a comparison can be made at constant apparent current density. The slope of the E-logi relationship is also of paramount important in appraising electrode performance. Some electrode may be poor electrocatalysts in terms of exchange current density but good electrocatalysts at high over-potentials if the slope has an exceptionally low value.

However, at the very high currents usually required in practical applications, factor other than strictly electrochemical ones contribute to the enhanced performance of electrodes (such as the cost per unit product in the industry).

2.4.2 Electrocatalysts in H_2 anodes of PEMFC

The heart of PEMFC is the membrane electrode assembly (MEA). This is constructed from the anode and cathode comprising the electrocatalysts bonded to the faces of a solid polymer membrane.

When we chose electrocatalyst, the first consideration is its catalytic ability, the electrochemical stability of the substrate is also important. In this basis the Pt maybe the best catalyst for most anodic and even cathodic reaction taking place in the fuel cells, especially in acidic solutions [100-102]. For fuel cell, the most popular and widely used fuel is hydrogen, so Pt become the first choice, from then on people tried a lot of Pt-alloys [103-105] and other metals, such as various transition metals, Pd-Ag, Raney-nickel [106-111], etc. When Pt used as H_2 anode for PEMFC, it is consist of finely dispersed Pt particles that are deposited on a high surface area support. The support permits greater efficiency in use of the metal by increasing the active metal surface and by facilitating to poisoning. Perhaps the greatest value of a support is that it provides a further control over selectivity [112].

But in the presence of specific poisons such as carbon monoxide, the oxidation rates are noticeably decreased. So a lot of Pt-bimetallic alloys have been developed [113-120].

2.4.3 Reaction mechanism of H_2 anode

Hydrogen is the practical fuel for use in the present generation of fuel cells (especial in PEMFC). Hydrogen has high electrochemical reactivity, the characteristic of hydrogen as an energy carrier has been extensively discussed in the past [121-122]. Also, its reaction mechanisms are well understood, and are characterized by the relative simplicity of its reaction steps, which do not lead to side products. Here we recall this mechanism and hope it will be helpful for us to study other fuels mechanism.

The overall anodic processes are considered to take place in the following partial reaction steps:

(a) Transport of molecular hydrogen to, and adsorption on, the electrode surface

$$H_2 \rightarrow H_{2,\,ad} \qquad (2\text{-}3)$$

(b) Hydration and ionization of the adsorbed hydrogen

- Tafel reaction (dissociation of the molecules into atoms)

$$H_{2,\,ad} \rightarrow H_{ad} + H_{ad} \qquad (2\text{-}4)$$

- Volmer reaction (hydration and ionization at discrete sites on electrode surface)

$$H_{ad} + H_2O \rightarrow H_3O^+ + e^- \qquad (2\text{-}5)$$

- Hydration and partial ionization, proceeding in a quasi-single step (Heyroisky-Volmer mechanism)

$$H_{2,\,ad} + H_2O \rightarrow H_{ad} + H_3O^+ + e^- \qquad (2\text{-}6)$$

$$H_{ad} + H_2O \rightarrow H_3O^+ + e^- \qquad (2\text{-}7)$$

(c) Transport away of H_3O^+ ions

The above division of the possible reaction steps corresponds with the reaction mechanism denoted Tafel-Volmer and Heyroisky-Volmer.

For gas diffusion electrodes, diffusion processes in the pores must always be considered. Because of potential drop in the pores, anodic current continues to increase with rising over-potential until the oxygen-charging region of electrode potential is reached.

2.4.4 Pt-alloys and synergistic effects

Pt is one of the best catalysts for the electrochemical oxidation of hydrogen. In the presence of specific poisons such as carbon monoxide, however, the oxidation rates are

noticeably decreased [123-124]. This has prompted considerable effort to develop an active hydrogen oxidation catalyst that is not affected by CO. Pt combined with other transition metals and oxides [125] have been investigated as CO-tolerant fuel cell anodes. According to these papers, the 8th group metals, Ru, Rh, Ir and Ni, when combined with Pt were all superior to Pt in their performance as anodes in CO-contaminated hydrogen.

Mckee and co-workers have postulated that the increased performance is due to the greater availability of active sites for hydrogen adsorption present on the Pt-transition metal composite catalysts. P.N.Ross and co-working deduced from their studies:

- The enhanced activity of Pt-Rh alloys was not due to a tolerance of the alloy towards CO but was due to an intrinsically greater catalytic activity of the alloy for hydrogen oxidation. This enhanced activity was related to the electronic properties of the alloy, the maximum occurring for an alloy with exactly one unpaired electron per atom.
- The absolute activity of Pt-Ru alloys for the oxidation contaminated hydrogen is a complex function of temperature and electrode potential, the variation of electrocatalytic activity with alloy composition indicates only dilution of the activity of the more active component at 110- 160°C or from 0-0.3V [126].

Recently, the synergistic system is used to explain different kinds of results in electrocatalysis studies [127-128]. A synergistic system in electrocatalysis may be

defined as one in which a mixed material is more effective than either material alone. The characteristic of a synergistic system may be dressed according to the variations of the specific activity (S_0) with the electrocatalyst parameter (e.g. wt%, electrochemically active surface area, etc.). Here, the specific activity is the true activity or the current density at a given overpotential (generally at 0.9v) per unit of true Pt surface area is identified by the H-adsorption area using cyclic voltammetry ($m^2.g^{-1}$). In each synergistic system, the variation in S_0 with the electrochemical surface (S_{pt} in m2.g-1) would indicate evidence of the maximum in the curve S_0 against S_{pt}. The synergistic system will be the product of at least one of these two processes:

- An electronic effect due to the interaction between the dispersed materials and the support. In this case the synergistic effect may induce a decrease in the activation energy or/and the order of the reaction.
- An increase in the active sites at the electrocatalyst surface. In this case, the synergistic effect may induce a non-variation in the activation energy and the order of the reaction.

Identification of the exact process may be achieved by studying the effect of the nature of dispersed materials and the support on the true heat of activation (E_0) and on the order of the reaction. In effect, from the Temkin relation [129-130]

$$E_a = E_0 + \Sigma\, n_i\, q_i \qquad (2\text{-}8)$$

Where E_0 is the true activation energy, n_i the order of the reaction for reactant i and q_i its isothermic heat of adsorption which may be considered as a constant in a first approximation. The variation of Ea with n for the same reaction will give E_0, and q_i and may be used to demonstrate the electronic effect. If no electronic effect is observed, it may be concluded that the synergistic effect is due to an increase in the active sites at the electrocatalyst surface.

CHAPTER 3

EXPERIMENTAL SECTION

3.1 Electrode preparation for half cell

The high surface area working electrodes preparation consisted of different carbon-supported catalysts bonded with 30% (w/w) Teflon powder to form a film. The weight of carbon-supported electrocatalysts is 40mg, the weight of Teflon is 16.9mg. The detailed method is as following: Mold pressing the mixed powders for 5 minute to get a dry film, then cutting it to tiny parts, mixing these tiny parts well; pressing and cutting again, repeating this procedure until the film is very fine and cut it again. Putting these tiny parts on an aluminium sheet into a mould, then pressed it at 280°C under 2 atm for 5 min to get the electrode we need.

As Teflon presents nonwetting electrode/electrolyte interface, we impregnate the electrodes with 0.1-0.5 mg/cm^2 Nafion using a 5% solution of Nafion ionomer (1100 EW) in lower aliphatic alcohol (Aldrich) to enhance the wettability of the electrode/electrolyte interface.

The working electrode geometric area is about 1.3 cm^2. A copper sheet that is a little smaller than electrode in surface area then is attached to the electrode. Between the electrode and the copper we added some conductivity graphite to bind them. A copper

wire is welded to the back of the copper. So prepared electrode is put in a mould, then supported and surrounded by epoxy (adding 20% hard to epoxy) from copper backside. When the working electrode is prepared according to this procedure it has only one surface side that can react in electrolyte. The counter electrode is a platinum plate separated from the working electrode compartment by a fine glass frit. The reference electrode is a standard hydrogen electrode connected with a lugging capillary.

Three series of working electrodes have been prepared:

- The carbon-supported 10% noble metal electrocatalysts electrodes (Pt, Ru, Rh, Ir, Pd).
- The carbon-supported 5%Pt plus each of the oxides (RuO_2, SnO_2, Fe_3O_4, WO_3).
- The carbon-supported 10% binary Pt-noble metal alloys and ternary alloys electrocatalyst electrodes (Pt-Ru, Pt-Rh, Pt-Ir, Pt-Pd, Pt-Co-Cr, Pt-Co-Ni).

All noble metals and their alloys used powder products purchased from E-TEK Corporation. The composition of each series electrode is shown in table 3-1.

Table 3-1: Composition of half cell electrodes

Electrodes	electrocatalysts powder	Taflon powder
Pt/C	40mg 10% Pt/C	16.9mg
Ru/C	40mg 10% Ru/C	16.9mg
Rh/C	40mg 10% Rh/C	16.9mg
Ir/C	40mg 10% Ir/C	16.9mg
Pd/C	40mg 10% Pd/C	16.9mg
Pt-Ru/C	40mg 10% Pt-Ru/C (1:1 a/o)	16.9mg
Pt-Rh/C	20mg 20% Pt-Rh/C (80:20 a/o) + 20mg Vulcan xc-72	16.9mg
Pt-Ir/C	40mg 10% Pt-Ir/C (80:20 a/o)	16.9mg
Pt-Pd/C	20mg 10% Pt/C +20mg 10% Pd/C	16.9mg
Pt-Co-Cr/C	40mg 10% Pt-Co-Cr/C (2:1:1 a/o)	16.9mg
Pt-Co-Ni/C	40mg 10% Pt-Co-Ni/C (2:1:1 a/o)	16.9mg
Pt-Metal Oxides*	38mg 5% Pt/C + 2mg Metal Oxides	16.9mg

*: In this case, we remark it as 5% Pt-5% Metal Oxides. Then for 10% Metal Oxides the amount of Metal Oxides is 4mg, … etc.

3.2 Half cell

The working electrodes were tested in a half-cell system [131-134] as shown as Figure 3-1. The electrolytes are acetals (Methylal, Ethylal, 1,3-dioxolane) solved in various supporting reactant grade solutions of H_2SO_4, $HClO_4$ or H_3PO_4 purchased from Fisher. At first we have tested methylal in different acid (H_2SO_4, $HClO_4$, H_3PO_4), and the concentration range of methylal is 0.01M-2M. After we found that the best acid suit for electrolyte in our testing is 1M H_2SO_4 solutions, we fixed the electrolyte to 1M H_2SO_4 solutions. All of steady-state galvanostatic polarization curves of these three acetals were carried out in 1M sulfuric acid solutions, which are mixed with 0.5M or 1M acetals at different temperatures.

3.3 Polarization curves set up

All of the steady-state galvanostatic polarization results have been achieved PAR a potentiostat/galvanostat Model 273, a 5208 Two phase Lock-in Analyzer, monitored by a PC.

Three temperatures have been used to testing, because of different boiling point of acetals. For avoiding evaporation of acetals, the testing temperature of half cell must be lower than boiling point of acetals, which are 42.3°C for methylal / 88°C for ethylal / 74°C for 1,3-dioxolane.

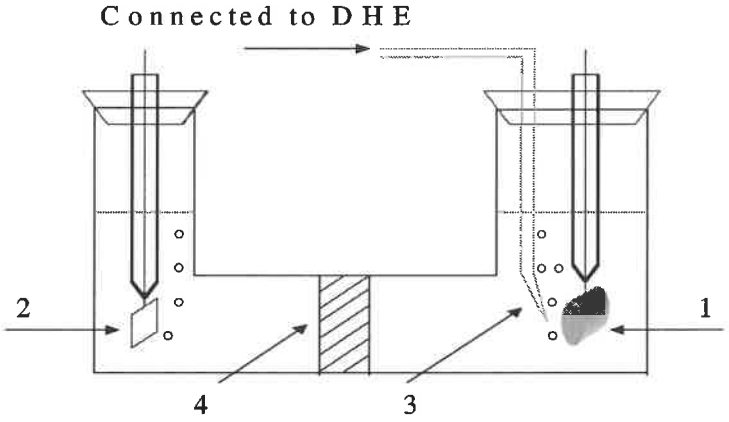

1: working electrode
2: counter electrode
3: luggin capillary
4: porous glass frit

Figure 3-1 Schematic of half cell system

3.4 MEA preparation

Electrodes for fuel cell station testing are fabricated according to the following procedures:

Anodes:

When we begin to prepare the anodes, we first built a standard commercial 2mg/cm^2 Pt-Ru/C (40% Pt-Ru/C, 1:1 a/o) anode. Due to high electrical resistance among our fuel cell system, this standard anode did not perform as we expected. We have to increase anode loading from 2mg to 4mg per cm^2, the details of preparing electrode is described as following. The performance of prepared one is better than commercial one due to higher loading (Figure 3-2).

When we directly applied 4mg/cm^2 Pt-Ru/C (20% Pt-Ru, 1:1 a/o) electrocatalyst powder on blank carbon clothing, we found that the stability of electrode is very bad. Because the electrodes prepared by this way is very thick, the active area is highly hindered by carbon or PTFE (if using it). Therefore some of the electrodes still worked after a long time running on conditioning current density, at the same time other electrodes did not or worked very weakly. For decrease the thickness of electrode, the commercial electrode was taken as base electrode and different electrocatalysts painted on it. The loading of electrocatalysts (base + additive) was still controlled to have value of 4mg/cm^2.

For the reason of convenient comparison, the base electrode is always an ELAT Electrode loading 2.0mg/cm^2 Pt/Ru (40% Pt/Ru/C, 1:1 a/o) purchased from E-TEK Co. The surface area of electrode is 2.25cm^2 (1.5*1.5). Since the final loading of electrocatalysts should be 4.0mg/cm^2, the contribution loading of additive was always 2.0mg / cm^2, therefore how much additive needed in each case can easily be calculated out.

The adding electrocatalysts and base electrocatalyst will be laid on two layers and cannot be mixed together automatically, and the layer we painted will be front one contacted directly to fuel, so this additive layer does not only have function as modifying part but also as active site supplier. For this reason we must use mixed adding electrocatalysts, which should be different electrocatalysts mixed with active site supplier Pt-Ru. In our experiments the one of mixed adding electrocatalyst is 20% Pt-Ru (1:1 a/o) on a carbon supports (Vulcan XC-72) purchased from E-TEK Co., and this is basic one, the amounts of Pt-Ru were varied by mixed with different quantities of other carbon-supported electrocatalysts (Pt-Ir, Pt-Sn, Pt-Pd, Pt-Rh purchased from E-TEK Co.) or various oxides (such as RuO_2 powder purchased from Fisher Scientific Co.). The composition of different electrodes is shown in table3-2, the different composition have been applied so that the added loading of electrodes can be around 2mg/cm^2 for most of them.

Table 3-2: composition of electrodes (surface area 2.25cm^2)

Electrodes	basic added electrocatalyst	other added electrocatalysts
Pt/Ru	20% Pt/Ru: 22mg	Null
Pt/Ru + Pt/Sn	20% Pt/Ru: 11mg	20% Pt/Sn: 11mg
Pt/Ru + Pt/Ir	20% Pt/Ru: 11mg	20% Pt/Ir: 11mg
Pt/Ru + Pt/Pd	20% Pt/Ru: 11mg	20% Pt/Pd: 11mg
Pt/Ru + Pt/Rh	20% Pt/Ru: 11mg	20% Pt/Rh: 11mg
Pt/Ru + Pt(O)x	20% Pt/Ru: 11mg	40% Pt(O)x: 5mg
Pt/Ru + RuO_2	20% Pt/Ru: 17mg	99.9% RuO_2: 4mg
Pt/Ru + Pt/Cr	20% Pt/Ru: 17mg	10% Pt/Cr: 10mg
Pt/Ru + Pt/Cr/Ni	20% Pt/Ru: 17mg	10% Pt/Cr/Ni: 10mg

The mixture of powders is added by 0.1 ml 5% (W/W) Nafion 1100EW (Aldrich) solution and 0.1ml DMF (Aldrich), and then the mixture are agitated in ultra-sonic bath for 5min to totally mix them. After that the mixture is painted carefully on the catalyst side of electrode cloth stated as above. The total loading of anode is still controlled to about 4.0mg/cm^2. The Nafion solution is to improve the three-dimensional reaction zone that also improves the solubility of O_2 and fuel at the interface and bonding between the membrane and the electrodes. DMF can bond electrocatalyst and prevent the breaking of electrode when it is dried.

According to M. S. Wilson's thin film catalyst layers explanation, for increase the contact area between the polymer electrolyte and the platinum clusters, completely eliminating the Teflon component is a good choice. So here we use two group electrodes, one is only Pt-Ru/C that we added 30% PTFE as a binder, another group is Pt-Ru/C + different electrocatalysts that we do not add PTFE as a binder. Therefore we can compare PTFE-included Pt-Ru/C electrode to literature ones that already has a lot of results, meantime the no-PTFE ones can compare to PTFE-included Pt-Ru/C one.

The painted electrodes are re-impregnated with 5% (W/W) Nafion 1100EW solution by a brush coating method. The electrodes are dried in air, after that the electrodes are kept in a vacuum oven for 2 hours at 60°C and then 12 hours at 25°C in order to allow the evaporation of the organic solvents and ensure the homogeneity of the protonic film in the active layer.

Cathode:

The cathode is prepared similarly to anode, but the base is E-TEK ECC carbon cloth electrode (no catalyst) and the painting electrocatalyst is single 60% Pt/C on carbon supports (Vulcan XC-72) purchased from E-TEK Co., the amount of powder is 15mg. Using as high as 60% Pt/C powder is to ensure getting the thinnest layer of electrode. The loading of cathode is also about $4mg/cm^2$.

A single cell assembly (MEA) is prepared by pressing a 12 cm^2 (3*4) Nafion 117 membrane together with the anode and cathode under a pressure of 3000kg at 120°C for 5 min. The pretreatment of membrane is as following:

- Wash in acetone and rinsing by de-ionized water
- Kept in 5% H_2O_2 solution for 1 hour at 80°C
- Rinse with de-ionized water repeatedly
- Kept in renewed 5% H_2O_2 solution for another 1 hour at 80°C
- Rinse with de-ionized water repeatedly
- Kept in boiling de-ionized water for 1 hour
- Kept in 1M H_2SO_4 solution for 24 hours
- Rinse with de-ionized water repeatedly
- Store in de-ionized water

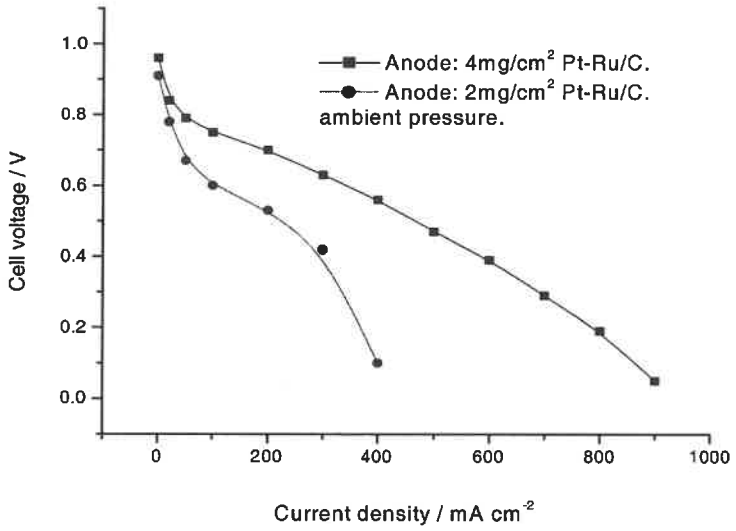

Figure 3-2 Polarization curves for a single MEA at H_2/O_2 reactants. T_{cell}: 60°C. Membrane: Nafion 117. Cathode: 4mg/cm^2. Anode: commercial Pt-Ru/C loading 2mg/cm^2 (40% Pt-Ru/C, 1:1 a/o). Prepared Pt-Ru/C loading 4mg/cm^2.

3.5 Fuel Cell set up

The MEA is than incorporated in a single cell stack. Graphite plate is used as a current collector-with-gas-distributor in this stack and copper is also used as current collector, Teflon reinforced fiber sheet of 0.25mm thickness as a gasket is moulded between MEA and graphite plate. The stack is installed in a fuel cell station with all their peripheral components (include heat controllers, humidification, flow meters, pressure regulator, pump, heat cylinder for fuel evaporations, etc.), the system for aceatls as fuel is shown as Figure 3-3, if the fuel is H_2 the heat cylinder is replaced by a humidifier and there is no pump.

The cell is operated with pure oxygen and fuels. When the fuel is hydrogen the pressure is at atmosphere or 25 psi, the temperature of fuel cell is 60°C and humidifiers of O_2/H_2 are 75C°/80°C, the stoichiometry of O_2/H_2 is 2:1.5. When the fuels are acetals, the fuels are in liquid condition (mixed with distilled water) at the vessel, they are then pumped to pass through the heat cylinder and evaporated to reach anode. The pressure of either O_2 or acetals is one atmosphere. Both gas flow rate is about 0.2 ml/s. O_2 is humidified by bubbling in stainless steel container filled with distilled water, fuels are humidified by passing distilled water of heat cylinder. The feeding acetals are impregnated acetals solution, which are: methylal/water: 76ml/72ml (1/4 M); ethylal/water: 104ml/144ml (1/8 M); 1,3-dioxolane: 74ml /72ml (1/4 M).

The fuel cell is kept stable under open circuit for 1 hour then 0.2A for 24 hours in H_2/O_2 condition before testing. Due to different boiling point of acetals the cell is operated at temperatures in the range of 45°C to 100°C, and the heating cylinder is always at least 2-3 degree higher than boiling point of acetals. Because of easy poisoning trend of 1,3-dioxolane, the testing of 1,3-dioxolane was carried on after finishing the methylal and ethylal testing. Each testing at least repeated twice, the repeatability is good except 1,3-dioxolane, which the performance decreases dramatically after a few minutes late and the EMA was also poisoned.

The fuel cell station is a GlobeTech Model GT60 modified by our group so that fuels different from hydrogen can be easily applied on it, the system is connected to a PC.

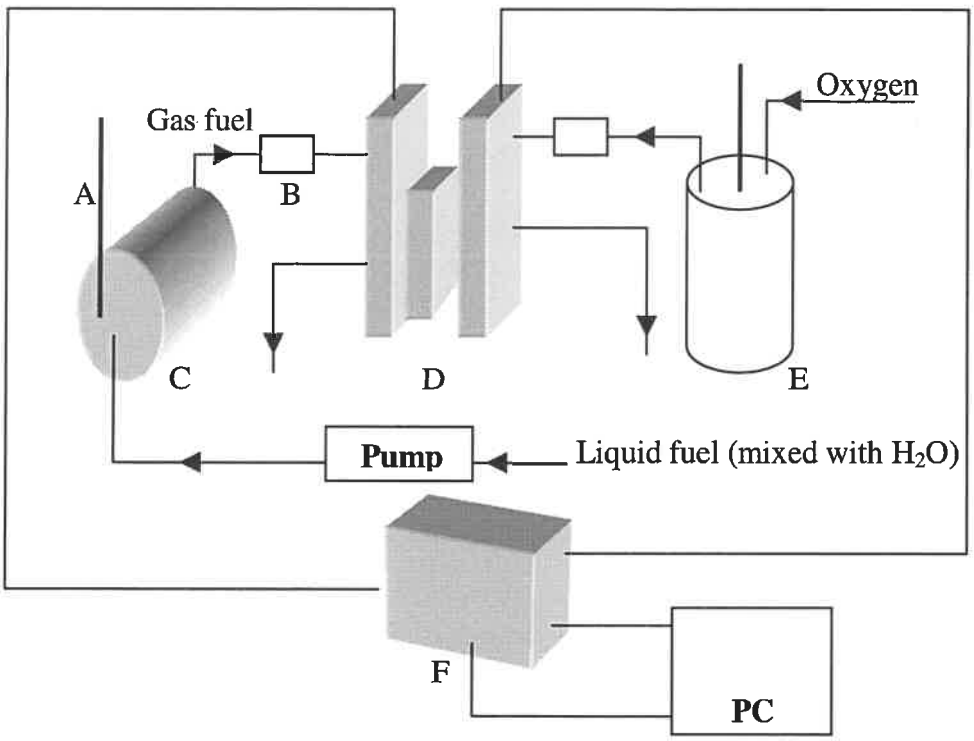

A: Thermostatic
B: Flow meter
C: Heat cylinder + humidifier
D: Fuel cell stack
E: Humidifier
F: HP Electronic load box

Figure 3-3 Schematic of fuel cell station connection

CHAPTER 4

RESULTS AND DISCUSSION

4.1 Half cell anodic polarization curves

4.1.1 Electrolyte acid

The steady-state galvanostatic polarization studies consisted of measuring a series of electrodes in acid electrolyte using a standard three-electrodes half cell. The three kinds of electrolyte acids have been tested to find the best electrolyte suitable for the testing. The concentration of acid is fixed to 1M, then 1M methylal is added to the acids. The best acid electrolyte for steady-state galvanostatic polarization studies is sulfuric acid (Figure 4-1). With temperature increased from 25°C to 60°C the overpotential in these three acids has a big drop. Next we tried different concentrations of methylal (0.01 to 2M), the optimum value is 1M (Figure 4-2). When methylal concentration is 0.1M, the reaction overpotential is very high even at low current densities. It means methylal concentration lower than 0.1M cannot support its direct electro-oxidation in this system.

4.1.2 Open-circuit potential

The open-circuit potential of different electrodes in methylal is shown in table 4-1. The open-circuit potential of electrode in different acetal solutions is shown as table 4-2.

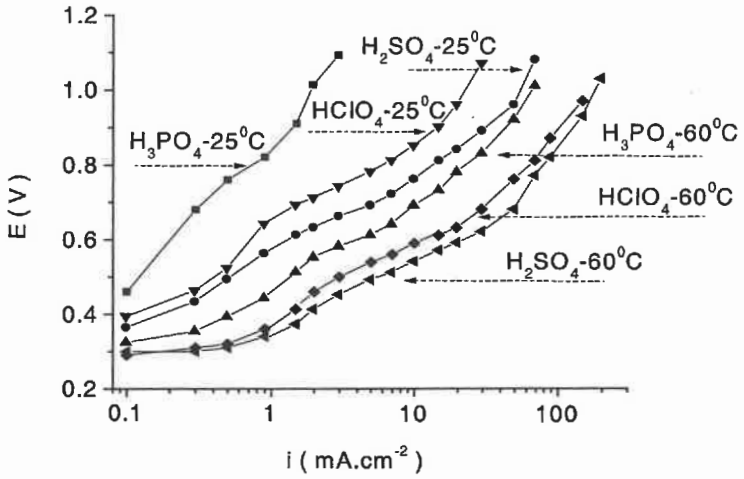

Figure 4-1 Steady-state galvanostatic polarization curves of direct elecrto-oxidation of 1M methylal in different 1M acid solutions. Electrode: 5% Pt - 10% RuO_2/C.

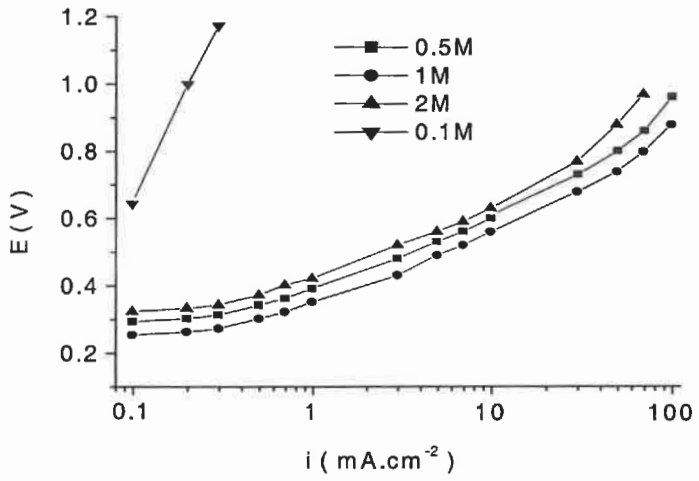

Figure 4-2 Steady-state galvanostatic polarization curves of direct electro-oxidation of methylal (0.1M-2M) in 1M sulfuric acid solutions at 25°C. Electrode: (5%Pt-10%RuO_2)/ C.

Table 4-1: Open-circuit potential for direct electro-oxidation of methylal on different electrodes in 1M H_2SO_4 + 1M methylal. (mV vs SHE)

Electrodes	E_o (25°C)	E_o (60°C)	Electrodes	E_o (25°C)	E_o (60°C)
10%Pt/C	310	350	10%Pt-Pd/C	300	400
10%Ru/C	490	520	5%Pt-Co-Cr/C	320	350
10%Rh/C	390	420	5%Pt-Co-Ni/ C	220	290
10%Ir/C	230	260	5%Pt-5%RuO_2/C	300	---
10%Pd/C	490	480	5%Pt-10%RuO_2/C	280	---
10%Pt-Ru/C	310	350	5%Pt-10%SnO_2/C	300	---
10%Pt-Rh/C	300	440	5%Pt-10%WO_3/C	390	---
10Pt-Ir/C	330	350	5%Pt-10%Fe_3O_4/C	380	---

Table 4-2: Open-circuit potential of electrode 5%Pt-10%RuO_2/C in different solutions. Supported electrolyte: 0.5M acetals + 1M H_2SO_4

V_{oc} (mV vs SHE)

	25°C	40°C	60°C	80°C
Methylal	280	380	------	------
Ethylal	160	360	230	200
1,3-dioxolane	410	------	350	------

It can be seen the most of electrodes have an open-circuit potentials values at 220mv to 350mv. In this study the values of E_o increase a little with temperature. The open-circuit potential is a mixed potential resulting from the electrochemical reactions related to hydrogen atoms formed by the dissociate adsorption of the organic molecules or water and then ionisation of adsorbed hydrogen atoms. The measured open-circuit potentials are close to the value for the hydrogen ionisation reaction:

$$H_{ads} = H^+ + e^- \qquad (4\text{-}1)$$

It means the dissociate chemisorption of the C-H and O-H bonds occurs readily at the interface, resulting in adsorbed hydrogen [135].

Ethylal has a lower open-circuit potential than methylal and 1,3-dioxolane, it means maybe that ethylal has more activated C-H bonds compared to latter, and then has a higher coverage of the surface adsorbed by hydrogen atoms. The acid-catalysed hydrolysis of aceatls can yield formaldehyde, formic acid and methanol, just as we show in equations (4-4) to (4-13). For all three kinds of acetals, when temperature increased from 25°C to 40°C or 60°C, the open-circuit potential increases a little, it maybe due to the intermediate hydrolysis products methanol appearance rather than formaldehyde and formic acid. It was then suggested that the products of acid hydrolysis might actually be determining factor for the observed open-circuit potential. When temperature still rise to 80°C, the open-circuit potential has a tendency to go down, it maybe due to more and more hydrolysis products accumulated and facially ready to oxidize.

4.1.3 Direct electro-oxidation of methylal

The effect of the electrode materials based on 10% single noble metals on the polarization curves is shown in Figure 4-3. From this curve it can be seen that Pt/C is the best catalyst for oxidation of methylal, the others do not have good performances for electro-oxidation of methylal even at 60°C. The volcano behaviour was observed for the current density to metal atomic radius plots at a given potential 0.7v (Figure 4-4).

For secondary series electrodes, they are compared to Pt/C and Pt-Ru/C at 25°C, the results are shown in Figure 4-5 and 4-6. From these curves it can be seen that among electrodes based on Pt/C, Pt-Ru/C, Pt-RuO_2/C, Pt-SnO_2/C Pt-WO_3/C, Pt-Fe_3O_4/C, the 10%Pt-Ru/C or 10%Pt-10%RuO_2/C based electrodes are the best ones. At a given current the overpotential of the reaction increases in the order Pt-RuO_2 < Pt-Ru <Pt-Fe_3O_4 < Pt-SnO_2 < Pt-WO_3, only when current density is high than 10mA.cm^{-2}, the Pt-Ru/C is better than Pt-RuO_2/C.

On the other hand for a fixed concentration of Pt in the Pt-RuO_2 alloy, the overpotential changes with the RuO_2 concentration in the electrode. For RuO_2 concentration from 5% to 40% w/w, the lowest overpotential is obtained on 5%Pt-10%RuO_2 (Figure 4-7). These different results may be explained by the synergetic effect that between Pt and the ruthenium oxides for this reaction, the optimum value obtained for the overpotential when %RuO_2 changes supports this synergetic effect. The determination of the electrochemical active surface area of the various electrodes for this reaction is under

active investigation. This may help in the understanding of the effect of this parameter on the observed electrochemical activity.

For the third series electrode, the results are shown in Figure 4-8 and Figure 4-9. It can be seen that the best electrode among them is Pt-Ru alloy, Pt-Ir alloy also show a good properties at two temperatures, and Pt-Co-Cr has a big improvement as temperature rises to 60°C. The overpotential increases in the order Pt-Ru < Pt-Ir< Pt-Co-Cr< Pt-Rh< Pt-Pd. Similar volcano behaviours were observed for the current density to difference of binary metal atomic radius plots at a given potential Figure 4-10.

From above figures, it can be seen almost for all of the electrodes, when temperature rising from 25°C to 60°C, the performance of I-V has a big improvement. Figure 4-11 gives a good example of electrode 5% Pt-10% RuO_2.

The results of long-time stability for open circuit potential are shown in Figure 4-12. The temperature is room temperature. We just compare two kinds of electrodes. It is clear that in the experiment condition the Voc is down with the times going on. At the same time it should give us the indication the hydration products of methylal, such as formaldehyde, formic acid should be easier oxidized, with times going on the hydrolysis process become stable so the methylal direct electro-oxidation should also be independent on time after the hydrolysis process become stable. The different electrodes times-I-V curves support this deduction (Figure 4-13 and Figure 4-14).

The activities decrease of Pt-Co-Ni electrode maybe due to the active channel block by Co-Ni bind (Figure 4-15 and Figure 4-16). The Pt-metal oxides binary alloy electrodes usually cannot compete to Pt-Ru electrode except Pt-RuO_2 electrode, the later is dramatically better than other similar electrodes (Figure 4-17). Even running at given current density for a long time it is also shown as good stability as this of Pt-Ru (Figure 4-18).

The reaction of direct oxidation of methylal in this half-cell is as shown in Eq. (4-2), compared to oxidation of methanol Eq. (4-3), the reaction of oxidation of methylal produce more number of electrons (16) than that of methanol:

$$(CH_3O)_2{\bullet}CH_2 + 4H_2O = 3\ CO_2 + 16\ H^+ + 16e^- \qquad (4\text{-}2)$$

$$CH_3OH + H_2O = 6H^+ + CO_2 + 6e^- \qquad (4\text{-}3)$$

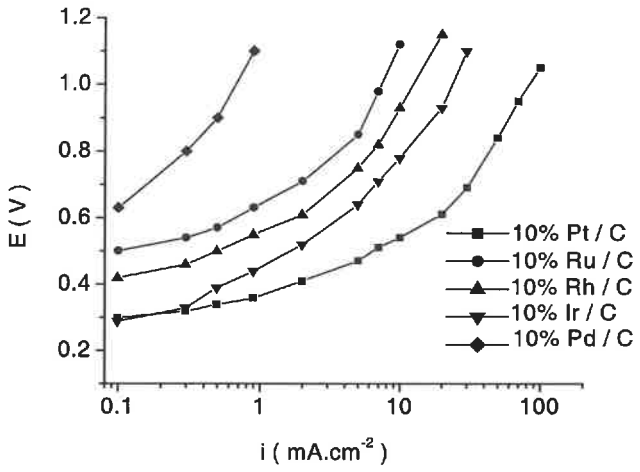

Figure 4-3 Steady-state galvanostatic polarization curves of direct electro-oxidation of methylal using different noble metal electrodes at 60°C. Electrolyte: 1M H_2SO_4 + 1M methylal.

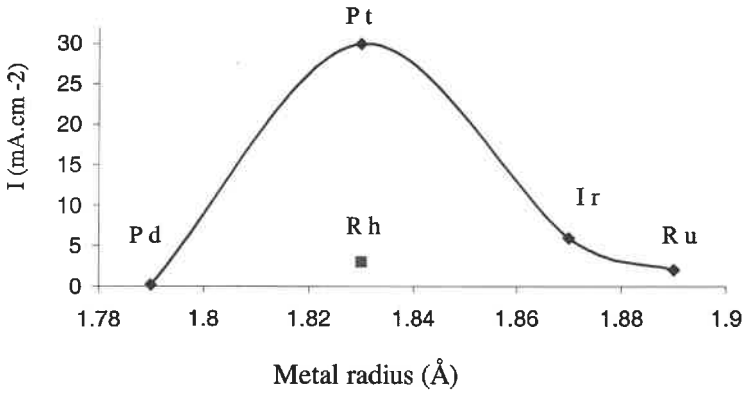

Figure 4-4 Current density of methylal direct electro-oxidation at E = 0.7V as a function of the noble metals radius. Electrolyte: 1M H_2SO_4 + 1M methylal at 60°C.

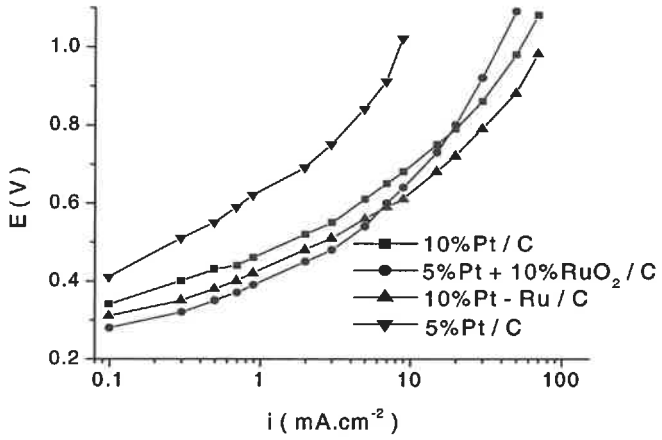

Figure 4-5 Steady-state galvanostatic polarization curves of different catalyst electrodes in 1M methylal + 1M H_2SO_4 solution at 25°C.

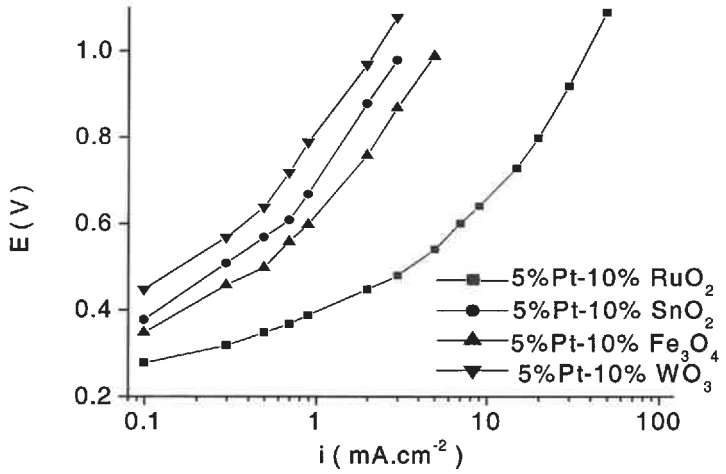

Figure 4-6 Steady-state galvanostatic polarization curves of different kind catalyst electrodes in 1M methylal+1M H_2SO_4 solution at 25°C.

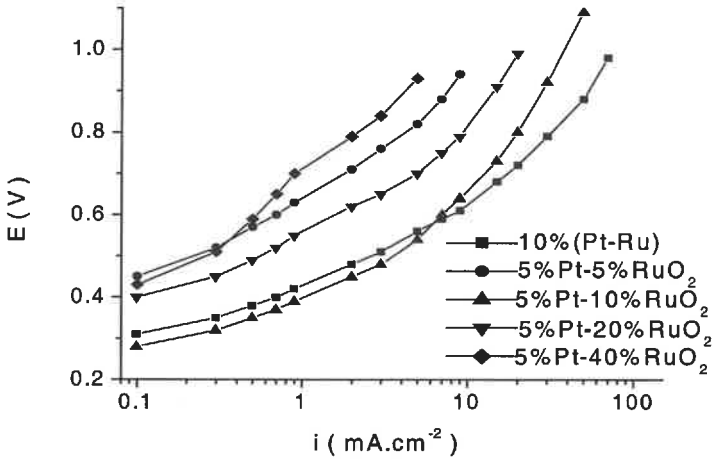

Figure 4-7 Steady-state galvanostatic polarization curves of different percentage RuO_2 catalyst electrodes in 1M methylal + 1M H_2SO_4 solution at 25°C.

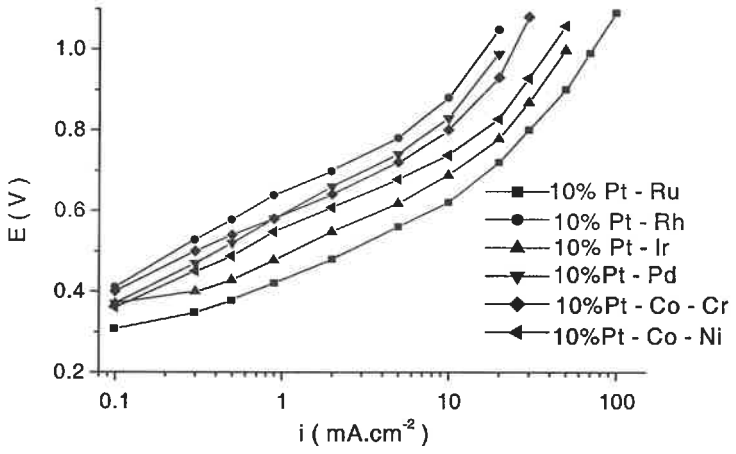

Figure 4-8 Steady-state galvanostatic polarization curves of direct electro-oxidation of methylal on different electrodes in 1M methylal + 1M H_2SO_4 solution at 25°C.

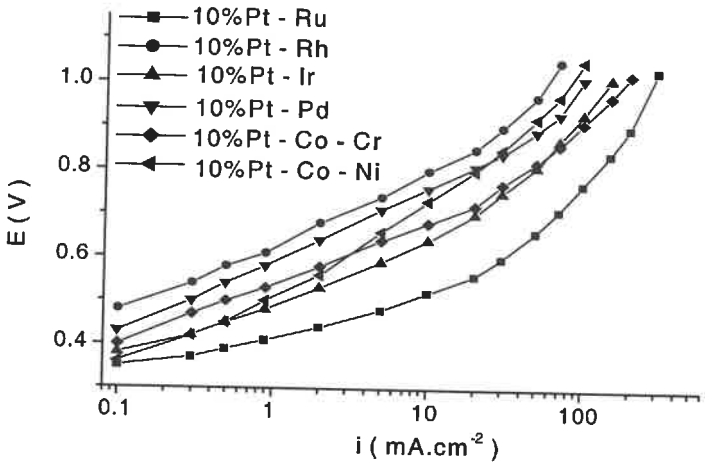

Figure 4-9 Compare to the Figure 4-8 for the same electrodes at same condition except temperature is 60°C.

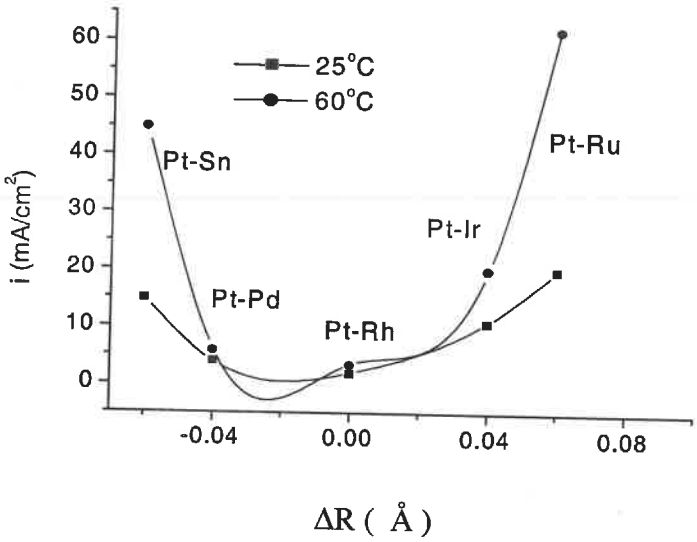

Figure 4-10 Current density of 1M methylal direct electrooxidation in 1M H_2SO_4 at E=0.7v as a function of ΔR of binary metals. $\Delta R = R_m - R_{Pt}$, where R is metal radius and m = Pd, Ir, Rh, Ru.

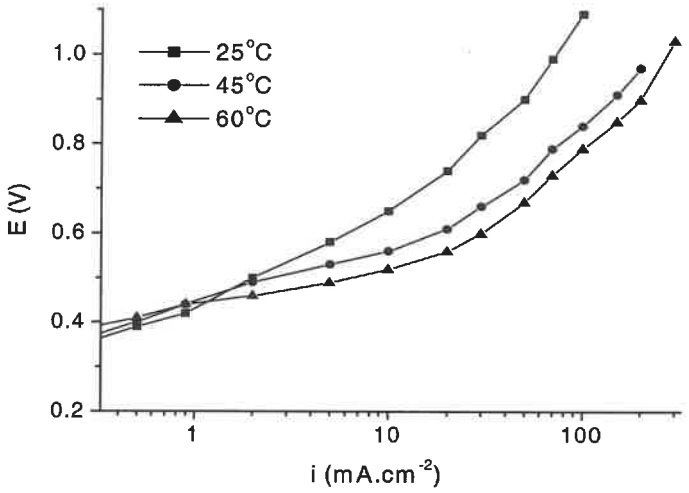

Figure 4-11 Steady-state galvanostatic polarization curves of methylal direct electro-oxidation at different temperatures. Electrolyte: 1M methylal + 1M H_2SO_4 solution. Electrode: 5% Pt-10%RuO_2/C

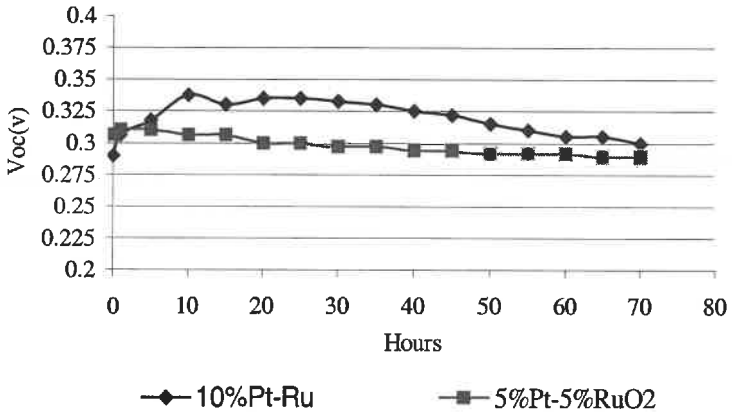

Figure 4-12 Stability of open circuit potential. Electrolyte: 0.5M methylal + 1M H_2SO_4.

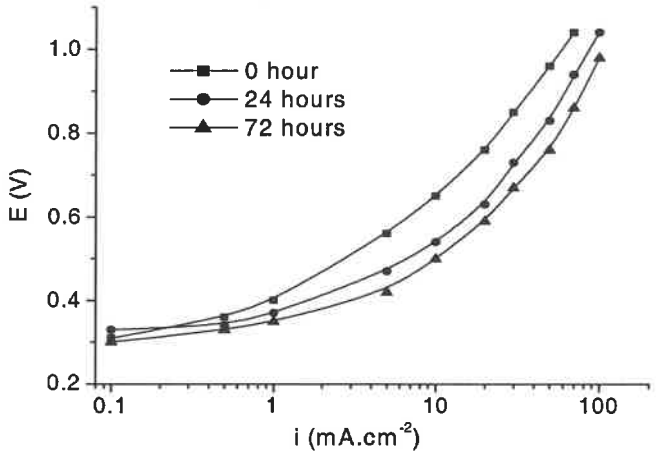

Figure 4-13 Steady-state galvanostatic polarization curves of direct electro-oxidation of 0.5M methylal in 1M H_2SO_4 solutions after different hours. Electrode: 10%Pt-Ru.

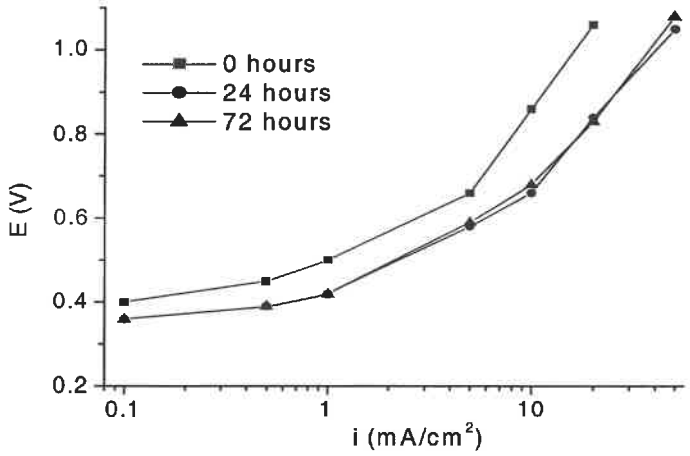

Figure 4-14 Steady-state galvanostatic polarization curves of direct electro-oxidation of 0.5M methylal in 1M H_2SO_4 solutions after different hours. Electrode: 10% Pt-Rh.

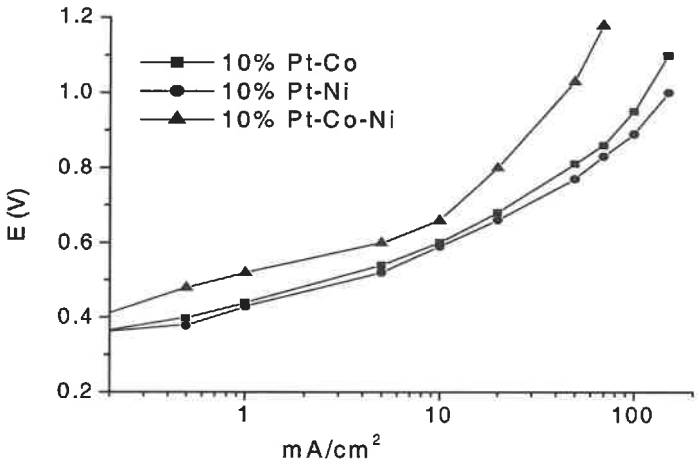

Figure 4-15 Steady-state galvanostatic polarization curves of direct electro-oxidation of 0.5M methylal in 1M H_2SO_4 solutions after different hours. Electrode: 10% Pt-Rh.

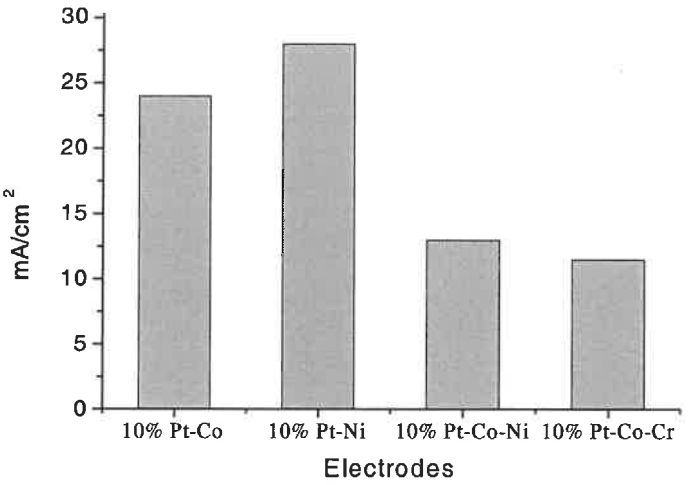

Figure 4-16 Current density of methylal direct electro-oxidation in 1M H_2SO_4 at E=0.7V as a function of electrodes at 25°C.

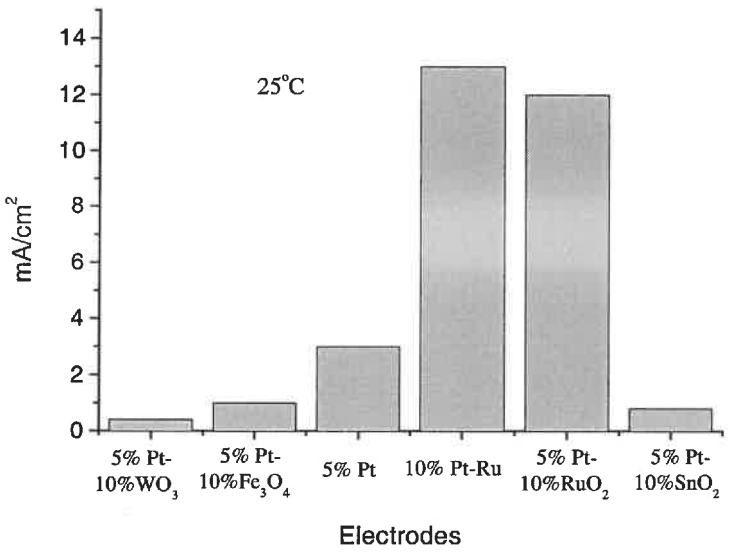

Figure 4-17 current density of methylal direct electro-oxidation in 1M H_2SO_4 at E=0.7v as a function of electrodes.

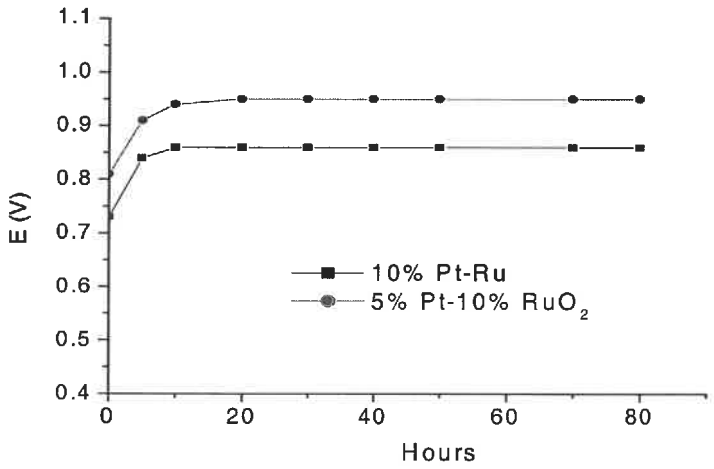

Figure 4-18 Longevity of 1M methylal direct electro-oxidation in 1M H_2SO_4 at 20mA/cm^2.

4.1.4 Direct electro-oxidation of ethylal and 1,3-dioxolane

As our previous works showed above that the best characteristics of methylal electro-oxidation are obtained with sulfuric acid among H_2SO_4, $HClO_4$ and H_3PO_4 solutions. For ethylal and 1,3-dioxolane they also have similar results. So we focus our supporting electrolyte on 1M sulfuric acid solutions.

Figure 4-19 shows the direct electro-oxidation polarization curves (I-V) for 1M methanol and 1M methylal in a supporting solution of 1M H_2O_4. From the curves it is shown that the performance of methylal oxidation is better than that of methanol. This is an indication that acetals are more easily electro-oxidized than alcohols. The study of the electro-oxidation of other acetals may help to sustain this result.

The polarization curves of ethylal and 1,3-dioxolane in 1 M H_2SO_4 on various electrodes (including Pt mixed with metal oxides) were drawn and similar trends to those obtained on methylal electro oxidation were observed. From these polarization curves, it was shown that, for the same supporting electrolyte and electrode material, the electro-oxidation of ethylal performs better than that of methylal. The analysis of the hydrolysis products of methylal and ethylal revealed the presence of methanol and formaldehyde [131]. However, the hydrolysis products were not detected in the electrolyte following the lengthier experiments because they could be oxidized very easily at the electrode to carbon dioxide. The polarization curves also show that some

oxide-based electrocatalysts exhibit good performance for the electro-oxidation of these fuels.

Figure 4-20 and 4-21 show the steady-state polarization curves of the electro-oxidation of 0.5M ethylal and 1,3-dioxolane in 1M H_2SO_4 at 25°C on various electrodes. From these curves that obtained on various single metal-based electrodes, it can be seen that the best characteristics are obtained with the electrode based on 10% Pt. The effect of fuel concentration on polarization was also studied, it was found that the optimum concentration of ethylal, i.e. that which yields current voltage curves with the lowest overpotential, is 0.5 M.

The polarization curves of the methylal, ethylal and 1,3-dioxolane in 1M H_2SO_4 on various electrodes, including electrodes Pt mixed with metal oxides show similar trends. As examples of this, the polarization curves of the electro-oxidation of 1,3-dioxolane on various Pt/metal-oxide electrodes are shown in Figure 4-22. The best performances were obtained on Pt-RuO_2 and Pt (O_x) with the same supporting electrolyte. The bar chart representation of the electro-oxidation current densities on various electrode materials obtained at 0.60 V for methylal, ethylal and 1,3-dioxolane is shown in Figure 4-23. For the same electrode material, the electro-oxidation of ethylal performs better than that of either methylal or 1,3-dioxolane. For example, the overpotential of the electro-oxidation of acetals on Pt-Ru increases in the order: ethylal < 1,3-dioxolane < methylal. But on Pt-RuO_2, the overpotential increases in the order: ethylal < methylal < 1,3-dioxolane.

For electrodes based on different concentrations of RuO_2 mixed with 5% Pt, the overpotential first decreases to a minimum when [RuO_2] increases to 10% and then increases strongly with [RuO_2] (Figure 4-24). The lowest overpotential is obtained with 5% Pt-10% RuO_2. These results may be explained by the synergetic effect between Pt and the ruthenium oxides as we pointed out above. Similar results were obtained for direct anodic methanol oxidation [132]. This is now well documented.

It has been shown that Pt-Ru; Pt-Sn; Pt (O)x; Pt-RuOx; Pt-MnOx; and Pt-Fe_2O_3 electrodes can sustain electro-oxidation of ethylal and 1,3-dioxolane during the steady-state experiments without noticeable hysteresis in the polarization curves. This is an indication that these electrodes are resistant to the effects of poisoning. Figure 4-25 and 4-26 shown the Pt-binary electrodes performance, there also have similar trend as methylal on these electrodes.

For the electro-oxidation of all three acetals, 10% Pt/Ru (1: 1) is a better catalyst than 5% Pt-5% RuO2. For ethylal electro-oxidation, 10% Pt/Sn (1:1) is the best catalyst and 10% PtOx is the worst catalyst. By contrast, for 1,3-dioxolane, 10% Pt/Sn (1:1) and 10% PtOx are comparable in terms of activity (Figure 4-23). This indicates that we may have a change of the reaction rate of the electro-oxidation of the acetals according to the catalyst anode material composition. New analysis of the hydrolysis products of methylal and ethylal revealed the presence of methanol and formaldehyde. However, the hydrolysis

products were not detected in the electrolyte after long-term electro-oxidation experiments very likely because they were anodically oxidized to carbon dioxide.

The mechanism of acetals hydrolysis has been documented by M.Beaujean et al. from Lambiotte [138], which is the company produces and sells acetals. The results they have obtained can be summarized as follows: Acetals hydrolyse in an acid medium and in the presence of water (Table 4-4), but are relatively stable in a neutral or in a basic medium. At a pH level of 3.63, no detectable hydrolysis of methylal was observed in a 30-70% mixture with water at 20°C after 3 months. The hydrolysis level of methylal increases when the pH level decreases. The hydrolysis level of methylal increases from 0.55% at pH 2.95 to 35.26% at pH 0.96. Similar results were obtained with ethylal, for which a hydrolysis level of 33% was shown at pH 0 and 4% at pH 1. For 1,3dioxolane, the hydrolysis level decreases from 9% at pH 0 to 0% at pH 1. At pH 0, the hydrolysis level of methylal is higher than that of ethylal, which is higher than that of 1,3dioxolane. Methyl formate, formic acid, methanol and formaldehyde are the main hydrolysis products of acetals. The same results were obtained in our work.

The data in Figure 4-20 and 4-21 obtained with the noble-metal catalysts are evaluated in Figure 4-27 by plotting the current densities at 0.70 V vs SHE vs the atomic radius of their respective metal. Volcano behaviors were obtained. The highest current density was obtained with platinum and rhodium and the lowest was obtained with palladium and ruthenium. Binary-alloy-based catalysts show an interesting correlation between the

current density and ΔR ($\Delta R = R_{metal} - R_{pt}$) as shown in Figure 4-28. The lowest current density is obtained when ΔR is close to zero and catalytic activity of the binary catalyst increases with |ΔR|. Accordingly, the highest values of current density are obtained for Pt-Sn and Pt-Ru. The same results were obtained with methanol electro-oxidation. This may explain why the Pt-Ru alloy has been the best choice up to now for the methanol fuel cell anode [139, 140] and why Pt-Sn might be intrinsically the second best active binary alloy for methanol oxidation. This also explain why Pt-Ru and Pt-Sn have shown to be the efficient catalysts for the electro-oxidation of dimethoxymethane, trimethoxymethane and 1, 3, 5-trioxane. This might help in the selection of alloys for the electro-oxidation of acetals from a combination of catalytic binary alloys having particular value of ΔR. Consequently, new binary alloys could be designed for direct acetal fuel cells.

Current vs. overpotential curves of the electro-oxidation of ethylal on Pt-Ru were drawn after various hydrolysis times (Figure 4-29). As may be seen, in the high current density regions, the curves improved to a measurable degree with an increase in time. At a current density of 20 $mA.cm^{-2}$, the overpotential decreases by 200 mV after 72 hours, and the open circuit potential changes by less than 50 mV after the same amount of time (Figure 4-30). This improvement is very likely due to acetal hydrolysis.

This variation might be related to the change in fuel composition due to hydrolysis. Chemical hydrolysis products are certainly involved in the improvement of the acetal

electro-oxidation reaction. It may be seen that the electro-oxidation polarization curves improved with the increase in hydrolysis time. This improvement due to the hydrolysis of ethylal was also observed for methylal and 1,3-dioxolane. Analysis of the anode effluent streams for by-products showed that carbon dioxide was the only detectable product in the case of methylal, ethylal and 1,3-dioxolane. For the acid (pH = 0.5) hydrolysis of methylal, ethylal and 1,3-dioxolane over 72 hours, the hydrolysis reaction products were also analyzed by gas chromatographs. Methanol, methyl formate, formic acid and formaldehyde were obtained as hydrolysis by products.

However, these hydrolysis products were not detected in the anode effluent streams. It is quite likely that the hydrolysis products could have been very easily oxidized at the anode, leaving no soluble products to accumulate in the solution. This is in agreement with results obtained on the electro-oxidation of dimethyl orthoformate ($(CH_4O)_2CH_2$), trimethyl orthoformate ($(CH_3O)_3CH_2$) and trioxane ($(CH_3O)_3$) [].

From the polarization curves shown in Figure 4-23, the best characteristics are obtained in the ethylal solution at room temperature among these acetals. When current density is over 100mA.cm^{-2}, there are side reactions to occur in ethylal and 1,3-dioxolane solutions; when the current density is over 150mA.cm^{-2}, side reaction also occurs in methylal solution. The over voltage of the electrooxidation at current densities higher than 2 mA/cm^2 increases in the order ethylal < 1,3-dioxolane < methylal.

4.1.5 Proposed reactions

Based on the reaction product analysis, the following half-cell electro-oxidation reactions can be proposed. This may involve the production of some hydrolysis by-products followed by complete electro-extraction to carbon dioxide.

i) For methylal:

Hydrolysis:

$$(CH_3O_2)\,CH_2 + H_2O \leftrightarrow CH_2O + 2CH_3OH \qquad (4\text{-}4)$$

$$CH_2O + H_2O \leftrightarrow CO_2 + 4H^+ + 4e^- \qquad (4\text{-}5)$$

$$2CH_3OH + 2H_2O \leftrightarrow 2CO_2 + 12H^+ + 12e^- \qquad (4\text{-}6)$$

The complete electro-oxidation of methylal to carbon dioxide is:

$$(CH_3O)_2\,CH_2 + 4H_2O \leftrightarrow 3CO_2 + 16H^+ + 16e^- \qquad (4\text{-}7)$$

ii) For ethylal:

Hydrolysis:

$$(CH_3O)_2\,(CH_2)_3 + 3H_2O \leftrightarrow 4CH_3OH + CH_2O \qquad (4\text{-}8)$$

$$CH_2O + H_2O \leftrightarrow CO_2 + 4H^+ + 4e^- \quad (4\text{-}9)$$

$$4CH_3OH + 4H_2O \leftrightarrow 4CO_2 + 24H^+ + 24e^- \quad (4\text{-}10)$$

The complete electro-oxidation of ethylal to carbon dioxide is:

$$(CH_3O)_2(CH_2)_3 + 8H_2O \leftrightarrow 5CO_2 + 28H^+ + 28e^- \quad (4\text{-}11)$$

iii) For 1,3-dioxolane:

Similar hydrolysis products, which may include methanol, methyl formate, formic acid and/or formaldehyde, would be expected from the hydrolysis of 1,3-dioxolane in an acid electrolyte.

Hydrolysis:

$$C_3H_6O_2 + 2H_2O \leftrightarrow CH_2O + 2\,CH_3OH \quad (4\text{-}12)$$

The complete electro-oxidation of 1,3-dioxolane is:

$$C_3H_6O_2 + 4H_2O \leftrightarrow 3CO_2 + 14H^+ + 14e^- \quad (4\text{-}13)$$

The above equations indicate that the complete electro-oxidation of the acetals produces more electrons than the complete electro-oxidation of methanol:

$$CH_3OH + H_2O \leftrightarrow CO_2 + 6H^+ + 6e^- \qquad (4\text{-}13)$$

The high number of electrons produced from acetal electro-oxidations may explain why the polarization curves of acetals are better than that of methanol. This is supported by the direct electro-oxidation overpotential curves for methanol and methylal in 1M H_2SO_4 solutions at 25°C and by the bar chart representation of the direct electro-oxidation current density for acetals (Figure 4-19 and 4-23).

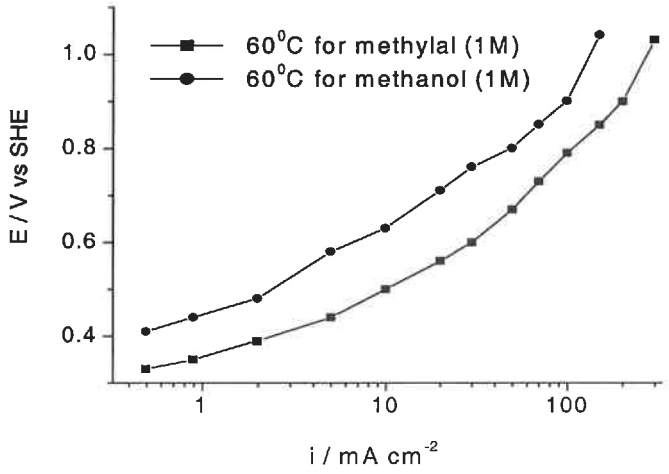

Figure 4-19 steady-state galvanostatic polarization curves of electro-oxidation of methylal and methanol in 1M H_2SO_4. Electrode: 5% Pt-10% RuO_2.

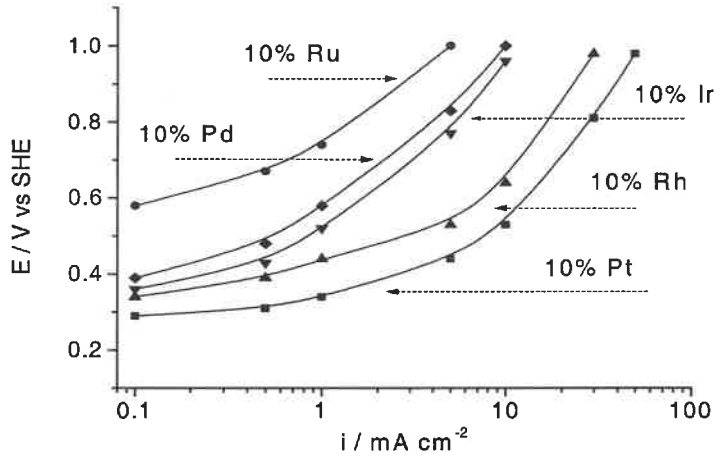

Figure 4-20 polarization curves for direct electro-oxidation of 0.5M ethylal on different single noble metal electrodes at 25°C.

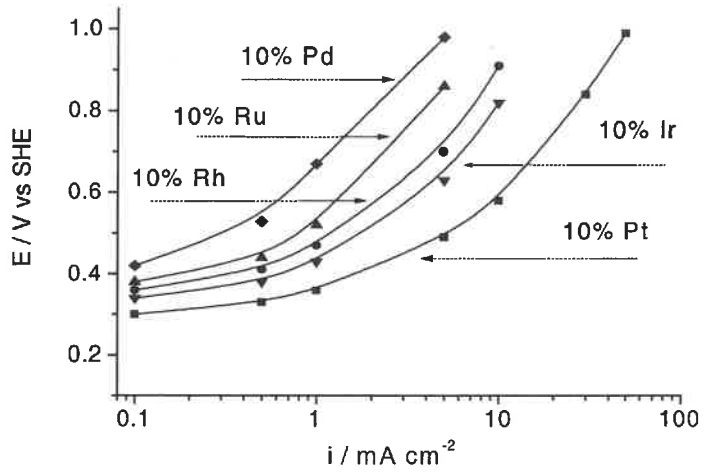

Figure 4-21 polarization curves of direct electro-oxidation of 0.5M 1,3-dioxolane on different single noble metal electrodes at 25°C.

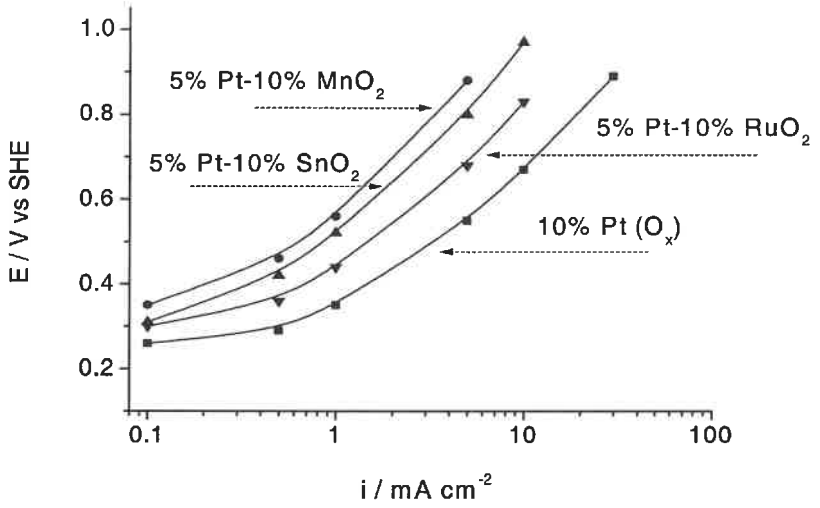

Figure 4-22 I-V polarization curves for direct oxidation of 0.5M 1,3-dioxolane in 1M H_2SO_4 at 25°C.

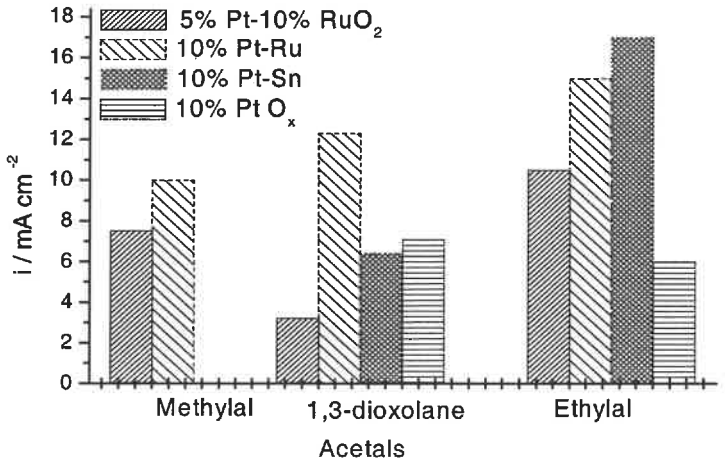

Figure 4-23 Bar chart representation of direct electro-oxidation current density for methylal, 1,3-dioxolane and ethylal in 1M H2SO4 at 25°C and 0.6 Volt vs SHE on various electrode materials.

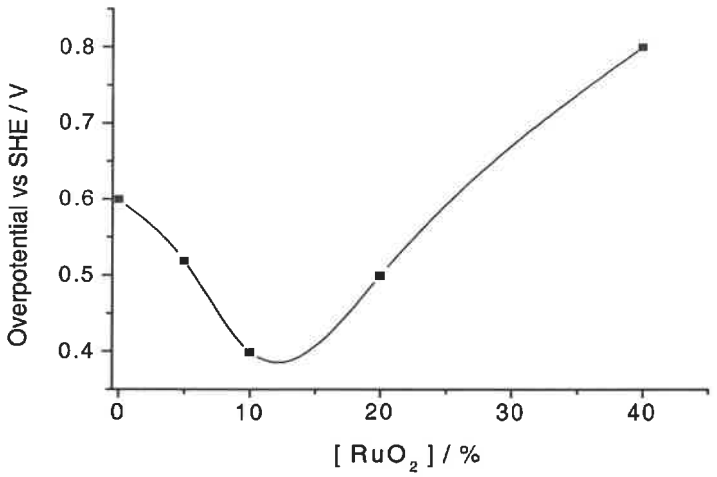

Figure 4-24 Variation of the electro-oxidation potential with RuO_2% mixed in 5% Pt electrode at 0.5M ethylal + 1M H_2SO_4. Current density: 5mA.cm^{-2}.

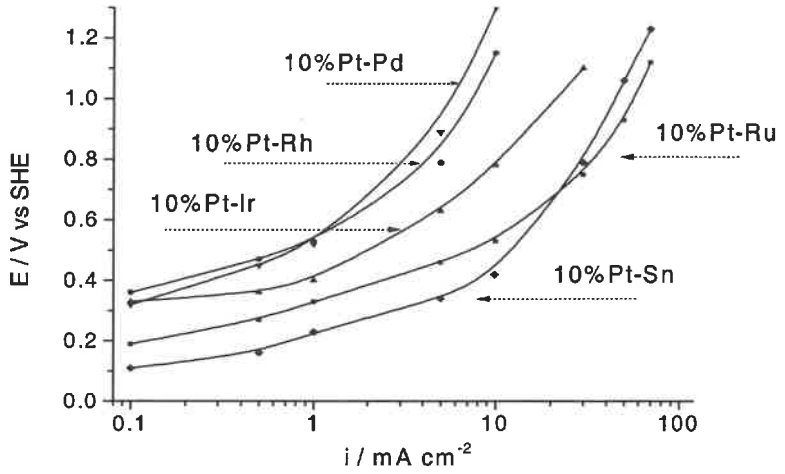

Figure 4-25 I-V polarization curves of direct electro-oxidation of ethylal (0.5M) in 1M H_2SO_4 solutions at 25C.

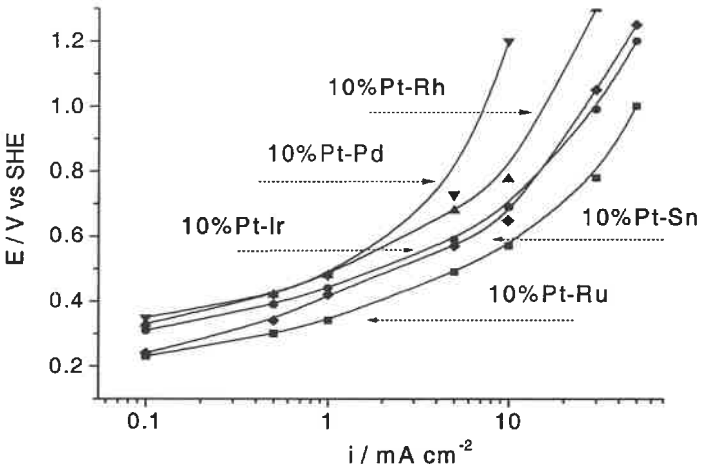

Figure 4-26 Steady-state galvanostatic polarization curves for direct electro-oxidation of 0.5M 1,3-dioxolane in 1M H_2SO_4 at 25°C.

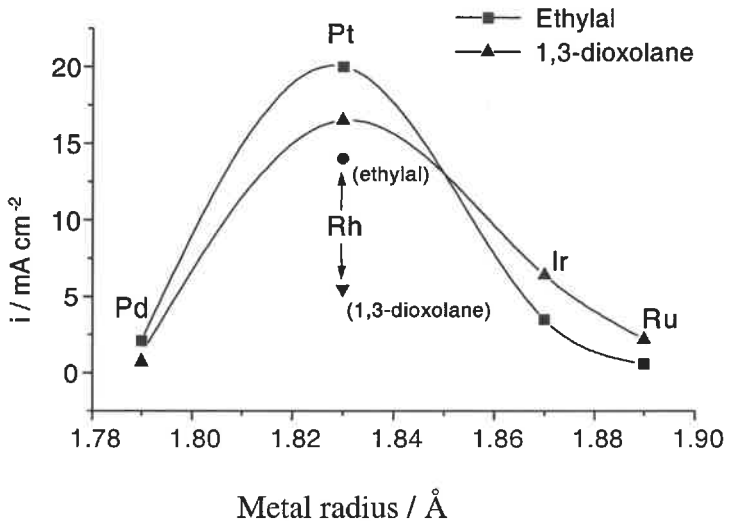

Figure 4-27 Current density vs radius for single noble metals used as catalysts in the direct electro-oxidation of 0.5M acetals in 1M H_2SO_4 at 25°C at 0.70 Volt.

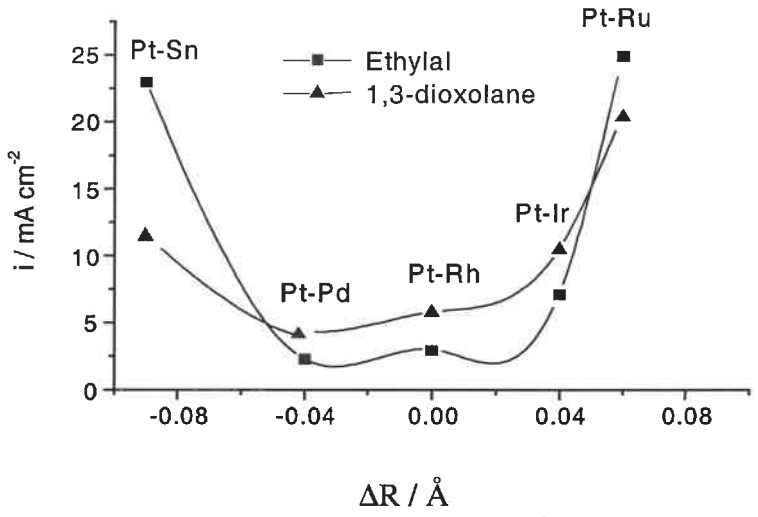

Figure 4-28 Current density vs (R_{metal} - R_{pt}) radius for binary metals used as catalysts in the direct electro-oxidation of 0.5M acetals in 1M H_2SO_4 at 25°C at 0.70 Volt.

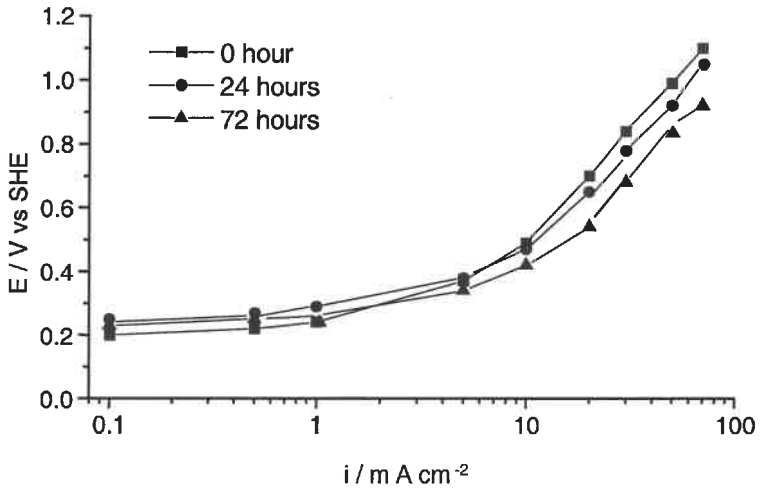

Figure 4-29 Steady-state polarization curves of 0.5M ethylal direct electro-oxidation after different hours in 1M H_2SO_4 at 25°C.

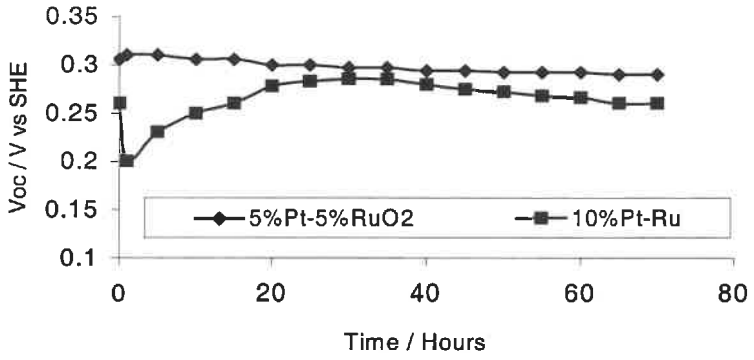

Figure 4-30 Long-term stability of open-circuit potential of 0.5M ethylal in 1M H_2SO_4 at 25°C.

Table 4-4

Hydrolysis level (%) variation with pH of acetals in H_2SO_4 during a 5-hour period at 20°C [14]

Acetals/pH	0	1	3
Methylal	52%	4%	0%
Ethylal	33%	22%	0%
1,3-dioxolane	9%	0%	0%

Table 4-5

Variation in the overpotential during the electro-oxidation of methylal, ethylal and 1,3-dioxolane in 1 M H_2SO_4 at 25°C on Pt/Ru and on $PtRuO_2$ for 20 $mA.cm^{-2}$

Acetals/V at 20 $mA.cm^{-2}$	Methylal	Ethylal	1,3-dioxolane
Pt-Ru	0.65	0.40	0.50
Pt-RuO_2	0.75	0.65	0.85

4.2 PEMFC curves

Polarization curves were recorded and used to compare the performances of the various MEAs prepared.

4.2.1 H_2/O_2 polarization curves on different electrodes

All electrodes (MEA) prepared by us have been conditioned in H_2/O_2 PEMFC to stabilize and optimize. The cathodes in all MEA are the same type 4mg/cm^2 Pt/C-prepared from 60% Pt/C E-TEK powder. The fuel cell testing temperature is kept at 60°, the hydrogen humidifier is 80°C and oxygen humidifier is 75°C. The electrodes would first be conditioned in ambient pressure then in pressure P_{H2}/P_{O2}: 20psi/25psi.

Figure 4-31 gives the curves with anode 4mg/cm^2 Pt-Ru/C applied in H_2/O_2, Figure 4-32 also gives power density curves in ambient pressure. It is clear, as expected, the performance is improved as pressure increased. At ambient pressure the power density of this electrode can reach to 160 mW.cm^{-2}. In this testing condition the electrocatalyst Pt-Ru is not as good as Pt, but it is a good reference for the other electrodes we prepared. Compared them in either hydrogen or acetals reactants, we can get a series data to find if there is different performances trend between hydrogen and acetals.

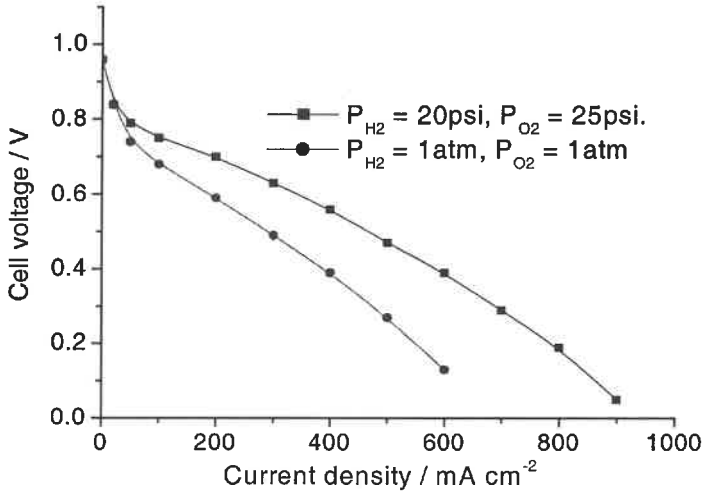

Figure 4-31 Polarization curves for a single MEA at H_2/O_2 reactants. T_{cell} = 60°C. Electrode area: 2.25cm^2. Membrane: Nafion 117. Cathode: 4mg/cm^2 Pt/C, Anode: 4mg/cm^2 Pt-Ru/C- prepared by our lab.

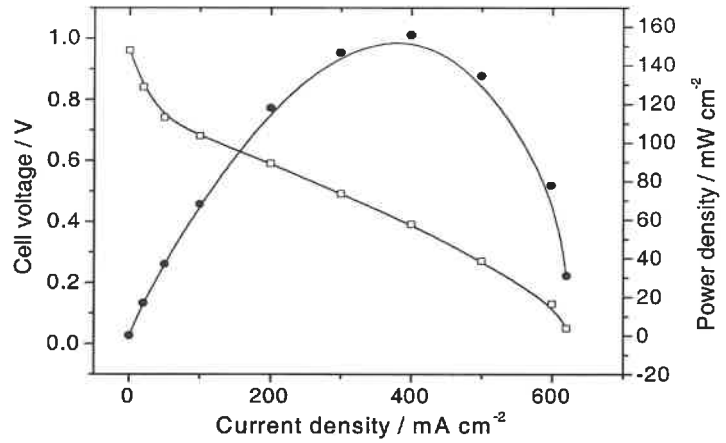

Figure 4-32 Polarization and power density curves for a single MEA at H_2/O_2 reactants. Pressure: ambient, T_{cell} = 60°C. Electrode area: 2.25cm^2.Membrane: Nafion 117. Cathode: 4mg/cm^2 Pt/C, Anode: 4mg/cm^2 Pt-Ru/C- prepared by our lab.

Figure 4-33 to 4-36 gives the polarization curves of a series MEA (different anodes) in ambient pressure. We can see that (Pt-Ru + Pt-Sn)/C has a best performance in H_2/O_2, its power density can reach 270 mW. cm^{-2}. Figure 4-37 to 4-38 gives a comparison of these electrodes at different operation pressures. All the curves show that Pt-Ru is not as good as other electrodes. One reason may be due to the difference between the methods preparing them. Just as we described in section 3-2, in Pt-Ru/C we used 30% PTFE as a binder. As M. S. Wilson et al explained, a catalyst site must satisfy three criteria for it to contribute to the electrochemical reaction in a fuel cell. The criteria are proton access, gas access, and electronic path continuity. The structure and composition of an electrode can affect all three of these parameters in varying degrees. To maximize catalyst utilization, it is desirable to satisfy these three criteria for as many of the catalyst sites as possible.

When you use this typical method to prepare a fuel cell gas diffusion electrode the catalyst layer of the electrode consist of 2 nm diameter platinum particles supported by carbon black. This layer sits on top of a base layer of carbon black, which is spread over carbon cloth or carbon paper. The entire structure is bonded together with 25 to 50wt % PTFE (just as Pt-Ru/C we prepared). In phosphoric acid fuel cells, the liquid electrolyte seeps into the hydrophobic catalyst layer to provide ion access to the catalyst sites. In the case of PEMFCs, access of the ionomer electrolyte to the platinum particles within the catalyst layer is achieved by impregnating the active (catalyzed) side of the electrode with a solubilized form of the ionomer Nafion. Impregnation is carried out by brushing or spraying the recast solution onto the front side of the electrode.

This mode of construction introduces several difficulties in the case of the PEMFC. For example, the erratic thickness of a typical catalyst layer, combined with variations in the impregnation depth of the recast ionomer, result in areas where the catalyst layer is not fully impregnated and areas where the ionomeric additive could extend into the electrode further than the catalyst layer, thus introducing an unnecessary transport barrier to the diffusion of gas through the backing. It is difficult to match the impregnation depth exactly with the depth of the catalyst layer in an electrode of this construction.

Although PTFE is effective as a binder and imparts hydrophobicity to the gas diffusion regime of the electrode, no particular advantage is realized by the presence of PTFE in the immediate vicinity of the catalyst sites. This statement is counter to the prevailing philosophy that the PTFE is necessary to provide hydrophobic regions within the catalyst layer through which the gas can access the catalyst. An ideal gas conduit would be a pore lined with only a thin coating of PTFE (for hydrophobicity) to allow a passageway for the gas. However, in practice, discrete and dense clumps of PTFE are formed because the melt does not wet the carbon particles uniformly. Thus, when the recast ionomer is applied to the electrode later in the impregnation step, much of the carbon surface is already covered with PTFE and many of the pores are blocked.

Even if the PTFE is evenly distributed throughout the pores, the advantages normally associated with PTFE cannot be capitalized upon to improve the performance of the

catalytic layer. The high solubility of oxygen in PTFE is useful only to those catalyst particles at the interface of PTFE and the carbon support. However, sites that are totally enveloped by PTFE are denied proton access and cannot contribute to the electrochemical process. This is demonstrated in liquid electrolyte by the decrease in catalyst active area with the increase of PTFE weight percent in gas diffusion electrodes. Incidentally, PTFE is no more efficient in transporting oxygen than either the ionomer or water. The permeability of oxygen through hydrated Nafion and through water is both considerably greater than through PTFE. Therefore, a pore filled with the former materials will transmit oxygen at a higher rate than a solid pore filled with PTFE. In summary, PTFE can increase the diffusivity of gases only in the sense that it provides hydrophobicity to an open pore to prevent it from being clogged with water. Although this property is desirable in the gas diffusion portion of an electrode, a penalty is paid in the catalytic region due to the lack of utilization of the catalyst in completely dry and/or PTFE-coated pores.

The use of Nafion as a binder introduces certain structural advantages over conventional electrodes that utilize a rigid support with respect to the bonding of the electrode to the PEM. Upon hydration, the dimensions of a hydrophilic ionomer membrane increase a fair amount and the swelling from the osmotic forces exert substantial forces. In a PEMFC with a large cross-sectional area, the relatively rigid Telfon-bonded carbon matrix of a conventional electrode structure cannot easily accommodate variations in the swelling of the membrane if the membrane water content varies substantially. The stress is most

probably relieved by the electrode partially delaminating from the membrane or by cracking in the electrode. Thus, startup and shutdown (hydration/dehydration) cycles decrease the longevity of the cell.

The latter electrode structure (no PTFE electrodes) presented here attempts to improve upon the previous construction by significantly increasing the contact area between the polymer electrolyte and the platinum clusters. This increase is achieved in two ways. First, the supported catalyst and the ionomeric additive are cast together to form the catalytic layer. This assures that the thickness of tile catalyst layer coincides with the depth of the ionomer. Second, the contact area between the ionomer additive and catalyst is increased by completely eliminating tile PTFE component and by improving the dispersion of the ionomer throughout the catalyst layer. The latter is accomplished by blending the solubilized ionomer and the platinized carbon into a homogeneous "ink", from which the thin film catalyst layer of the electrode is cast.

The gas diffusion portion of the electrode consists of a separate Teflonized carbon cloth backing that is stacked behind the thin film to provide support and to provide a hydrophobic distribution network for the gases. This two-part construction of the electrode hydrophobic backing and hydrophilic catalyst layer - allows each of the two regions to be fabricated separately with the properties that best suit the function of each region.

The thickness of the catalytically active region is usually determined by the depth of proton penetration, which is a function of' the specific protonic conductivity, the volume fraction and the distribution of the ionomeric electrolyte within the electrode structure. However, increasing the volume fraction of the ionomeric electrolyte also increases the thickness of the electrode and, hence, the mass transport barrier and the electronic impedance of the electrode, both of' which are detrimental effects. Thus, above a certain optimum, the potential drop across the catalyst layer increases with tile Volume fraction of the ionomer.

The last of the three criteria is the access of gas. In our new type of thin film catalyst layer, the gas is not provided with a network of hydrophobic pores within the catalyst layer; thus, gas diffusing through the catalyst layer must traverse pores filled with water and/or ionomer. However, the permeability of oxygen through recast ionomeric films is sufficient such that a 5μm diffusion pathway through the ionomer to the catalyst particles will not introduce significant oxygen transport losses on the cathode side of the fuel cell. Consequently, a PTFE-free thin film catalyst layer with an effective tortuosity thickness of 5μm or less should be able to sustain current densities equivalent to a much thicker electrode that uses in extensive network of gas distribution pores.

For the electrodes that prepared by the same method, their performances have the order (Pt-Ru + Pt-Sn) > (Pt-Ru + Pt-Pd) > (Pt-Ru + Pt-RuO_2) > (Pt-Ru + Pt-Ir), it is shown that

Pt-Sn has the strongest synergetic effect on Pt-Ru, and Pt-RuO_2 has similar synergetic effect as Pt-Pd on Pt-Ru.

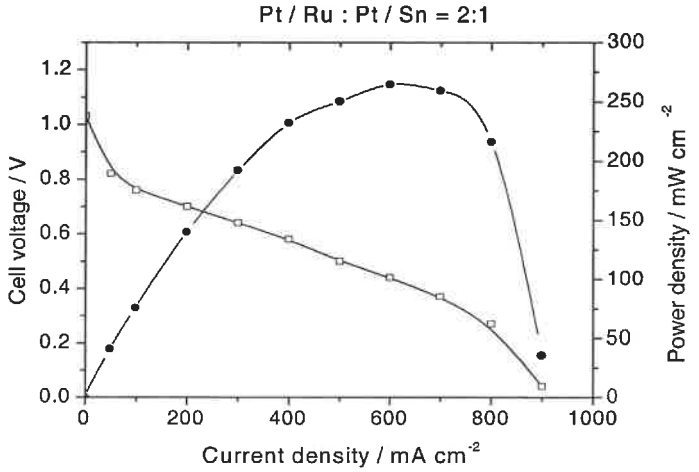

Figure 4-33 Polarization and power density curves for a single MEA at H_2/O_2 reactants. Pressure: ambient, T_{cell} = 60°C. Electrode area: 2.25cm^2. Membrane: Nafion 117. Cathode: 4mg/cm^2 Pt/C, Anode: 4mg/cm^2 (Pt-Ru + Pt-Sn/C)- prepared by our lab.

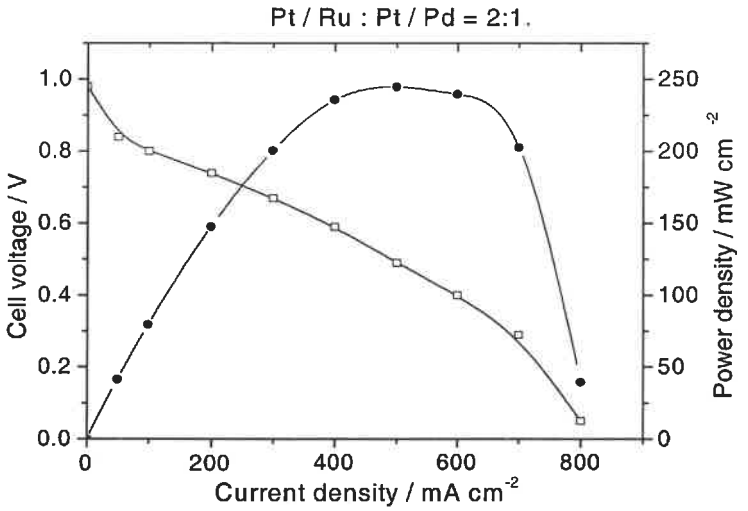

Figure 4-34 Polarization and power density curves for a single MEA at H_2/O_2 reactants. Pressure: ambient, T_{cell} = 60°C. Electrode area: 2.25cm^2. Membrane: Nafion 117. Cathode: 4mg/cm^2 Pt/C, Anode: 4mg/cm^2 (Pt-Ru + Pt-Pd/C)- prepared by our lab.

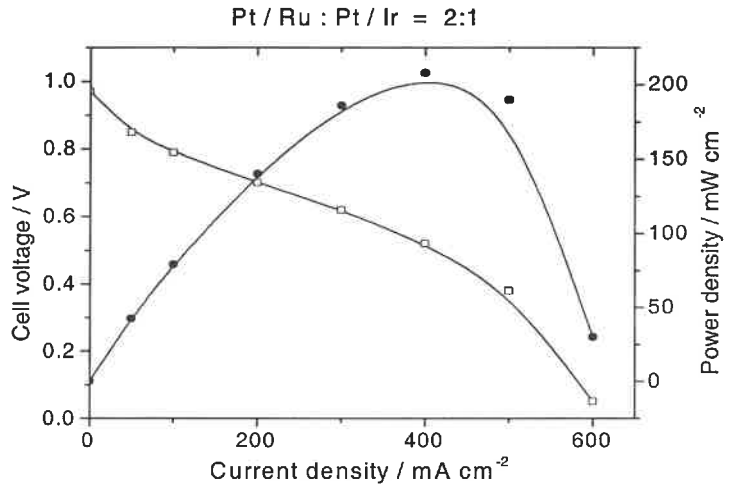

Figure 4-35 Polarization and power density curves for a single MEA at H_2/O_2 reactants. Pressure: ambient, T_{cell} = 60°C. Electrode area: 2.25cm^2. Membrane: Nafion 117. Cathode: 4mg/cm^2 Pt/C, Anode: 4mg/cm^2 (Pt-Ru + Pt-Ir/C)- prepared by our lab.

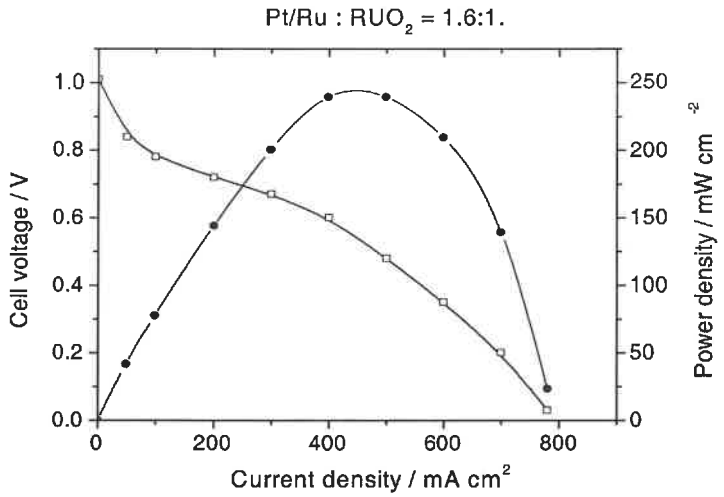

Figure 4-36 Polarization and power density curves for a single MEA at H_2/O_2 reactants. Pressure: ambient, T_{cell} = 60°C. Electrode area: 2.25cm^2. Membrane: Nafion 117. Cathode: 4mg/cm^2 Pt/C, Anode: 4mg/cm^2 (Pt-Ru + RuO_2/C)- prepared by our lab.

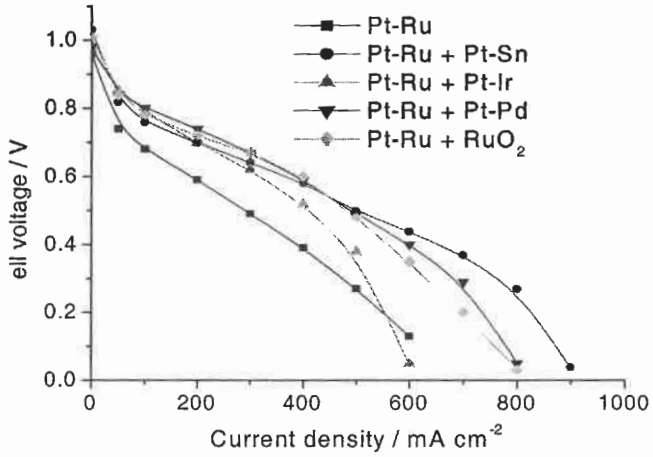

Figure 4-37 Polarization curves for a single MEA at H_2/O_2 reactants. T_{cell}: 60°C. Membrane: Nafion 117. Pressure: ambient. Cathode: 4mg/cm^2 Pt/C (60% Pt/C), Anodes: different composition as shown.

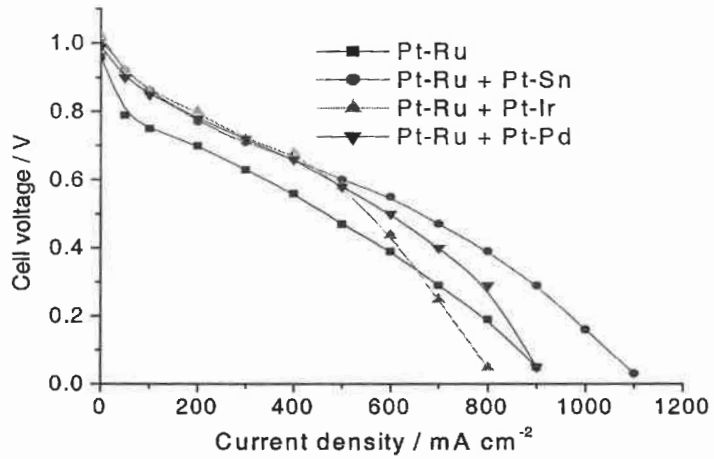

Figure 4-38 Polarization curves for a single MEA at H_2/O_2 reactants. T_{cell}: 60°C. Membrane: Nafion 117. Pressure: P_{H2}/P_{O2} = 20psi/25psi. Cathode: 4mg/cm^2 Pt/C (60% Pt/C). Anodes: different composition as shown.

4.2.2 Acetals/O_2 polarization curves on different electrodes

For acetals as fuel we used a cylinder as a heater, this cylinder has a bi-function to evaporate the liquid and then to humidify the so-produced gas. One side of cylinder is connected to a pump and another side is connected to fuel cell stack, so the produced fuel gas is always at ambient pressure. As we explained above, duo to different boiling point the testing temperatures have different values. For methylal the temperature of fuel cell is 60°C, for ethylal and 1,3-dioxolane the temperatures are 85°C and 90°C.

4.2.2.1 Methylal/O_2

Figure 4-39 to 4-43 show different MEA's polarization curves for methylal as fuel. The Figure 4-44 is the comparison of different electrodes. From these figures we can see for all these electrodes methylal shown some kind of reaction activity, but the region is narrow. But in (Pt-Ru + Pt-Sn) it has a big improvement, the open circuit potential is 0.74v, the power density can reach to 28 $mW.cm^{-2}$. Just as in hydrogen fuel, (Pt-Ru + Pt-Pd) is better than (Pt-Ru + Pt-Ir).

We already know that methylal is almost completely hydrolyzed in a direct oxidation fuel cell that employs an acid doped polymer electrolyte to form a mixture of methylformate, methanol and formic acid [136]. The anode performance improves in the sequence of methanol, methylal, formic acid, and methylformate solutions. However, the methylal

solution at room temperature does not hydrolyze without an acid catalyst. So we can imagine that only at high temperature there are hydrolysis products of methylal in our cylinder, at 60°C to 80°C we expect it is only methylal deliver to MEA. Then similar hydrolysis occurred at the Nafion/electrode interface, the resulting products, formic acid/formaldehyde could be oxidized at the electrode and also be converted to carbon dioxide according to following processes:

$$(CH_3O)_2CH_2 + H_2O \rightarrow 2CH_3OH + HCHO \text{ (acid-catalyzed)} \qquad (4\text{-}14)$$

$$HCHO + H_2O \rightarrow CO_2 + 4H^+ + 4e^- \qquad (4\text{-}15)$$

Therefore poisoning effect is inevitable to all these electrodes just like methanol electrooxidation. The performance of Pt-Ru-Sn in our studies shows that this electrode has good resistance to CO/CO_2 poison. From these curves we can guess that the product composition of electrooxidation of methylal is dependent on the electrocatalyst materials. Such differences have been observed in the oxidation of methanol on Pt and Pt-Ru catalysts where the kinetic of oxidation and the stability of intermediates is altered by the chemisorption characteristics of the Ru sites. Differences in product composition can also arise from the extreme water activity at the site of reaction. In water-deficient environment other oxygen-deficient intermediate products such as dimethyl ether or methyl formate could be formed electrochemically. This confirms that in order to attain complete oxidation of the organic molecules, the nature of the electrocatalyst and electrolyte are of fundamental importance.

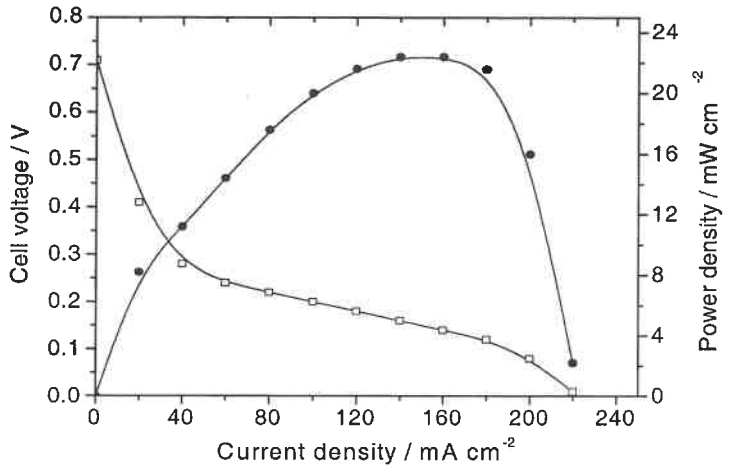

Figure 4-39 Polarization and power density curves for a single MEA at ethylal/O_2 reactants. Pressure: ambient, T_{cell} = 90°C. Electrode area: 2.25cm^2. Mole ratio of water/Ethylal: 8. Membrane: Nafion 117. Cathode: 4mg/cm^2 Pt/C, Anode: 4mg/cm^2 Pt-Ru/C- prepared by our lab.

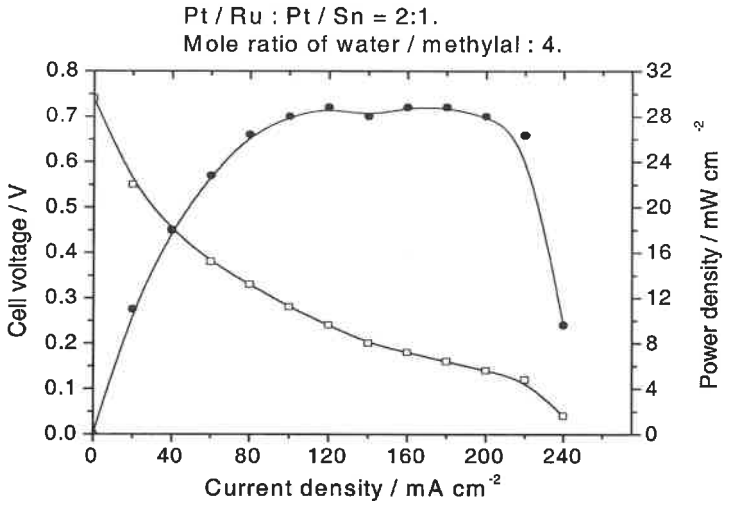

Figure 4-40 Polarization and power density curves for a single MEA at Methylal/O_2 reactants. Pressure: ambient, T_{cell} = 60°C. Electrode area: 2.25cm^2. Membrane: Nafion 117. Cathode: 4mg/cm^2 Pt/C, Anode: 4mg/cm^2 (Pt-Ru + Pt-Sn/C)- prepared by our lab.

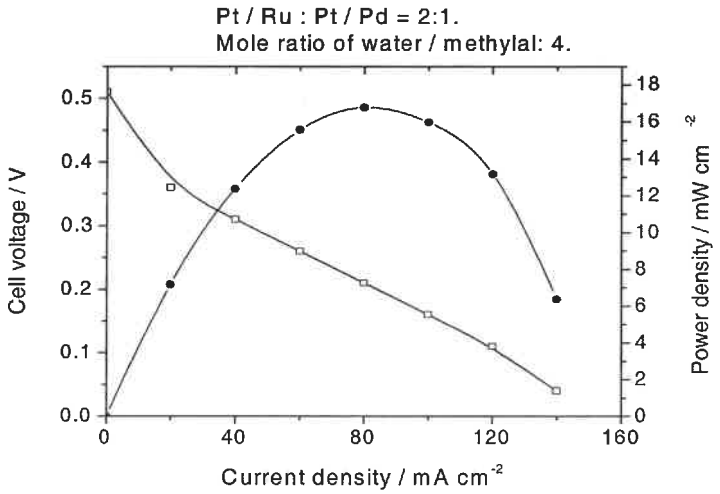

Figure 4-41 Polarization and power density curves for a single MEA at Methylal/O_2 reactants. Pressure: ambient, T_{cell} = 60°C. Electrode area: 2.25cm^2. Membrane: Nafion 117. Cathode: 4mg/cm^2 Pt/C, Anode: 4mg/cm^2 (Pt-Ru + Pt-Pd/C)- prepared by our lab.

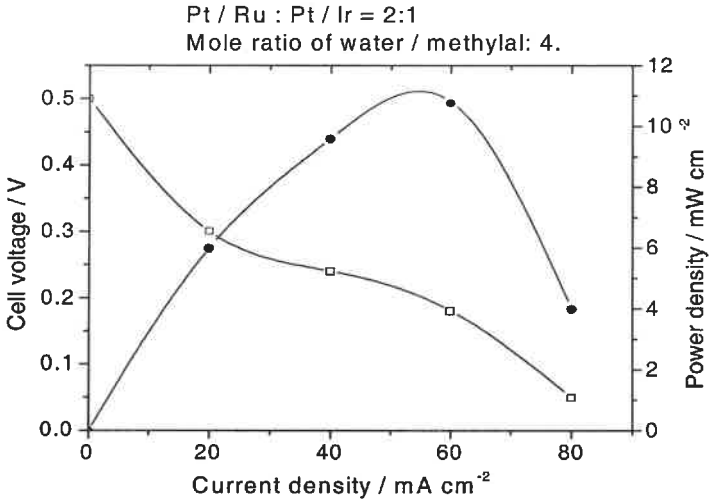

Figure 4-42 Polarization and power density curves for a single MEA at Methylal/O_2 reactants. Pressure: ambient, T_{cell} = 60°C. Electrode area: 2.25cm^2. Membrane: Nafion 117. Cathode: 4mg/cm^2 Pt/C, Anode: 4mg/cm^2 (Pt-Ru + Pt-Ir/C)- prepared by our lab.

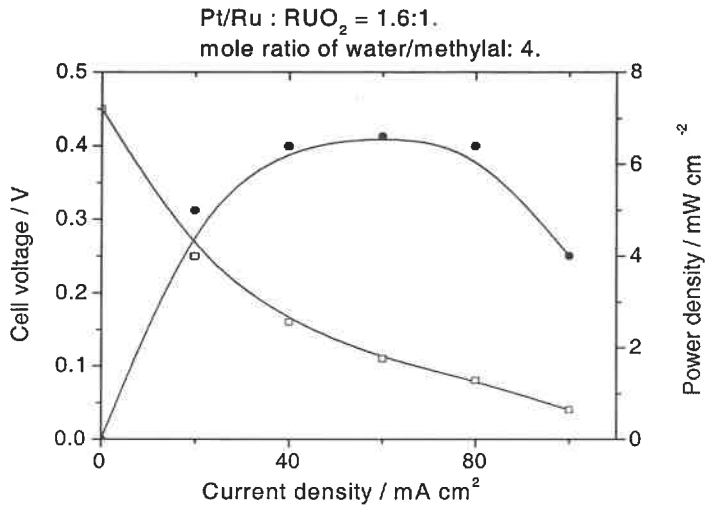

Figure 4-43 Polarization and power density curves for a single MEA at Methylal/O_2 reactants. Pressure: ambient, T_{cell} = 60°C. Electrode area: 2.25cm^2. Membrane: Nafion 117. Cathode: 4mg/cm^2 Pt/C, Anode: 4mg/cm^2 Pt-Ru + RuO_2/C- prepared by our lab.

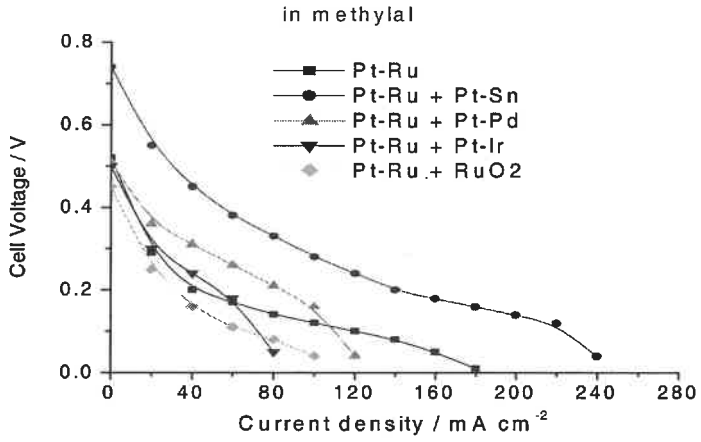

Figure 4-44 Polarization curves for a single MEA at methylal/O_2 reactants. T_{cell}: 60°C. Membrane: Nafion 117. Pressure: ambient. Cathode: 4mg/cm^2 Pt/C (60% Pt/C). Anodes: different composition as shown.

From the experience based on methanol electrooxidation, we know for single noble metals only Pt seems to be able to adsorb methanol and to break the C-H bonds. Acetals PEMFC have the same result. Unfortunately, the dissociative adsorptions of methanol or acetals lead to the formation of strongly adsorbed residues acting as poisons for the electrooxidation catalysts. The "in situ" IR spectroscopic reflectance techniques showed that the main species responsible of the poisoning phenomena are adsorbed CO, either linearly or bridge bonded to the platinum surface. The formation of CO leads to the high overpotentials observed during the electrooxidation of methanol in a DMFC. However fundamental works have shown that the CO poisoning is less important on highly dispersed platinum than on smooth platinum. The tremendous development of the H2/O2 PEMFC during the last decade have shown that it is now possible to conceive catalytic electrodes very active for hydrogen oxidation with a platinum loading as low as 0. 1 mg/cm^2. Unfortunately, it is clear that, as least in a near future, such a small loading is not suitable for the electrooxidation of methanol or acetals, even if the electrode poisoning of such highly dispersed platinum catalysts is weaker.

The challenge remains then to reduce or to avoid the formation of such strongly adsorbed CO species or to favor their oxidation at low potentials. This can be obtained only by modifying the superficial electrode structure in order to change the kinetics of adsorption and oxidation of species linked at the electrode surface. Different metals added to platinum have been proposed, but only a few of them give encouraging results.

All previous fundamental works confirmed that if platinum is essential as the main component of the organic fuel (acetals or methanol) anode catalysts in a PEMFC, its modification is absolutely necessary, with at least two added components. Improvement of these plurimetallic catalysts is the key points for the development of organic fuel PEMFCs, in several directions: enhancement of the activity by modification of the composition, and increase of the stability, especially concerning the corrosion and/or the superficial enrichment in one component.

The components added to platinum should have several properties, which restrict greatly their choice. The pH of the membrane leads to the necessity to have a metal, stable in acid media, but sufficiently oxidizable to increase the concentration at the electrode surface of adsorbed OH species, which participates directly to the electrooxidation of CO. Until now the best additive is, without doubt, ruthenium, which is widely recognized as one main component of a DMFC anode. Ruthenium is covered with adsorbed OH species at very low potentials (around 0.2V/RHE) and consequently favors the electrooxidation of the methanol or acetals adsorption residues, which need OH species to be transformed in carbon dioxide. Fundamental "in situ" IR reflectance spectroscopic experiments showed that with a Pt/Ru electrode the oxidation of adsorbed CO species does occur at potentials at least 200 mV below than those observed with pure platinum.

The mechanism of the electro-oxidation of methanol was thoroughly studied on Pt-Ru electrodes of various structures, in all these different studies, it appears clearly that the

addition of Ru to platinum leads to an electrooxidation of methanol starting at more negative potentials. Some discrepancies exist concerning the optimum composition of the bimetallic electrode. However, comparison measurements of the electrocatalytic activity obtained with well-defined alloys, and those with highly dispersed Pt-Ru/C, confirms that the optimum ruthenium composition for methanol electrooxidation is from 15-25 % atomic ratio. This result holds between room temperature and 60°C. An important point should be mentioned concerning the electrooxidation of CO on Ru and Pt-Ru bimetallic catalysts: the optimum Ru composition is then around 50%, and the electrooxidation of CO is possible on a pure Ru electrode, conversely to that of methanol which is completely absent at a Ru surface. This observation suggests that, even if methanol clearly leads to the formation of adsorbed poisons, identified as several CO species of different structures, the distribution of adsorbed species at the electrode surface is much more complicated, and some other species, different from CO, are always present at the platinum surface.

Among the other possible metals suitable to increase the activity of platinum, Sn was often considered. The main advantage of using tin is the low potential at which tin is partially covered by OH species. The electrooxidation of methanol, which needs adsorbed OH to be transformed in carbon dioxide, is thus possible at lower potentials. However, it seems that the conditions of preparation of Pt-Sn bimetallic electrodes are very particular, the difficulty being to maintain Sn in a metallic state. Recent new results with Pt-Sn dispersed into a conducting polymer have shown that this bimetallic catalyst

leads to a negative shift of the electrooxidation potentials of methanol. But these Pt-Sn electrodes greatly enhance the electrooxidation of gaseous CO, in a larger extent than Pt-Ru alloys. Finally, trimetallic Pt-Ru-Sn catalysts have also shown interesting results just like the results of our studies. But this catalyst's mechanism should be very complicated, we can only guess it has a synergistic effect, from our studies we see it does show synergistic effects of Pt-Ru and Pt-Sn. We already explained the mechanism of Pt-Ru on methanol or acetals, in the following we will also try to explain the mechanism of Pt-Sn on acetals or methanol.

For a meaningful mechanistic study, it is essential to assess the fundamental electrocatalytic activity of alloy electrodes as a function of their outermost layer composition, which may differ significantly from their bulk composition depending on both the catalyst preparation method (surface segregation effects) and the commonly applied pretreatment of the electrode prior to electrochemical measurements (preferential dissolution of the less noble alloying component at positive potentials). In addition, the true electrocatalytic activity must be clearly distinguished from mere changes in the real surface area in contact with the electrolyte, which cannot be achieved unambiguously for high-surface area alloy electrodes.

According to P. N. Ross et al research about methanol oxidation on Pt-Sn surface [142], Pt_3Sn is a particularly interesting alloy because it could in principle provide both functionalities postulated for alloy surfaces, i.e. an electronic as well as a

water-dissociating function. Pt_3Sn has a very negative heat of formation, i.e., a highly exothermic alloy, and is formally an intermetallic compound that occurs in an ordered crystal structure having Sn substituted for Pt at the corners of the unit cell. Modern band-structure calculations [143] confirm the existence of strong intermetallic bonding expected in such an alloy.

Because of the much lower surface energy of Sn, there is a large thermodynamic driving force for Sn enrichment in the surface relative to the bulk. Dilute alloys of Pt-Sn, e.g. 2 a/o Sn, have equilibrated surfaces highly enriched in Pt, typically 30-50% Sn. However, at the stoichiometric bulk composition of Pt_3Sn, the low index surfaces have ideally terminated planes that are either 25 % Sn (111) or 50% Sn (110 and 100). Any higher composition of Sn in the surface forms Sn-Sn bonds at the expense of Pt-Sn bonds in both the surface and the bulk, and this change is thermodynamically unfavorable. Hence, the Pt_3Sn crystal forms surfaces having 25 to 50 % Sn as well, so that Pt-Sn alloys have the unusual property that the surface composition is almost insensitive to the bulk composition, and is generally at least 25% Sn. This is a very different property than the Pt-Ru system, where thermodynamically Pt enrichment is favored, and Pt rich surfaces are easily achieved by annealing bulk alloys of varying composition.

A second and even more important contrast between Pt-Ru and Pt-Sn is revealed in UHV (ultra high vacuum) studies of CO thermal desorption spectroscopy (TPD), which demonstrate the strong electronic effect characteristic to the Pt-Sn system, consistent with

its strong intermetallic bonding mentioned above. Both the saturation coverage with CO and its adsorption energy are essentially identical on pure Pt and pure Ru single crystals ($E_{ads} \approx 30$ kcal/mole [144-145]) and thus, no significant changes in the behavior towards CO are expected upon the formation of a solid solution of Pt and Ru which does not exhibit any intermetallic compound formation. On the other hand, alloying with Sn causes both a reduction of the CO saturation coverage and a decrease in the CO adsorption energy by $\approx$ 5 kcal/mole [146]. This modified adsorption strength for CO clearly indicates the electronic effect of Sn adatoms on Pt, which may alter the purely bifunctional mechanism observed for Pt-Ru alloys (means with dissociative adsorption of water preferentially at Ru sites and the dissociative adsorption of organic fuel preferentially at Pt sites), in that it is apt to change the extremely high activity of electronically unperturbed Pt (in Pt-Ru) for the initial adsorption/dehydrogenation of methanol or acetals. At any rate, the activity of Pt-Sn alloy electrodes towards the oxidation of methanol or acetals cannot be predicted in a straightforward manner merely based on our understanding of the bifunctional mechanism on Pt-Ru alloys. Nevertheless, one would expect to observe the highest catalytic activity (if any) for Pt-Sn alloys with a rather low Sn surface compositions due to the fact that the initial dissociative adsorption of methanol or acetals will have to proceed via an ensemble of Pt surface atoms, similar to the situation with Pt-Ru. This optimum Sn surface composition, in analogy with Pt-Ru, would then be on the order of 10-20%, a composition which is not easily produced since it is a non-equilibrium composition.

Another important contrast between Pt-Sn and Pt-Ru is the stability of the admetal in electrolytic solution. Ru is stable in a Pt-Ru alloy surface up to a potential of ca. 0.7V in strong acid electrolyte. In normal polarization testing in a fuel cell, for example, one should not leach Ru from the surface. However, even at room temperature, Sn has a very narrow potential window of stability in strong acids, perhaps as low 0.5V, and even lower at higher temperatures. As a consequence, Sn dissolves from the surface at relatively low polarization, so one has to be extremely careful in testing the activity of either Pt-Sn solid electrodes or high surface fuel cell electrodes. The dissolution of Sn in the latter is probably ubiquitous in the literature, as it is quite common to polarize fuel cell electrode rather severely to explore the region of high current densities. There is an interesting compensating effect to the dissolution of Sn from the alloy surface; there is readsorption of the Sn onto the Pt surface at low potential, e.g. below 0.3V, which some investigator have termed underpotentially deposited (UPD) Sn, and this Sn adatom modified Pt surface is more active than Pt for methanol oxidation. It appears certain that virtually all fuel cell type Pt-Sn alloy catalysts are in reality adatom modified catalysts because of this dissolution/readsorption transformation of the Sn. The effect of UPD Sn on the activity of Pt for methanol oxidation is very sensitive to the Sn concentration in solution, with the maximum enhancement occurring at very low concentrations in solutions, e.g. 1μm, corresponding to very low surface coverage of the UPD Sn. But what we should keep in mind is that it is difficult to control the coverage of Sn via this surface transformation in-situ, which is probably the reason for the large discrepancies reported in the literature for Pt-Sn fuel-cell type electrodes.

Thus it is not difficult to understand the synergistic effects for this electrode coming from inter-complementary of each other. In our case the Pt-Ru-Pd also showed some kind of encouraging result although most of literatures have negative results about effect of Pd.

4.2.2.2 Ethylal or 1,3-dioxolane/O_2

Figure 4-45 to 4-49 showed different MEA's polarization curves for ethylal as fuel. The Figure 4-50 is the comparison of different electrodes for ethylal electro-oxidation. Figure 4-51 to 4-53 showed different MEA's polarization curves for 1,3-dioxolane as fuel. The figure 4-54 is the comparison of different electrodes for 1,3-dioxlane electro-oxidation. From the above figures we can see ethylal and 1,3-dioxolane have similar reaction trend as methylal, the mechanism of electrodes on acetals should has some kind of common characters. The (Pt-Ru + Pt-Sn) has a good performance. But in 1,3-dioxolane Pt-Ru-RuO2 shows better performance than that of on methylal and ethylal. In fact for all those electrode 1,3-dioxolane have a good performance at the staring phase of fuel cell testing, but for some of them such as Pt-Ru-Pd and Pt-Ru-Ir it is even difficult to complete one cycle before the performance quickly degrade. It may be indicated that 1,3-dioxolane produces more intermediate CO during electro-oxidation than ethylal and methylal do.

Figure 4-55 to 4-58 show acetals performance on same electrode, we can see ethylal always have a best performance among acetals except on Pt-Ru-RuO_2, on which 1,3-

dioxolane is better than other ones. But for different electrodes there still have small differences on performances of acetals, it may indicate the detailed mechanisms for acetals should have some kind of difference. More studies on these differences are necessary.

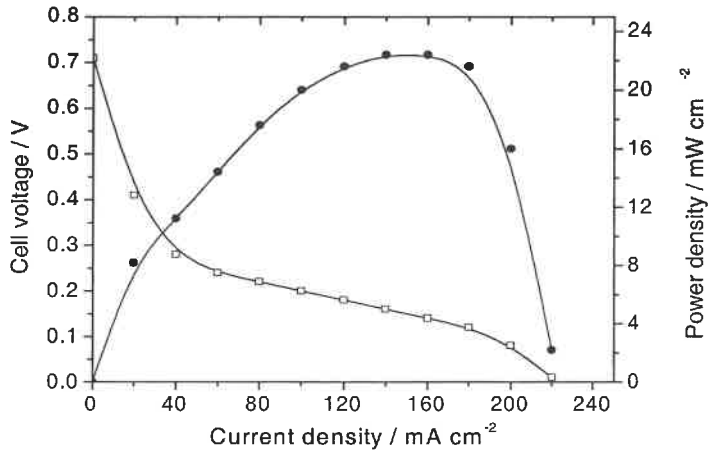

Figure 4-45 Polarization and power density curves for a single MEA at ethylal/O_2 reactants. Pressure: ambient. T_{cell} = 90°C. Electrode area: 2.25cm^2. Mole ratio of water/Ethylal: 8. Membrane: Nafion 117. Cathode: 4mg/cm^2 Pt/C, Anode: 4mg/cm^2 Pt-Ru/C- prepared by our lab.

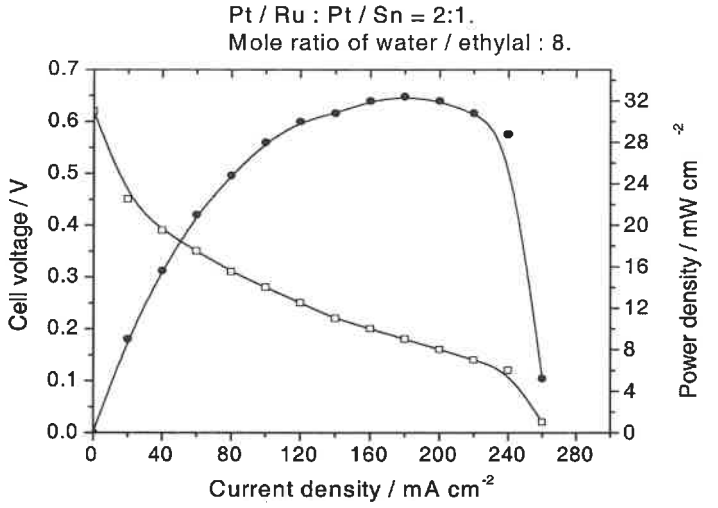

Figure 4-46 Polarization and power density curves for a single MEA at ethylal/O_2 reactants. Pressure: ambient, T_{cell} = 90°C. Electrode area: 2.25cm^2. Membrane: Nafion 117. Cathode: 4mg/cm^2 Pt/C, Anode: 4mg/cm^2 (Pt-Ru + Pt-Sn/C)- prepared by our lab.

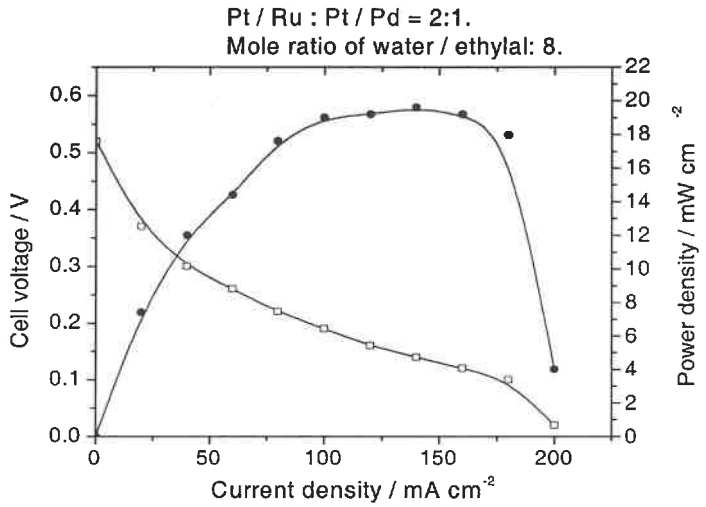

Figure 4-47 Polarization and power density curves for a single MEA at ethylal/O_2 reactants. Pressure: ambient, T_{cell} = 90°C. Electrode area: 2.25cm^2. Membrane: Nafion 117. Cathode: 4mg/cm^2 Pt/C, Anode: 4mg/cm^2 (Pt-Ru + Pt-Pd/C)- prepared by our lab.

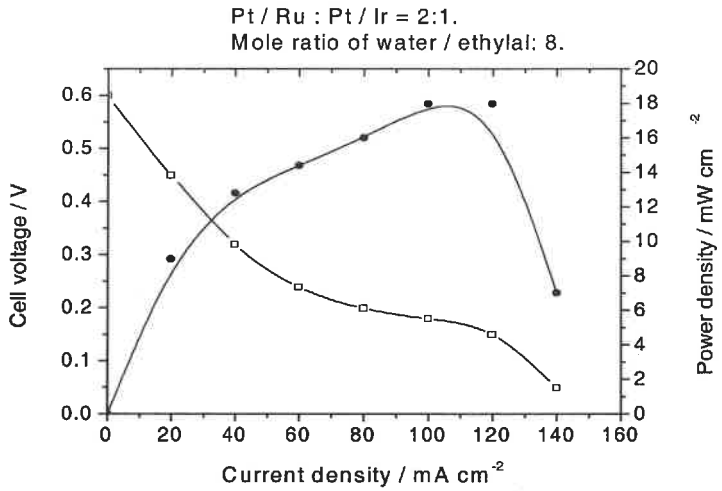

Figure 4-48 Polarization curves for a single MEA at Ethylal/O_2 reactants. Pressure: ambient, T_{cell} = 90°C. Electrode area: 2.25cm^2. Membrane: Nafion 117. Cathode: 4mg/cm^2 Pt/C, Anode: 4mg/cm^2 Pt-Ru + Pt-Ir/C- prepared by our lab.

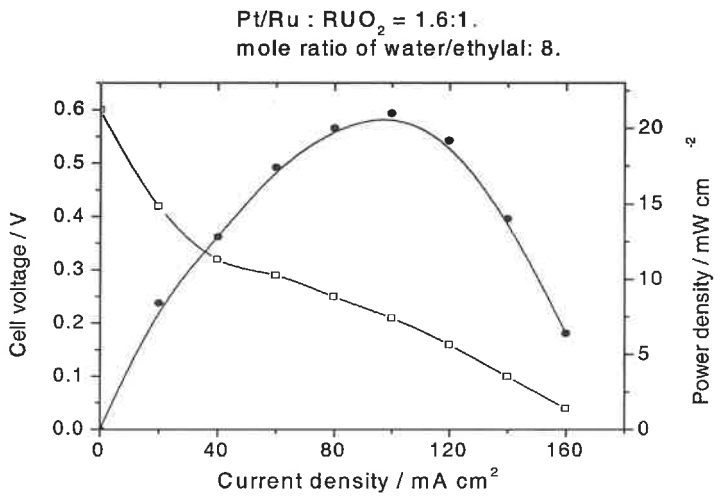

Figure 4-49 Polarization and power density curves for a single MEA at Ethylal/O_2 reactants. Pressure: ambient, T_{cell} = 90°C. Electrode area: 2.25cm^2. Membrane: Nafion 117. Cathode: 4mg/cm^2 Pt/C, Anode: 4mg/cm^2 Pt-Ru + RuO_2/C- prepared by our lab.

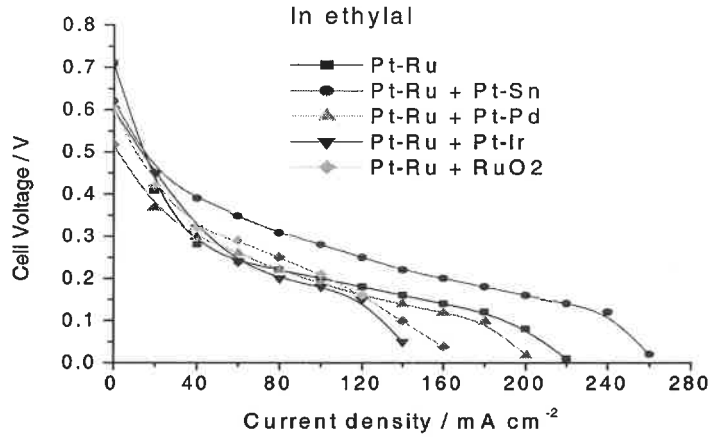

Figure 4-50 Polarization curves for a single MEA at ethylal/O_2 reactants. T_{cell}: 90°C. Membrane: Nafion 117. Pressure: ambient. Cathode: 4mg/cm^2 Pt/C (60% Pt/C). Anodes: different composition as shown.

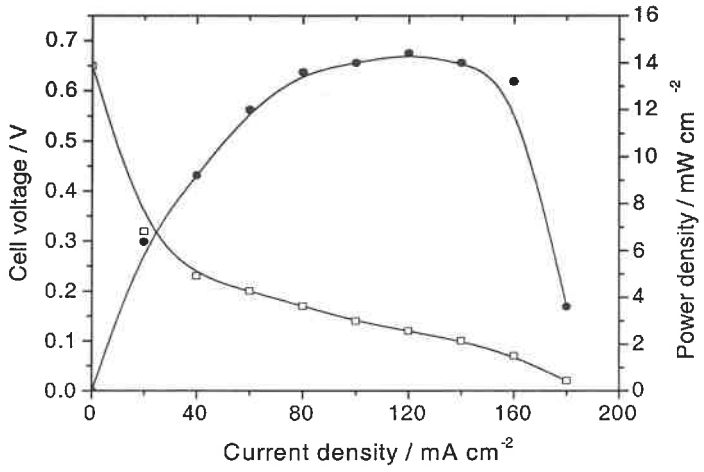

Figure 4-51 Polarization and power density curves for a single MEA at 1,3-dioxolane/O_2 reactants. Pressure: ambient, T_{cell} = 85°C. Electrode area: 2.25cm^2. Mole ratio of water/1,3-dioxolane: 4. Membrane: Nafion 117. Cathode: 4mg/cm^2 Pt/C, Anode: 4mg/cm^2 Pt-Ru/C- prepared by our lab.

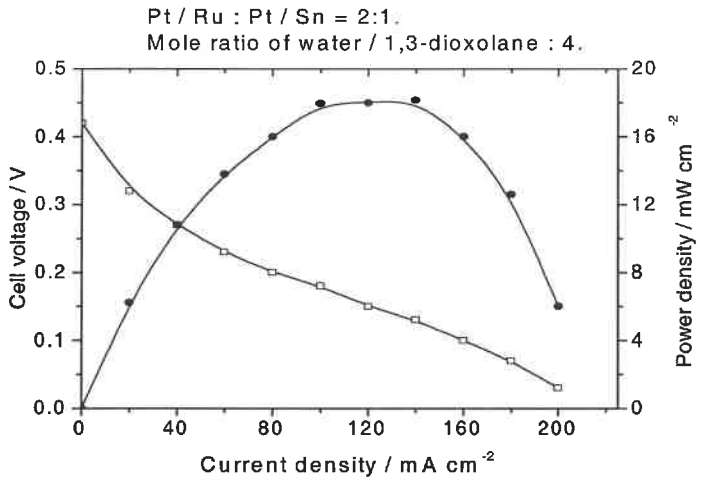

Figure 4-52 Polarization and power density curves for a single MEA at 1,3 - dioxolane/O_2 reactants. Pressure: ambient, T_{cell} = 85°C. Electrode area: 2.25cm^2. Membrane: Nafion 117. Cathode: 4mg/cm^2 Pt/C, Anode: 4mg/cm^2 (Pt-Ru + Pt-Sn/C)- prepared by our lab.

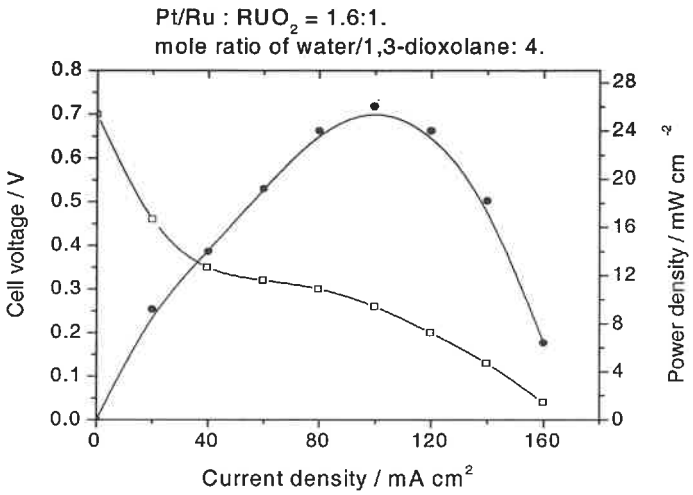

Figure 4-53 Polarization and power density curves for a single MEA at 1,3 - dioxolane/O_2 reactants. Pressure: ambient, T_{cell} = 80°C. Electrode area: 2.25cm^2. Membrane: Nafion 117. Cathode: 4mg/cm^2 Pt/C, Anode: 4mg/cm^2 (Pt-Ru + RuO_2/C)- prepared by our lab.

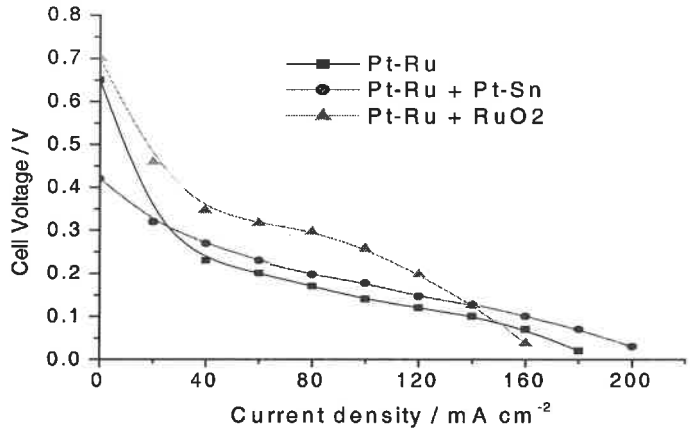

Figure 4-54 Polarization curves for a single MEA at 1,3-dioxolane/O_2 reactants. T_{cell}: 85°C. Membrane: Nafion 117. Pressure: ambient. Cathode: 4mg/cm^2 Pt/C (60% Pt/C). Anodes: different composition as shown.

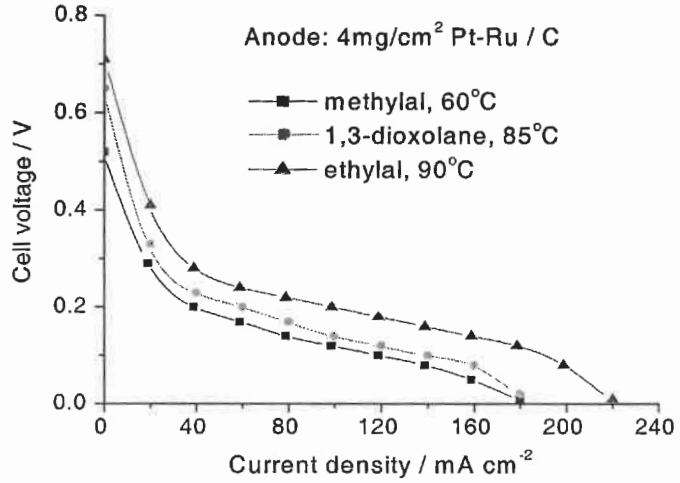

Figure 4-55 Polarization curves for a single MEA at acetals/O_2 reactants. Membrane: Nafion 117. Pressure: ambient. Cathode: 4mg/cm^2 Pt/C (60% Pt/C).

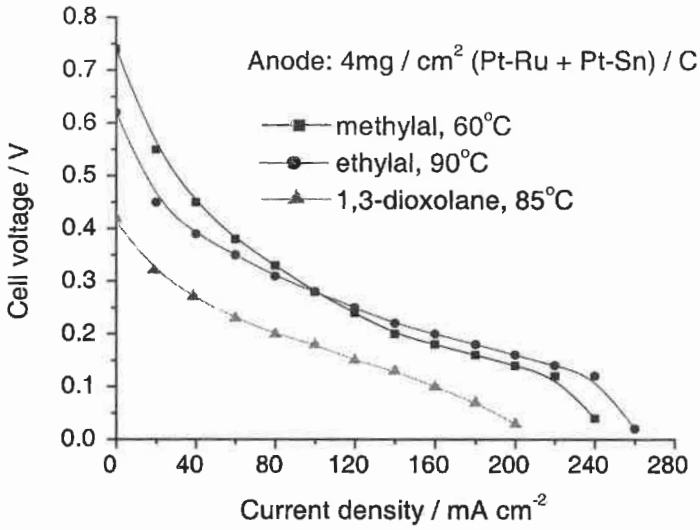

Figure 4-56 Polarization curves for a single MEA at aceatls/O_2 reactants. Membrane: Nafion 117. Pressure: ambient. Cathode: 4mg/cm^2 Pt/C (60% Pt/C).

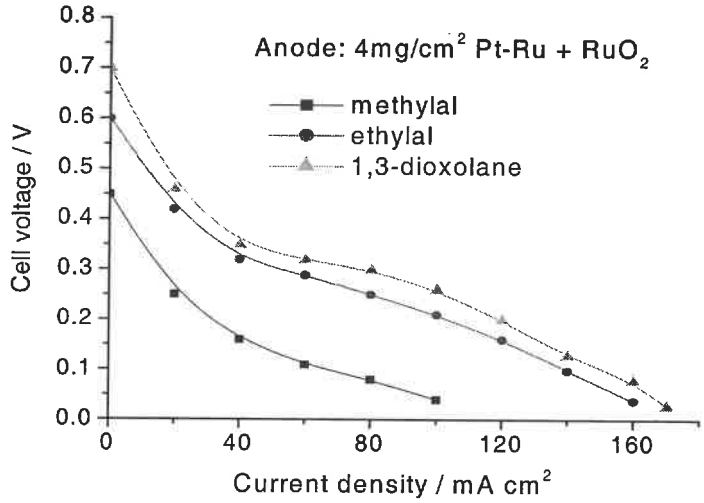

Figure 4-57 Polarization curves for a single MEA at acetals/O_2 reactants. Membrane: Nafion 117. Pressure: ambient. Cathode: 4mg/cm^2 Pt/C (60% Pt/C).

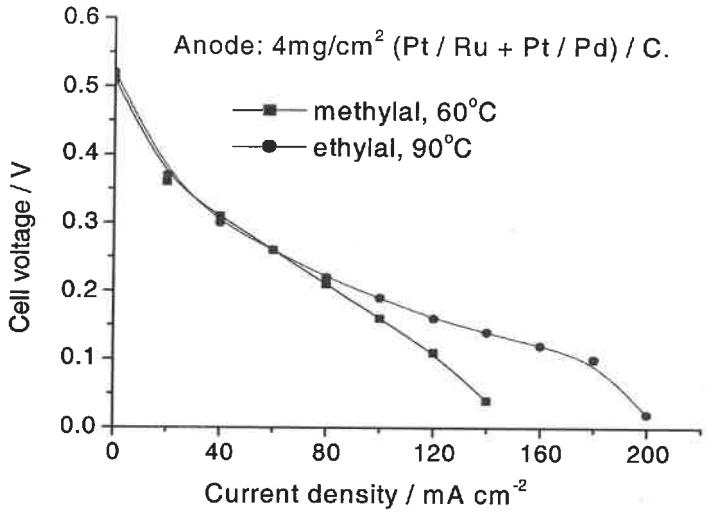

Figure 4-58 Polarization curves for a single MEA at acetals/O_2 reactants. Membrane: Nafion 117. Pressure: ambient. Cathode: 4mg/cm^2 Pt/C (60% Pt/C).

CONCLUSIONS AND RECOMMENDATIONS

- The applications of PEMFC in transportation and portable equipments need the development of new fuels and electrocatalysts for these systems.

- In this work, we have tested different types of electrodes in a half cell for direct electro-oxidation of acetals. It has been shown that Pt-Ru, Pt(O)x, Pt-Sn, Pt-RuO_2 and Pt-MnO_2 can sustain the electro-oxidation of acetals during the steady-state experiments without significant hysteresis in the polarization curves.

- The electro-oxidation of ethylal and 1,3-dioxolane were demonstrated for the first time in both half cell and fuel cell testing.

- New method of electrode preparation for PEMFCs has been developed. It has been shown in particular anodes, electrodes fabricated by this method exhibited interesting performance in PEMFCs. It was shown that these electrodes exhibited synergetic effects.

- It has been shown that liquid ethylal when used at 88°C at atmospheric pressure in PEMFC, performed better than PEMFC based on methylal (42°C) or 1,3-dioxolane (74°C) fuels.

- Volcano behaviour was observed for acetals electro-oxidation on Pt, Ru, Rh, Pd, Ir etc. at $i_{700mv} = f(R)$, where R is the metal radius. The same behaviour was obtained on Pt-Ru, Pt-Rh, Pt-Sn, Pt-Pd etc. at $i_{700mv} = f(\Delta R)$, where ΔR is the difference of the metal radius. The optimum current is obtained when $R \approx 1.83$Å for single noble metal based electrocatalysts. The optimum current is obtained when $|\Delta R|$ ($\Delta R = R_{metal}-R_{pt}$) is higher for Pt-metal alloys based electrocatalysts: Pt-Sn; Pt-Ru.

- It has been shown that acetals exhibited better performance than methanol on a half cell testing.

- It has been shown that direct acetal PEMFCs based on (Pt-Ru + Pt-Sn), (Pt-Ru + Pt-Pd), (Pt-Ru + Pt-Ir), (Pt-Ru + RuO_2) exhibited better performances than the cells based on single electrocatalysts (Pt-Ru, Pt-Pd, Pt-Sn Pt-Ir etc.). Among these anodes it was shown that (Pt-Ru + Pt-Sn) exhibited the best performance when using ethylal or methylal; (Pt-Ru + RuO_2) exhibited the best performance when using 1,3-dioxolane.

- These different electrodes have shown some resistant to the CO/CO_2 poisoning during ethylal and methylal fuel cell testing. Some electrodes (Pt-Ru + RuO_2, Pt-Ru + Pt-Sn) showed very good resistant to the CO/CO_2 poisoning during fuel cell testing based on 1,3-dioxolane. It has shown that CO/CO_2 poisoning of 1,3-

dioxolane electro-oxidation is very severe than that of ethylal and methylal. It seems that 1,3-dioxolane produces more intermediate CO during electro-oxidation.

- Ethylal is the best fuel among acetals in the half cell and fuel cell testing. It has also been stable in our testing.

- From these results, it could be seen that methanol can be replaced by acetals on PEMFC applications because acetals fuel cells perform better than methanol fuel cells.

Based on the results obtained in this work, we recommend carrying on the works on the development of PEMFCs in future. For a better understanding of the mechanism of acetals electro-oxidation and the improvement of the corresponding PEMFC performance, the following aspects should be considered:

- Determination of the cross-over rate of acetals through Nafion 117 and other membranes.

- Determination of the kinetic parameters of acetals electro-oxidation.

- To characterize the composition, size, distribution and morphology of the particles of the electrocatalysts prepared in this work using electron microscopy and X-ray diffraction techniques.

- Determination of the mechanism of PBI conductivity in acetal PEMFCs.

- Determination of the performance of direct liquid feed acetal PEMFCs. Our preliminary results indicated the direct liquid feed acetal is feasible.

- Some other types of acetals must be also considered for PEMFC.

REFERENCES

1. K. V. Kordesch, J. C. T. Oliveira, "Fuel Cells", Ullmann's Encyclopedia of Industrial Chemistry, Fifth Edition, VCH, Weinheim, Germany, Vol. A 12, pp. 55-83.

2. General Electric Co., Aircraft Equipment Div. Feasibility Study of SPE Fuel Cell Power Plant for Automotive Applications, Final Study Report PO –L61-3863 V-1, prepared for Los Alamos National Laboratories, Nov. 17, 1981.

3. K. B. Prater, Journal Power Sources **29** (1990) 239

4. S. Mukerjee, S. Srinivasan, A. J. Appleby, Electrochimica Acta **38** (12) (1993) 1661.

5. H. F. Creveling, "Research and Development of a Proton Exchange Membrane (PEM) Fuel cell System for Transportation Applications": Abstracts, 1992 Fuel Cell Seminar, Tucson, AZ, Nov. 29-Dec. 2, 1992.

6. Fuel Cell News, **X**, 283, Summer, Fall, 1993.

7. R. A. Lemons, Journal Power Sources **29** (1990) 239.

8. K. B. Prater, Journal of Power Sources **37** (1992) 181.

9. Daimler Benz, Media Information, "Daimler-Benz report breakthrough in alternate power technology-Presentation electric automobile", Stuttgart/Ulm, Germany, April 13, 1994.

10. Daimler Benz, High Tech Report, 3/1994.

11. Ballard Power Systems Inc, Annual report 1994.

12. A. P. Meyer, J. V. Clausi, J. C. Trocciola, "The IFC Proton Exchange Membrane Fuel Cells", 33rd International Power Sources Symposium, Proc., June 1988, pp. 799-802, The Electrochem. Soc., Inc., Pennington 1988.

13. Energy Partners, "The Green Car™ Program", Overview, 1993.

14. Energy Partners, "Energy Partners Corporate Capabilities", Information brochure 1993.

15. Energy Partners, "Brief on the Closed Loop Fuel Cell Power System", 1993.

16. Fuel Cell News, Vol. X, Nov. 4, Winter 1994, pp.9.

17. J. F. McElroy et al., "SPE Hydrogen-Oxygen Fuel Cells for Rrigorous Naval Applications", 34th International Power Sources Symp., Cherry Hill, NJ, 1990. Proceedings pp. 403-407, Publ. by IEEE Service Center, 1990.

18. M. J. Rosso, P. M. Golben, J. J. Orlando, 0. J. Adlhart, 33th Power Sources Symposium, 13-16 June 1988, The Electrochem. Soc., Inc., Pennington, NJ.

19. K. Strasser, Journal of Power Sources **37** (1992) 209.

20. W. Drenckhahn, K. Hassmann, "Brennstoffzellen als Energiewandler", Sonderdruck aus Energiewirtschaftliche Tagesfragen **43** (6) (1993) pp. 382-390.

21. Siemens, PEM-Brennstoffzellen, Wirtschaftlichkeit an Bord - mit Elektrotechnik von Siemens, Brochure, 1994.

22. O. J. Adlhart, P. Rohonyi, D. Modroukas, and J. Driller, ASAIO Journal 1997, p. 214-219.

23. M. Ishizawa, K. Kimata, Y. Kuwatw, T. Yamashita, NTT Review Vol. 9 No. 5 Sep. 1997, p. 65-69.

24. M. Ishizawa, K. Kimata, Y. Kuwata, M. Takeuchi, T. Ogata, Electronics and Communications in Japan, Part 1, Vol. 82, No. 7, 1999, p.35-43.

25. D. Browning, P. Jones, K. Packer, Journal of Power Sources **65** (1997) 187-195, p. 187-195.

26. Kordesch Karl, Fuel cells and their applications (1996), p. 75.

27. S. Kamasaki, Sh. Sekido, Y. Miura, "Characteristics of Fuel Cell Hydrogen Electrodes Combined with SPE Nafion", Memoirs of Faculty of Technology, Tokyo Metropolitan University, No. 38, 1988, p. 141.

28. K. V. Kordesch, Electrochimica Acta **16**, (1971) 597.

29. S. Srinivasan, E. A. Ticianelli, C. R. Derouin, A. Redondo, "Advances in Solid Polymer Electrolyte Fuel Cell Technology with Low Platinum loading Electrodes", J. Power Sources **22** (1988) 359-375.

30. E. A. Ticianelli, C. R. Derouin, A. Redondo, S. Srinivasan, J.Electrochem. Soc. **135** (1988) 2209.

31. E. A. Ticianelli, J. G. Beery, S. Srinivasan, J.Appl. Electrochem. **21** (1991) 597.

32. Kordesch Karl, Fuel cells and their applications (1996), p. 77.

33. A. C. Ferreira, S. Srinivasan, "High Power Densities and Energy Efficiencies in PEMFCs using 0.05 mg Pt/cm^2 Gas Diffusion Electrode", ECS, Spring Meeting, San Francisco (CA), May 22-27, 1994, 969.

34. Ballard Advanced Materials, "Development and Evaluation of a Low-Cost Solid Polymer Electrolyte", IEA Workshop, Ottawa, Canada, Sept. 14-15, 1992.

35. T. D. Gierke, G. E. Munn, F. C. Wilson, J. Polym. Sci. Polym. Phys. **19** (1981) 1687.

36. PEM Brennstoffzellen, Brochure, Siemens KWU FRN4, Erlangen, Germany, D-91050 (Dec. 1992).

37. K. Strasser, "PEM Fuel Cells for Energy Storage Systems", IECEC '91, 26th Intersociety Energy Conversion Engineering Conference, Boston, Massachusetts, August 4-9, 1991, p. 636.

38. A. J. Appleby "Fuel Cells for Traction Applications - An Overview", Proceedings from a symposium on Feb. 8, 1994 at the Royal Swedish Academy of Engineering Sciences, IVA, Stockholm, Sweden, pp. 13-60.

39. M. Wakizoe, J. Kim. S. Srinivasan, and J. Me. Breen, "A Novel Method for Determination of Transport Parameters of H2 and 02 in Proton Exchange Membrane Fuel Cells", in Proceedings of the Symposium on "atteries and Fuel Cells for Stationary and Electric Vehicle Applications", ed. by A. R. Landgrebe, Z. Takehara, Proceedings Volume 93-8, p.310-323.

40. Yu-Min Tsou, M. C. Kimble, R. E. White, J. Electrochem. Soc. **139** (1992) 1913.

41. Kordesch Karl, Fuel cells and their applications (1996), p. 83.

42. Kordesch Karl, Fuel cells and their applications (1996), p. 87.

43. Kordesch Karl, Fuel cells and their applications (1996), p. 88.

44. "Fuel Cell Test at Siemens", Polymer Electrolyte Membrane- B ren nstoffzellen (PEMBZ), Siemens KWU FRN 4, Erlangen, D-91050, Dec. 1992.

45. R, A. Lemons, J. Power Sources **29** (1990) 251.

46. M. S. Wilson, T. E. Springer, T. A. Zawodzinski, S. Gottesfeld, "Recent Achievements in Polymer Electrolyte Fuel Cell (PEFC) Research at Los Alamos National Laboratory", IECEC 1991 – 26th Intersociety Energy Conversion Engineering Conference, Bosteon (MA), Aug. 4-9, 1991, p. 636-641.

47. M. Waidhas et al., "Research and Development of Low Temperature Fuel Cell at Siemens", 1994 - Fuel Cell Seminar, San Diego (CA), Nov/Dec. 1994, p. 477

48. S. Gottesfeld, J. Pafford, J. Electrochem. Soc. **135** (1988) 2651.

49. R. A. Lemons, J. Power Sources **29** (1990) 251.

50. S. Mukerjee, S. Srinivasan, A. J. Appleby, Electrochimica Acta **38** (12) (1993) 1661.

51. H. F. Creveling, "Research and Development of a proton-Exchange-Membrane Fuel cell System for Transportation Applications": Abstracts, 1992 Fuel Cell Seminar, Tucson, AZ, Nov. 29-Dec.2, 1992.

52. R. A. Lemons, J. Power Sources **29** (1990) 239.

53. W. Dödnitz, G. Gutmann, P. Urban, Daimler-Benz AG in "New Materials for Fuel Cell Systems II", O. Savadogo, P. R. Roberge, Editors, p. 14., Éditions de l'École Polytechnique de Montréal, Montréal, Canada (1997).

54. D. P. Wilkinson and A. E. Steck in "New Materials for Fuel Cell Systems II", O. Savadogo, P. R. Roberge, Editors, p. 27., Éditions de l'École Polytechnique de Montréal, Montréal, Canada (1997).

55. D. S. Watkins, K. W. Dircks and D. Epp, Canadian Patent 1,305,212 (1988).

56. D. P. Wilkinson, H. H. Voss, J. Dudley, G. J. Lamont and V. Basura, US Patent 5,432,021 (1995).

57. D. P. Wilkinson, H. H. Voss, J. Dudley, G. J. Lamont and V. Basura, US Patent 5,482,680(1996).

58. S. Gottesfeld and J. Pafford, J. Electrochem. Soc., Vol 135, 2651 (1988).

59. D. P. Wilkinson, H.H. Voss, K. B. Prater, G. A. flards, T. R. Ralph and D.Thompsett, European Patent Application 96302406.2 (1996).

60. A. Aramata and M. Masucla, J. Electrochem. Soc., 138, 1949 (1991).

61. S. R. Narayanan, H. Frank, B. J. Nakamura, M. Smart, W. Chun, G. Halpert, J. Kosek and C. Cropley, Electrochemical Society Proceedings Volume 95-23, 278 (1995).

62. X. Ren, M. S. Wilson and S. Gottesfeld, J. Electrochem. Soc., 143,L12-L 15 (1996).

63. S. Surampudi, S. R. Narayanan, E. Vamos, H. Frank, G. Halpert, A. LaConti, J. Kosek, G. K. S. Prakash and G.A. Olah, J. Power Sources, 47, 377 (1994).

64. S. R. Narayanan, G. Halpert, W. Chun, B. J. Nakamura, T.I. Valdez, H. Frank and S. Surampudi in "Proceeding of the 37th power sources conference 96", (1996).

65. K.M. Colbow, G. Bolli, J. St-Pierre and D. P. Wilkinson, in "Electrochemical Society Proceedings", Volume 96-8, p.332, The Electrochemical Society, Pennington, New Jersey, 1996.

66. U.S. Department of Energy Report, LANL No. 9-X53-D6271-1 (1984).

67. D. S. Watkins, K. W. Dircks and D. G. Epp, US Patent No. 4 988 583 19 No 5,108,849 (1992).

68. H. H. Voss, D. P. Wilkinson and D. S. Watkins, US Patent No. 5,260,143 (1993); US Patent No. 5,441, 819 (1995).

69. H. H. Voss and C. Y. Chow, US Patent No 5,230, 966 (1993).

70. N. J. Fletcher, C. Y. Chow, E. G. Pow, B. M. Wozniczka, H. H. Voss, G. Hornburg and D. P Wilkinson, US Patent No 5,547,776 (1996).

71. K. B. Washington, D. P. Wilkinson and H. H. Voss, US Patent No 5,300,370(1994).

72. M. S. Wilson, T. E. Springer, J. R. Davey and S. S. Gottesfeld, Electrochemical Society Proceedings, Vol. 95-23, pl 15 (1995).

73. D. P. Wilkinson, H. H. Voss and K. B. Prater, US Patent No. 5,252,410 (1993).

74. C. Chow, D. S. Watkins, K. B. Washington and S. Ramji, US Patent No. 5,284,718 (1994).

75. A. E. Steck and J. Wei, US Patent No. 5,464,700 (1995).

76. P. Gibb, H. H. Voss, W. Schlosser and E. G. Pow, US Patent No 5,484,666 (1996).

77. K. B. Washington, 1. T. Kenna, S. N. Ramji and G. A. James,US Patent No 5,514,487(1996).

78. K. B. Prater, J. Power Sources, 61, 105 (1996).

79. D. P. Wilkinson, H. H. Voss and K. B. Prater, J. Power Sources, 49, 117 (1994).

80. H. H. Voss, D. P. Wilkinson, P. G. Pickup, M. C. Johnson and V. Basura, Electrochim. Acta, 40, 321 (1995).

81. D. P. Wilkinson, H. H. Voss, D. S. Watkins and K. B. Prater, US Patent No 5,366,818 (1994).

82. D. P. Wilkinson, H. H. Voss, N. Fletcher, M. C. Johnson and E. Pow, US Patent Application Serial No. 08/721,214 (filed September 26, 1996).

83. K. Kinoshita, in Electrochemical Oxygen Technology, p. Sponsered by The Electrochemical Society, John Wiley & Sons, Inc. (1992).

84. N. J. Fletcher, G. J. Lamont, H. H. Voss and D. P. Wilkinson, US Patent 5,470,671 (1995).

85. G. A. Hards, T. R. Ralph, D. P. Wilkinson and S. A. Campbell, Program and Abstracts of the Fuel Cell Seminar, P. 544, Nov. 17 - 20, Orlando, Florida, 1996.

86. J. Wei, C. Sone and A. E. Steck, US Patent 5,498,639 (1996).

87. A. E. Steck, in "New Materials for Fuel Cell Systems I", O. Savadogo, P. R. Roberge, T. N. Vezirogle, Editors, p.74, Éditions de l'École Polytechnique de Montréal, Montréal, Canada (1995).

88. O. Savadogo, Journal of New Materials for Electrochemical Systems 1, PP.47-66 (1998).

89. A. J. Appleby and F. R. Foulkes, "Fuel Cell Handbook", Krieger Publishing Company, Malabar, Florida, 1993.

90. D. T. Tran, O. A. Velev, I. J. Kakwaii, S. Gainburzev, F. Sirnoneaux, T. R. Lalk and S. Srinivasan, Meeting Abstracts of Batery Division, Fall Meeting of The Electrochemical Society, Abstract 101, p.132, October, 1996.

91. D. P. Wilkinson, G. J. Lamont, H. H. Voss and C. Schwab, US Patent No 5,521,018 (1996).

92. D .P. Wilkinson, G. J. Lamont, H. H. Voss and C. Schwab, US Patent No 5,527,363 (1996).

93. K. B. Washington, D. P. Wilkinson and H. H. Voss, US Patent No 5,300,370(1994).

94. Otto J. Adlhart, P. Rohonyi, D. Mordroukas, J. Driller, ASAIO Journal 1997, **43**, p. 214-219.

95. M. Ishizawa, K. Kimata, Y. Kuwata, M. Takeuchi, T. Ogata, Electronics and Communications in Japan, Part 1, Vol. J81-B-I, No. 1, January 1998, p. 29-37.

96. D. Browning, P. Jones, K. Packer, J. of Power Sources **65** (9197) p.187-195.

97. H. Amanauma, Y. Kuwata, M. Adachi, I. Ishizawa, T. Ogata, Field test of fuel cell energy system for telecommunication co-generation system. Tech Rep IEICE 1996, PE96-24, P.7-14.

98. M. Ishizawa, Y. Kuwata, Y. Takeechi, K. Kimata, T. Ogata, Portable fuel cell system for Telecommunications use. Denki Kagaku 1996, **3**(6).

99. M. Ishizawa, Y. Kuwata, Y. Takeechi, K. Kimata, T. Yamashita, Introduction of portable fuel cell systems. NTI Rev. 1997, **9** (65-69).

100. A. N. Frumkin, Z. Physik. Chem., Leipzig, 207, p321, 1957.

101. A. N. Frumkin, Advances in electrochemistry and electrochemical engineering, Vol.3, John Wiley, New York, 1963.

102. M. S. Wilson, S. Gottesfeld, J. Appl. Electrochemistry., 22.p 1, 1992.

103. S. Mukerjee, S. Srinivasan, J. Electroanal. Chem., 357, p201, 1993.

104. V. M. Jalan and D. A. Landsman, US Patent 5, 186, 110, 1980.

105. P. Stonehart, Ber. Bunsenges. Physik. Chem. 94, p913, 1990.

106. S. Trasatti, J. Electroanal. Chem., 33, p351, 1971.

107. L. 1. Krishtalik, J. Electroanal. Chem., 130, p9, 1981.

108. O .Savadogo, J .Electrochem. Soc., 139, p1982, 1992.

109. O. Savadogo, S. Levesque, J. Appl. Electrochem., 21, p457, 1991.

110. H. Dumont, P. Los, A. Lasia, H. Menard and L. Brossard, J. Appl. Electrochem., 23, p684,1993.

111. H. Dumont, P. Los, H. Menard , L. Brossard, B. Salvato and 0. Vittori, Int. J. Hydrogen Energy, 18, p719, 1993.

112. P. N. Rylander, Catalytic hydrogenation over platinum metals., Academic Press, New York~ 1967.

113. D. W. Mckee, A. J. Scarpellino, Electrochem. Tech., 6, p101, 1969.]

114. P.N.Ross, K. Kinoshita, A. J. Scarpellino, P. Stonehart, J. Electroanal. Chem., 59, p177, 1975.

115. F. L. Williams and M. Boudart, J. Catal., 30, p1504, 1972.

116. S. Mosdale, P. Stevens, Solid State Ionics., 61, p251, 1993.

117. H. A. Gasteiger, N. Markovic, P. N. Ross, E. J. Cairns, J. Phys. Chem., 98, p617, 1994.

118. S. R. Wang, P. S. Fedkiw., J. Electrochem. Soc., 139, p1608, 1992.

119. J. B. Goodenough, A. Hamnet, B. J. Kennedy, R. Manoharn, S. A. Weeks, J. Electroanal. Chem., 240, p133, 1988.

120. C. Gutierrez, J. A. Caram, B. Beden, J. Electroanal. Chem., 305, p289, 1991.

121. T. N. Vezinglue, F. Barbier, Int.J.Hydrogen Energy., 17(7), p527,1992.

122. Fuel cell Development Information Center, Fuel Cells Now., Oct. 1994.

123. W. Vogel, J. Moolhuysen, Electrochim. Acta., 20, p79, 1975.

124. H. P. Dhar, L. G. Christner, A. K. Kush, , J. Electrochem. Soc., 134, p3021, 1987.

125. L. W. Niedrach, 1. B. Weinstock, Electrochem. Tech., 3, p270, 1967.

126. P.N.Ross, K. Kinoshita, A. J. Scarpellino, P. Stonehart, JElectroanal. Chem., 63, p97, 1975.

127. O. Savadogo, 1st International Symposium on New Materials for Fuel Cell System., O. Savadogo, P. R. Roberge et T. N. Veziroglu (eds.), Ecole Polytechnique de Montreal, p551, 1995.

128. N. M. Ristic, J. M. Jaksic and M. M. Jaksic, 1st International Symposium on New Materials for Fuel Cell System., O. Savadogo, P. R. Roberge et T. N. Veziroglu (eds.), Ecole Polytechnique de Montreal, p577, 1995.

129. M. Sye in "Semiconductor Devices" Ed. John Wiley and Sons, 1982.

130. J. A. Dalmon in "Catalyst par les metaux", B. Imelik, G. A. Martin et A. J. Renouprez Ed., Editions du CNRS, p253 1984.

131. O.Savadogo and A. Essalik, J. Electrochem.Soc., 141, L92 (1994).

132. O.Savadogo and A. Essalik, J. Electrochem.Soc., 143, 1814 (1996).

133. O.Savadogo and P. Beck, J. Electrochem.Soc., 143, 3482 (1996).

134. O.Savadogo and M. Lacroix, secondry International Symposium on "New Materials for Fuel Cell Systems", O.Savadogo, O.R.Roberge (eds.), Édition de le École Polytechnique de Montréal (Canada), P872 (1997)..

135. S. R. Narayanan, E. Vamos, S. Surampudi, H. Frank, G. Halpert, G. K. Surya Prakash, M. C. Smart, R. Knieler, and A. Olah, J. Electrochem.Soc., 144, 4195 (1997).

136. R.M. Moore, S. Gottesfeld and P. Zelenay, in "Proceedings of the Second International Symposium on Proton Conducting Membrane Fuel Cells", Eds. S. Gottesfeld, T. F. Fuller and G. Halpert, The Electrochemical Society, Pennington, New Jersey, 1999, Proceedings Volume 98-27, p. 388.

137. H.Chagnon and O.Savadogo, in "Extended Abstracts, Proceeding of the 3rd International Symposium on New Materals for Electrochemical Systems", Ed. O.Savadogo, Montreal, Canada, July 4-8, 1999, p.145.

138. M. Beaujean et al., Technical Report, Lambiotte et Cie, S.A., July 1995.

139. A. Fisher, M. Götz and H. wendt in "Second International Symposium on New Materials for Fuel Cell Systems", Eds. O. Savadogo and P. R. Roberge, Montreal, Canada, July 6-10, 1997, p.489.

140. M. Götz and H. wendt, Electrochim. Acta, **43**, (1998) 363.

141. J. T. Wang, W. F. Lin, M. Weber, S. Wasmus and R. F. Savinell, Electrochimica Acta, Vol. 43, No. 24, pp. 3821-3828, 1998.

142. P. N. Ross, Jr. and H. A. Gasteiger, "Proceedings of the First International Symposium On the New materials for Fuel Cell Systems", O.Savadogo, O.R.Roberge (eds.), Édition de le École Polytechnique de Montréal (Canada), P.286 (1997).

143. P. N. Ross, J. Vac. Sci. Technol. A 1992, 10, 2546.

144. B. E. Hayden, A. M. Bradshaw, Surf. Sci. 1984, 125, 787.

145. T. Engel, G. Ertl, Adv. Catal. 1979, 28, 1.

146. A. H. Haner, P. N. Ross, U. Bardi, A. Atrei, J. Vac. Sci. Technol. A 1992, 10, 2718.